

THESIS

**BIODEGRADATION OF DINITROTOLUENE
BY *PSEUDOMONAS PR7* IN A FLUIDIZED BED BIOREACTOR**

Submitted by

Katherine Keesling Whitty

**Department of Chemical
and Bioresource Engineering**

In partial fulfillment of the requirements

for the degree of Master of Science

Colorado State University

Fort Collins, Colorado

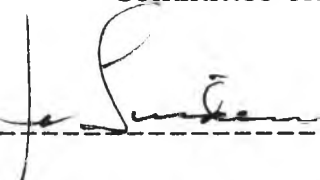
Spring 1997

COLORADO STATE UNIVERSITY

January 21, 1997

WE HEREBY RECOMMEND THAT THE THESIS PREPARED UNDER
OUR SUPERVISION BY KATHERINE KEESLING WHITTY ENTITLED
BIODEGRADATION OF DINITROTOLUENE BY PSEUDOMONAS PR7 IN A
FLUIDIZED-BED BIOREACTOR BE ACCEPTED AS FULFILLING IN PART
THE REQUIREMENTS FOR THE DEGREE OF MASTER OF SCIENCE.

Committee on Graduate Work



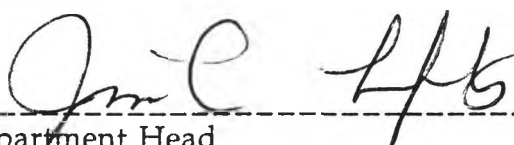
Katherine Keesling



Vincent A. Murphy

Kenneth F. Pearson

Adviser



Kenneth F. Pearson
Department Head

ABSTRACT OF THESIS

BIODEGRADATION OF 2,4-DINITROTOLUENE BY PSEUDOMONAS PR7

IN A FLUIDIZED-BED BIOREACTOR

2,4-Dinitrotoluene (DNT) has been listed as a priority pollutant by the U. S. EPA. It is a waste product in the production of 2,4,6-trinitrotoluene (TNT) and toluene diisocyanate. *Pseudomonas PR7* is able to completely degrade DNT via an oxidative pathway. Batch suspended-cell experiments were performed in order to determine the maximum specific growth rate μ_{\max} , and the Monod half-saturation constant, K_s . Parameter values of $\mu_{\max} = 0.1 \text{ h}^{-1}$ and $K_s = 14 \text{ mg/L}$ were obtained by fitting experimental data to the Monod model.

Immobilized-cell experiments in a fluidized-bed bioreactor (FBB) were performed in order to determine volumetric DNT degradation rate v for the biodegradation of DNT. A fluidized-bed bioreactor was chosen for study because (1) immobilization of cells onto particles allows for greater cell retention, and (2) fluidization of particles allows for mixing within the reactor. Greater cell retention allows for higher flow rates of liquid through the reactor and adequate mixing can alleviate the problem of low oxygen availability and other accumulation or depletion problems which occur in packed beds. Fluidization of immobilized cells in the FBB was achieved by the upflow of air and liquid. Data from residence time distribution (RTD) analysis of the FBB suggests that it behaves as a stirred tank reactor with small plug-flow regions and dead zones. The fluidized-bed bioreactor performance was compared with that of suspended-cell experiments and packed-bed experiments through direct comparison of DNT loading versus

degradation rates. It was found that the fluidized-bed bioreactor performed as well as a previously reported system consisting of a packed-bed column in series with a stirred-tank reactor in one experiment using diatomaceous earth particles as the immobilization medium. The FBB did not perform as well as the packed-bed system in subsequent experiments using polycarbonate particles.

Katherine Keesling Whitty
Department of Chemical and
Bioresource Engineering
Colorado State University
Fort Collins, CO 80523
Spring 1997

ACKNOWLEDGEMENTS

This work was supported by Grant # F49620-90-C09076 from the Air Force Office of Scientific Research. In addition to support from the research grant, I would like to acknowledge the support given to me through stipends from the Department of Chemical and Bioresource Engineering and a fellowship from the Graduate School here at CSU. I am grateful for the education it has provided me. My thanks go to Jim C. Spain and Shirley Nishino for providing *Pseudomonas* PR7 and the intermediate compound 4-methyl-5-nitrocatechol and for their suggestions regarding the bacterium and the intermediates it forms.

I would like to thank my advisor Dr. Kenneth F. Reardon for his guidance and ardent support. I am fortunate to have gained him as a friend and as a mentor through this experience; his expertise, knowledge, and patience made this project possible and enjoyable.

I also owe appreciation to the members of my committee, Dr. Vince G. Murphy and Dr. James C. Linden. Both were always willing to help and gave sound advice along the way. They also contributed to the value of this thesis through their final suggestions.

I would like to offer my gratitude to many of the students in the Department of Chemical and Bioresource Engineering who gave me assistance, friendship, and moral support throughout this project. There are so many that I cannot name them all, but I would especially like to recognize Doug Mosteller, Jeff Conuel, Julie Rogers, Chris Cannizzaro, Hugh Graham, Traci Taggart, Leigh Ann Boyack, Adeyma Arroyo, Sergio Valentinotti, Victor Saucedo, Pat Gilcrease, Narendra Poflee, and Noushin Mirajalili for their help

and support. And I'd like to thank Linda Henk for her assistance and friendship. Thank you.

Above all, I would like to thank my parents—Elizabeth Macy and Bill Whitty—my brother Thomas Whitty, and my best friend Lori Erickson. Without their love and patience I would not have accomplished this task with my spirit intact.

LIST OF TABLES

| | Page |
|--|------|
| Table 2.1: Microorganisms that degrade DNT and other nitroaromatic compounds. | 8 |
| Table 3.1: Reagents A and B for the sulfanilamide method for nitrite ion concentration determination. | 52 |
| Table 4.1: Suspended-cell shake-flask experiments and conditions. | 60 |
| Table 4.2: Suspended-cell stirred bioreactor experiments and conditions; all batches inoculated with a 0.5%v/v inocula grown in 1000 µM DNT until MNC had just disappeared. | 68 |
| Table 4.3: Parameter values for best fit of Monod model to experimental data. | 69 |
| Table 5.1 | 87 |
| Estimated values of the Damköhler and observable Damköhler numbers and the Thiele and Observable moduli at various conditions where $D = 0.92 \times 10^{-5} \text{ cm}^2/\text{s}$ and $k_s = 0.003 \text{ cm/s}$. | |
| Table A1.1: Physical properties of selected nitroaromatic compounds. | 104 |
| Table A2.1: Preparation of Spain's Mineral Salts Base. | 106 |

LIST OF FIGURES

| | Page |
|--|------|
| Figure 2.1: Metabolic pathway for the oxidative biodegradation of 2,4-dinitrotoluene by <i>Pseudomonas</i> DNT (Suen and Spain, 1993). Enzyme systems involved are <i>dntA</i> , <i>dntB</i> , <i>dntC</i> , and <i>dntD</i> . | 12 |
| Figure 2.2: Schematic diagrams of bioreactor types discussed in section 2.5. | 19 |
| Figure 2.3: Various means by which cells might be immobilized (Karel, Libicki, 1985). | 22 |
| Figure 2.4: Schematics of four general methods of cell immobilization. | 23 |
| Figure 2.5: Representation of an immobilized-cell particle. | 25 |
| Figure 2.6: Calculated effectiveness factor as a function of the observable modulus (Bailey and Ollis, 1986). | 33 |
| Figure 2.7: Basic classification of gas-liquid-solid fluidization systems (Fan 1989). | 34 |
| Figure 2.8: Minimum liquid fluidization velocities at varying superficial gas velocities for two particle diameters and densities. | 36 |
| Figure 2.9: Minimum fluidization velocity for a range of particle densities. | 37 |
| Figure 2.10: Pressure drop versus superficial fluid velocity. Note that the pressure drop ceases to increase at the minimum fluidization velocity. | 38 |
| Figure 3.1: Schematic of the fluidized-bed bioreactor. | 47 |
| Figure 3.2: Calibration of HPLC analytical method for DNT. | 50 |
| Figure 3.3: Calibration of HPLC analytical method for MNC. | 50 |
| Figure 3.4: Standard calibration of sulfanilamide method for nitrite analysis. | 52 |
| Figure 3.5: Dry cell concentration versus optical density measured at 600 nm. | 53 |
| Figure 3.6: Typical BCA protein assay calibration. | 56 |
| Figure 3.7: Voltage signal from the multimeter attached to the spectrofluorometer as a function of CFUs/mL of <i>P. PR7</i> grown in DNT plus SMSB. | 57 |

| | | |
|--------------|--|----|
| Figure 4.1: | Cell growth and DNT degradation in Shake-Flask Experiment SF1. Initial phosphate buffer strength was increased two-fold. | 60 |
| Figure 4.2: | Shake-flask cultures SF1 (triangles), SF2 (circles), and SF3 (diamonds) with initial DNT concentration of 500 μM . | 61 |
| Figure 4.3: | Experiments SF4 (triangles) and SF5 (circles) with different initial DNT concentrations. | 61 |
| Figure 4.4: | Experiment SF6; initial DNT concentration was 220 μM . | 62 |
| Figure 4.5: | Experiment SF7; initial DNT concentration was 440 μM . | 62 |
| Figure 4.6: | Experiments SF6 (triangles) and SF7 (circles); initial DNT concentrations were 220 and 440 μM (40 and 80 mg/L) respectively. | 63 |
| Figure 4.7: | Monod model fit to experiment SF3. Model parameter values were: $\mu_{\text{max}} = 0.04 \text{ h}^{-1}$, $K_s = 14.97 \text{ mg/L}$, and $Y_{x/s} = 0.198$. | 65 |
| Figure 4.8: | Monod-model fit of BR1 experimental data is represented by the line. Initial DNT concentration = 146 mg/L; $Y_{x/s} = 0.33$; $\mu_{\text{max}} = 0.102 \text{ h}^{-1}$; $K_s = 35.20 \text{ mg/L}$. | 70 |
| Figure 4.9: | Model prediction of BR1 experimental data. Initial DNT concentration = 146 mg/L; $Y_{x/s} = 0.3$; $\mu_{\text{max}} = 0.1 \text{ h}^{-1}$; $K_s = 14.0 \text{ mg/L}$. | 71 |
| Figure 4.10: | Monod-model prediction of BR2 experimental data. Initial DNT = 146 mg/L; $Y_{x/s} = 0.3$; $\mu_{\text{max}} = 0.1$; $K_s = 14.0 \text{ mg/L}$. | 71 |
| Figure 4.11: | Monod-model prediction of BR4 experimental data. Initial DNT concentration = 160 mg/L; $Y_{x/s} = 0.3$; $\mu_{\text{max}} = 0.1$; $K_s = 14.0 \text{ mg/L}$. | 72 |
| Figure 4.12: | Monod-model prediction of BR8 experimental data, pH controlled at 5.5. | 72 |
| Figure 5.1: | Result of mixing study in the fluidized-bed bioreactor. | 77 |
| Figure 5.2: | Experimental results of mixing study with tank-in-series models for N=1, N=2, and N=5 tanks. | 78 |
| Figure 5.3: | Fluidized-Bed Bioreactor Experiment FBB1 using diatomaceous-earth particles and feed DNT concentrations of 1000 μM . | 79 |
| Figure 5.4: | DNT degradation rate in the fluidized-bed bioreactor as a function of dilution rate for Experiment FBB1. | 80 |
| Figure 5.5: | Experiment FBB2 using polycarbonate particles. | 81 |

| | | |
|--------------|---|-----|
| Figure 5.6: | Repeated fluidized-bed bioreactor experiment (FBB3) using polycarbonate particles. | 82 |
| Figure 5.7: | Experiment FBB4 using polycarbonate particles with pH controlled between 6.7 and 7.0 and DNT feed concentrations of 675 mM and 880 mM. Solid diamonds represent the effluent DNT concentration in mM. | 83 |
| Figure 5.8: | DNT degradation versus loading rates in the FBB for Experiment FBB2 using polycarbonate particles. | 84 |
| Figure 5.9: | DNT degradation rates versus loading rates for Experiment FBB3 with polycarbonate particles. | 85 |
| Figure 5.10: | Comparison of the fluidized-bed bioreactor experiments to previous experiments in a packed-bed with recycle system. | 86 |
| Figure 5.11: | SEM of the polycarbonate particles without bacteria attached. | 89 |
| Figure 5.12: | SEM of <i>Psuedomonas</i> PR7 bacteria attached to the surface of a polycarbonate particle that was incubated in an unshaken test tube of DNT and SMSB. | 89 |
| Figure 5.13: | SEM of <i>Psuedomonas</i> PR7 bacteria attached to the surface of a polycarbonate particle that was from the fluidized-bed bioreactor while growing on DNT. | 90 |
| Figure A3.1 | Calibration of DNT concentration versus absorption peak response at $\lambda = 230$ nm from HPLC analysis. | 108 |
| Figure A3.2 | Calibration of MNC concentration versus absorption peak response at $\lambda = 230$ nm from HPLC analysis. | 110 |
| Figure A3.3 | Calibration of nitrite ion concentration versus absorption at $\lambda = 543$ nm. | 112 |
| Figure A3.4 | Calibration of BCA method with protein concentration versus absorption at $\lambda = 562$ nm. | 114 |

TABLE OF CONTENTS

| | |
|--|-----------|
| Chapter I INTRODUCTION | 1 |
| 1.1 Problem Definition and Scope..... | 1 |
| 1.2 Research Goals..... | 2 |
| Chapter II BACKGROUND INFORMATION | 4 |
| 2.1 Toxicity of DNT | 4 |
| 2.2 Biodegradation of Xenobiotic Compounds..... | 5 |
| 2.3 Biodegradation of Nitroaromatics | 6 |
| 2.3.1 Biodegradation of Polar Nitroaromatics..... | 7 |
| 2.3.2 Biodegradation of Nonpolar Nitroaromatics..... | 9 |
| 2.3.3 Enzyme Systems in Oxidative Biodegradation | 10 |
| 2.3.4 Enzyme Systems in Oxidative Biodegradation of DNT | 11 |
| 2.4 Biodegradation Kinetics | 14 |
| 2.4.1 Modeling the Metabolism of a Substrate..... | 14 |
| 2.4.2 Biodegradation Kinetics for 2,4-Dinitrotoluene..... | 16 |
| 2.5 Bioreactor Types..... | 17 |
| 2.5.1 Immobilized versus Suspended Cells..... | 17 |
| 2.5.2 Chemostats (CSTRs) and Batch Bioreactors | 18 |
| 2.5.3 Packed Bed Bioreactors | 18 |
| 2.5.4 Fluidized-Bed Reactors..... | 20 |
| 2.5.5 Fluidized- versus Packed-Bed Reactors..... | 20 |
| 2.6 Immobilized Cells..... | 21 |
| 2.6.1 Types of Immobilized Cell Aggregates..... | 21 |
| 2.6.2 Immobilized Cells and Substrate Utilization | 23 |
| 2.6.3 External Mass Transfer | 25 |
| 2.6.4 Internal Mass Transfer Considerations..... | 29 |
| 2.7 Fluidized Bed Reactor..... | 33 |
| 2.7.1 Fluidization of Particles..... | 35 |
| Chapter III METHODS AND MATERIALS..... | 39 |
| 3.1 Microorganism..... | 40 |
| 3.2 Inocula..... | 41 |
| 3.3 DNT Recrystallization | 42 |
| 3.4 Media..... | 43 |
| 3.5 Batch Shake Flask Experiments..... | 43 |
| 3.6 Batch Stirred-Tank Bioreactor Experiments | 44 |
| 3.7 Fluidized-Bed Bioreactor..... | 45 |
| 3.7.1 Diatomaceous-Earth Particle Experiments..... | 46 |
| 3.7.2 Plastic Particle Experiments..... | 48 |
| 3.8 DNT and MNC Analyses | 49 |
| 3.9 Nitrite Analysis..... | 51 |
| 3.10 Cell Concentrations/Absorbance..... | 53 |
| 3.11 Residence Time Distribution (RTD) Analysis..... | 58 |

| | |
|--|-----|
| Chapter IV SUSPENDED-CELL EXPERIMENTAL RESULTS & DISCUSSION: Intrinsic Kinetics of Biodegradation of 2,4-DNT by <i>Pseudomonas</i> PR7 | 59 |
| 4.1 Batch Shake-Flask Experiments..... | 59 |
| 4.1.1 Results..... | 59 |
| 4.1.2 Analysis and Discussion..... | 63 |
| 4.1.3 Qualitative Results Observed..... | 66 |
| 4.2 Batch Stirred-Tank Bioreactor Experiments | 68 |
| 4.2.1 Results..... | 68 |
| 4.2.2 Analysis and Discussion..... | 69 |
| 4.3 Conclusions..... | 74 |
| Chapter V FLUIDIZED-BED BIOREACTOR RESULTS & DISCUSSION | 76 |
| 5.1 Mixing Analysis | 76 |
| 5.1.1 Results..... | 76 |
| 5.1.2 Analysis and Discussion..... | 77 |
| 5.2 DNT Degradation Experiments | 79 |
| 5.2.1 Results..... | 79 |
| 5.2.2 Analysis and Discussion..... | 83 |
| 5.3 Mass Transfer Considerations..... | 86 |
| 5.4 Conclusions..... | 90 |
| Chapter VI SUMMARY..... | 93 |
| References..... | 96 |
| Appendix I: Physical Properties of DNT and Other Nitroaromatics | 104 |
| Appendix II: Preparation of Spain's Mineral Salts Base..... | 105 |
| Appendix III: Calibrations of Analytical Methods..... | 107 |
| Appendix IV: SimuSolv™ Modeling and Simulation Software: user program and example of input data file | 115 |

Chapter I INTRODUCTION

1.1 Problem Definition and Scope

A class of pollutants that has caused a great deal of concern through the past several decades is the nitroaromatics. Many are readily absorbed through the skin and their toxic effects often target the blood, kidneys and liver. They are recalcitrant, meaning that they are resistant to natural means of degradation such as photodegradation or biodegradation when left in the environment. Because most of these compounds are toxic and have carcinogenic and mutagenic effects, many research projects have investigated treatment methods for nitroaromatics.

2,4-Dinitrotoluene (DNT) is a nitroaromatic compound that is listed as a priority pollutant by the U. S. Environmental Protection Agency (U.S. EPA). DNT is a major by-product of the production of 2,4,6-trinitrotoluene (TNT) as well as the starting material for a reagent used in the production of polyurethane foams. It is also used in the manufacture of some types of dyes and is therefore found in many industrial waste streams and has become a concern due to its toxicity and carcinogenicity. Problems with contamination of soil by DNT have arisen at various military and industrial sites. The inclusion of DNT in industrial waste streams is often undesirable or unfeasible because it can be difficult to treat via conventional water treatment methods and is toxic to many activated sludge systems in relatively low concentrations. A sudden spike of DNT in an influent wastewater stream can cause a decline in population and degradative activity of the activated-sludge.

For these reasons, investigations into alternative methods of treatment for DNT are important.

1.2 Research Goals

In this work, the degradative ability of the bacterium *Pseudomonas* PR7 was studied. Specifically, the kinetics of the metabolism of 2,4-dinitrotoluene by *Pseudomonas* PR7 (*P. PR7*) was studied in suspended-cell batch cultures with varying initial DNT concentrations. The growth of *P. PR7* on DNT is slow, such that a continuously fed culture of the bacteria must be operated at a low flow rate in order to ensure that the bacteria are not washed out of the reactor before they have had time to duplicate themselves.

Retaining a significantly active population within a bioreactor while operating at reasonably high flow rates is desirable, and can become challenging when dealing with slow-growing bacteria or minimal growth promoting conditions. Immobilization of cells onto the surface of a solid matrix such as glass, activated carbon, or even plastic is one method of increasing the retention of cells within a bioreactor. The use of immobilized cells is widespread throughout the fields of biotechnology and biochemical engineering. In addition to suspended *P. PR7* cells, immobilized *P. PR7* cells were used in this work to assess the biodegradative ability of the strain in treating aqueous DNT.

The goals of this study were to characterize the intrinsic kinetics of the biodegradation of DNT by *Pseudomonas* PR7 and to study the performance of a three-phase fluidized-bed bioreactor containing immobilized *P. PR7*.

The research goals were accomplished in the following manner:

- The kinetics of the biodegradation of DNT by *Pseudomonas* PR7 were studied using batch suspended-cell (SC) shake-flask and fermentor experiments with varying initial DNT concentrations.
- The performance of the bacteria in an immobilized-cell (IC) fluidized-bed bioreactor (FBB) was studied in continuous experiments in which the dilution rate and the inlet DNT concentration were varied.
- Volumetric degradation rates of DNT in SC continuous, IC packed-bed, and IC fluidized-bed experiments were used as a basis for the comparison of the different reactor schemes.

Chapter II BACKGROUND INFORMATION

2.1 *Toxicity of DNT*

The isomers of dinitrotoluene (2,4-dinitrotoluene, 2,6-dinitrotoluene, 2,3-dinitrotoluene, etc.) have been reported to cause hepatobiliary (liver) cancer in mammals by several sources (Sax and Lewis 1987; 1993; Stayner, Dannenberg et al. 1992). The carcinogen is also thought to cause ischemic cardiovascular disease in humans.

Chronic feeding studies in rats using technical grade DNT (mainly 2,4- and 2,6-dinitrotoluene) have demonstrated a statistically significant increase in the incidence of hepatocarcinomas (cancerous liver cells), bile duct carcinomas, and subcutaneous fibrosarcomas. A significant excess of hepatocellular carcinomas has been reported in rats fed the purified 2,6-DNT isomer, whereas similarly designed studies using the purified 2,4-DNT isomer resulted in a statistically significant excess of liver cancer in one study and no significant excess of liver cancer in two other studies (Stayner, Dannenberg et al. 1993). The potential for the 2,4-DNT isomer to cause cancer may be lower than for the 2,6-DNT isomer, but the 2,4-DNT isomer is never the less a potential carcinogen and should be handled with great care and proper protective clothing. An excess of hepatobiliary cancer was observed among workers exposed to DNT in a study by Stayner and coworkers. This excess was reported to be nearly statistically significant based upon the U.S. population, and was reported to be statistically significant based upon a more relevant comparison with an internal reference group (Stayner, Dannenberg et al. 1993). The excess in hepatobiliary cancer mortality found among DNT-

exposed workers in the study is similar to the findings from experimental studies of DNT-exposed animals.

The personal exposure limit (PEL) set forth by OSHA for 2,4-dinitrotoluene exposure is 1500 $\mu\text{g}/\text{m}^3$ (skin). The ACGIH threshold limit value (TLV) is a time-weighted average (TWA) of 1.5 mg/m³. 2,4-Dinitrotoluene is a poison by ingestion and by the subcutaneous route. It is an experimental carcinogen and neoplastigen (an agent which causes neoplasia, the abnormal state of cells characterized by the growth and development of tumors, especially malignant tumors) as well as an irritant and an allergen. It can cause anemia, methemoglobinemia, cyanosis, and liver damage. When heated to decomposition, it emits toxic fumes of NO_x (Sax and Lewis 1987). It is therefore not a good candidate for incineration. Physical properties of DNT and other nitroaromatic compounds are found in Appendix I.

2.2 Biodegradation of Xenobiotic Compounds

Biodegradation refers to the microbiological transformation of, and in some cases growth on, organic pollutants. Microorganisms have been exposed to aromatic hydrocarbons like benzene and toluene for millions of years. It is a reasonable hypothesis that many microorganisms have therefore developed the enzyme systems necessary to metabolize these and similar compounds into innocuous compounds and biomass. Most naturally occurring organic compounds can be degraded by some microorganism. *Burkholderia cepacia* alone is known to use over 100 carbon compounds (Prescott, Harley et al. 1993). The fact that many microorganisms are capable of degrading a wide variety of naturally occurring organic compounds helped spark the widespread realization that man-made compounds may also be

degraded by microorganisms. However, many man-made compounds which have only been present for an instant on the evolutionary time scale are foreign to the biosphere. These compounds, termed xenobiotics, are not always as easily transformed by organisms in the biosphere. But fortunately some are similar enough to natural compounds that upon exposure over a long enough period of time, microorganisms may evolve the enzyme systems necessary to degrade some of these xenobiotics.

Bioremediation is the use of biodegradation for the remediation of sites contaminated with hazardous organics. Field tests at various contaminated sites have demonstrated that bioremediation can be used to remediate contamination and that it can be more economical than remediation technologies such as soil vapor extraction, excavation, and incineration. Microorganisms are increasingly being studied and used for bioremediation. Applications include bioreactors of various configurations, composting, and in situ treatment through the introduction of microorganisms and nutrients into the soil.

2.3 Biodegradation of Nitroaromatics

Enzyme systems that oxygenate the aromatic ring have shown an ability to oxygenate the nitroaromatic ring of 2,4-dinitrotoluene. Several microorganisms are known to degrade DNT, but most do so reductively rather than oxidatively. This results in the formation of amino, azoxy, or nitroso compounds that are difficult to further degrade (Liu, Thomson et al. 1984; McCormick, Cornell et al. 1978; McCormick, Feeherry et al. 1976). The study and use of oxidative biodegradation of nitroaromatics has been reported in the literature, but not to the extent that reductive biodegradation has been. Therefore it is important to explore the oxidative biodegradation of

nitroaromatic compounds further. It has been reported that *Phanerochaete chrysosporium*, a lignin-degrading fungus, degrades DNT to carbon dioxide and water by first reducing one nitro group to an amine, and subsequently removing both nitro groups via reactions involving peroxidase enzymes (Valli, Brock et al. 1992). In contrast, the bacterium *Pseudomonas* PR7 utilizes dioxygenase and monooxygenase systems to metabolize 2,4-dinitrotoluene, oxidatively opening the aromatic ring rather than reducing it. Table 2.1 lists several known degraders of DNT and other nitroaromatic compounds.

2.3.1 Biodegradation of Polar Nitroaromatics

When studying the kinetics of biodegradation of a specific compound by a microorganism, knowledge of the pathway and any intermediates involved is an asset. As evidenced in Table 2.1, the biodegradation of polar nitroaromatic compounds by bacteria has been studied in a number of isolated pure cultures. *p*-Nitrophenol (Spain, Wyss et al. 1979) and *o*-nitrophenol (Zeyer and Kearney 1984) undergo an initial attack by a monooxygenase which results in the release of nitrite and the formation of the corresponding dihydroxy compound. In contrast, *m*-nitrophenol is first reduced to the corresponding aminophenol, which is further degraded by an unknown mechanism (Zeyer and Kearney 1984). 3,5-Dinitro-2-methylphenol (dinitro-*o*-cresol) can be degraded via either the oxidative (Gundersen and Jensen 1956) or the reductive route (Tewfik and Evans 1966). Nitrobenzoates appear to be degraded primarily by the oxidative pathway (1958; Cain 1966).

Table 2.1: Microorganisms that degrade DNT and other nitroaromatic compounds.

| <u>Compound</u> | <u>Microorganism</u> | <u>Mode of degradation</u> | <u>Reference</u> |
|---|---|--------------------------------------|---|
| Several nitroaromatics | Sewage microorganisms | reductive | (Hallas and Alexander 1983) |
| <i>m</i> -dinitrobenzene | 16 bacterial and fungal strains | aerobic conditions | (Dey, Kanekar et al. 1986) |
| nitro-compounds | Soil bacterium | | (Gundersen and Jensen 1956) |
| 3,5-dinitro- <i>o</i> -cresol | Soil microorganisms | reductive | (Tewfik and Evans 1966) |
| <i>o</i> -nitrophenol | <i>Pseudomonas putida</i> | oxidative | (Zeyer and Kearney 1984) |
| <i>m</i> -nitrophenol | <i>Pseudomonas putida</i> | reductive (1st step known) | (Zeyer and Kearney 1984) |
| <i>p</i> -nitrophenol | <i>Pseudomonas putida</i> | oxidative | (Spain, Wyss et al. 1979) |
| 2,6-dinitrophenol | <i>Alcaligenes eutrophus</i> | | (Ecker, Knackmuss et al. 1989) |
| nitrobenzoates | | oxidative | (Cain 1958; Cain 1966) |
| several mono- and dinitroaromatic compounds | <i>Clostridia</i> , sulfate-reducing, and methanogenic bacteria | reductive | (Gorontzy, Kuver et al. 1993) |
| 2-nitrotoluene | <i>Pseudomonas JS42</i> | oxidative | (An, Gibson et al. 1994) |
| TNT and other nitroaromatics | Mixed culture | reductive | (McCormick, Feeherry et al. 1976) |
| DNT | Mixed culture | 1 | (McCormick, Cornell et al. 1978) |
| DNT | Mixed culture | reductive | (Liu, Thomson et al. 1984) |
| TNT | Mixed culture | aerobic conditions | (Kulpa and Wilson 1991) |
| DNT | <i>Phanerochaete chrysosporium</i> | reductive and oxidative | (Valli, Brock et al. 1992) |
| TNT | <i>Phanerochaete chrysosporium</i> | aerobic conditions, nitrite released | (Fernando, Bumpus et al. 1990) |
| TNT | <i>Pseudomonas</i> species | nitrite released | (Unkefer, Alvarez et al. 1990) |
| TNT | <i>Pseudomonas fluorescens</i> | reductive | (Spain, Wyss et al. 1979) |
| DNT | <i>Pseudomonas</i> DNT | oxidative | (Spanggord, Spain et al. 1991; Suen and Spain 1993) |
| DNT | <i>Pseudomonas PR7</i> | oxidative | (Reardon and Spain 1995) this work |

2.3.2 Biodegradation of Nonpolar Nitroaromatics

Nonpolar nitroaromatics such as nitrobenzene and the nitrotoluenes are more resistant to microbial attack. Early work suggested that reduction was the primary reaction mediated by microorganisms. McCormick et al. (McCormick, Cornell et al. 1978; 1976) identified azoxy compounds and amino derivatives from the biotransformation of di- and trinitrotoluenes and Liu et al. (Liu, Thomson et al. 1984) identified amino and nitroso compounds from anaerobic biotransformation of DNT. Similarly, nitrobenzenes and nitrotoluenes were reduced in sewage (Hallas and Alexander 1983). However, none of the reduction products seemed to be further degraded, and in many instances they were more toxic than the parent nitro compounds. Dey and coworkers reported the isolation of 16 bacterial and fungal strains that were able to degrade *m*-dinitrobenzene (Dey, Kanekar et al. 1986). Several isolates able to degrade TNT by a reductive pathway were reported (Neumeier, Haas et al. 1989). Gorontzy and coworkers found that although growing cells of sulfate-reducing bacteria and *Clostridium* spp. carried out nitroreduction, methanogenic cells lysed in the presence of nitroaromatic compounds. Nevertheless, these suspensions of lysed methanogens converted nitroaromatics to the corresponding amino derivatives. Some of the nitroaromatics tested were transformed chemically by 1.5 mM quantities of culture media reducing agents like cysteine or sulfide (Gorontzy, Kuver et al. 1993).

In the past five to eight years, work from several laboratories has shown that nitrotoluenes can be biodegraded by an oxidative pathway. *Phanerochaete chrysosporium* completely mineralized TNT by an unknown mechanism under aerobic conditions (Fernando, Bumpus et al. 1990). Unkefer and coworkers isolated a *Pseudomonas* species that mineralizes TNT

with concomitant release of nitrite (Unkefer, Alvarez et al. 1990). Kulpa and coworkers have studied the aerobic degradation of TNT by a mixed culture (Kulpa and Wilson 1991). More recently, An and coworkers (An, Gibson et al. 1994) have reported on the oxidation of 2-nitrotoluene (2-NT) to 3-methylcatechol and nitrite by a new multicomponent enzyme system which they have designated 2NT 2,3-dioxygenase, utilized by *Pseudomonas* sp. strain JS42. The 3-methylcatechol is subsequently degraded by the *meta* ring fission pathway. These studies have created the framework upon which further investigations into the oxidative biodegradation of nitroaromatic compounds can be based.

2.3.3 Enzyme Systems in Oxidative Biodegradation

Pseudomonas PR7 was chosen for use in this study because of its ability to degrade 2,4-dinitrotoluene oxidatively and its similarity to the previously studied biodegradation pathway and enzyme systems of *Pseudomonas* DNT.

Pseudomonas PR7 belongs to a group of microorganisms known as the pseudomonads. Two important characteristics of pseudomonads are the relative nonspecificity of many of the induced enzyme systems and the convergence of pollutant degradation pathways. The nonspecificity of the induced enzymes allows for the simultaneous utilization of several similar substrates without an excess of redundant genetic coding for enzyme induction. The convergence of catabolic pathways allows for the efficient utilization of a wide range of growth substrates (Hutchinson and Robinson 1988).

In the metabolism of aromatic compounds, there are generally two types of enzyme systems induced: enzymes that incorporate one atom of molecular oxygen into an organic substrate, the monooxygenases, and

enzymes that incorporate two atoms of molecular oxygen, the dioxygenases (Spain, Zylstra et al. 1989). The enzymes synthesized for aromatic ring cleavage, either *meta*, *ortho*, or modified *ortho*, are most likely induced by a specific type of substrate. *Meta* ring fission occurs between the two and three positions on an aromatic ring and is generally active in the degradation of methyl-substituted aromatic substrates such as toluene. *Ortho* ring cleavage occurs between the one and two positions on an aromatic ring and is generally active in the degradation of halogen-substituted aromatic substrates. In the absence of *meta* cleavage pathway enzymes, an aromatic compound that would be more efficiently degraded by the *meta* pathway may be transformed by the modified *ortho* cleavage pathway instead. The modified *ortho* pathway involves less specific enzymes and cleaves the ring in the same manner as the *ortho* pathway (Haigler and Spain 1991).

A particular primary substrate is often responsible for inducing a large segment of an enzyme system, explaining why enzymes of only one pathway are synthesized during growth on a particular substrate even though a common intermediate for the various ring cleavage systems may be formed (Feist and Hegeman 1969). Of the three ring cleavage pathways, the *meta* pathway appears to have the least amount of specificity. Some researchers have suggested that this pathway came about through evolution in the catabolism of a wide variety of aromatic derivatives that presumably arose during the degradation of natural products (Feist and Hegeman 1969).

2.3.4 Enzyme Systems in Oxidative Biodegradation of DNT

In 1991, Spain and coworkers reported on the isolation and characterization of a *Pseudomonas* strain capable of using DNT as the sole source of carbon and energy (Spanggord, Spain et al. 1991). They also

presented evidence that the oxidative pathway of biodegradation involved dioxygenase and monooxygenase enzyme systems. The previously studied pathway by which degradation of DNT by *Pseudomonas* DNT occurs (Figure 2.1) has been very useful in this work because *P. PR7* is thought to follow the same pathway when degrading DNT.

The initial step in this pathway is an attack on DNT by a dioxygenase enzyme system (*dntA*) which results in the release of one nitrite group and

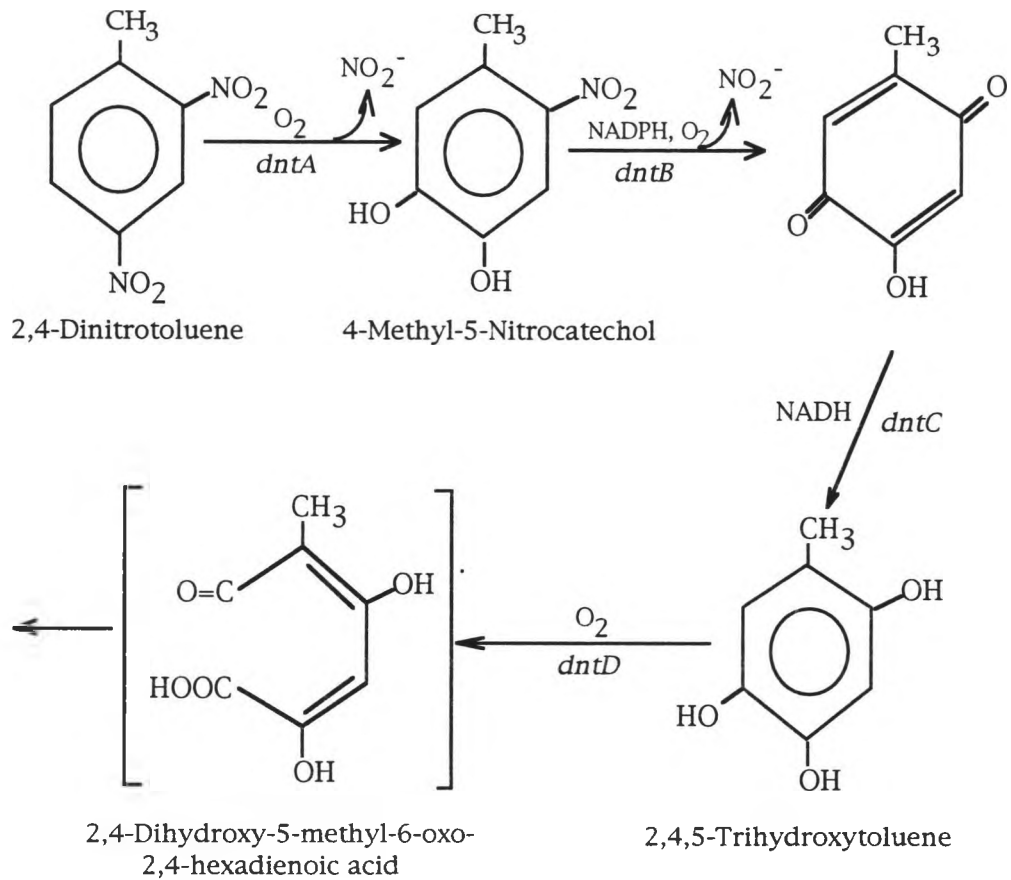


Figure 2.1: Metabolic pathway for the oxidative biodegradation of 2,4-dinitrotoluene by *Pseudomonas* DNT (Suen and Spain 1993). Enzyme systems involved are *dntA*, *dntB*, *dntC*, and *dntD*.

the formation of a bright yellow intermediate, 4-methyl-5-nitrocatechol (MNC) (Spanggord, Spain et al. 1991). A monooxygenase (*dntB*) system then catalyzes the oxidation of MNC to 2-hydroxy-5-methylquinone (HMQ) and nitrite. A quinone reductase (*dntC*) and 2,4,5-trihydroxytoluene oxygenase (*dntD*) catalyze further reactions to result in colorless ring fission products (Suen and Spain 1993). Because there is a transient accumulation of MNC and HMQ, the induction of the enzyme systems for DNT degradation is thought to be sequential. Further evidence indicating that the genes for DNT degradation are organized in three different operons supports this theory. However, in *Pseudomonas* PR7, induction of enzymes following initial dioxygenase attack appears to be simultaneous (Nishino 1994). There is a transient accumulation of MNC but no apparent accumulation of HMQ, suggesting that enzyme systems are induced simultaneously once MNC is produced.

Suen and Spain reported on the molecular basis of DNT degradation by the strain DNT. For that purpose, they cloned and characterized the genes for DNT degradation from *Pseudomonas* DNT. Initial studies revealed the presence of three plasmids. Mitomycin-derived mutants, which were deficient in either the DNT dioxygenase only or in both DNT dioxygenase and MNC monooxygenase, were isolated. Total plasmid DNA partially digested by *Eco*RI was cloned into a broad-host-range cosmid vector, pCP13. Recombinant clones containing genes encoding DNT dioxygenase, MNC monooxygenase, and 2,4,5-trihydroxytoluene oxygenase were characterized by identification of reaction products and the ability to complement mutants. Subcloning analysis suggested that the DNT dioxygenase is a multi-component enzyme system and that the genes for the DNT pathway are organized in at least three different operons. Although there are many

reports on the biochemical studies of nitroaromatic degradation, this was the first report on the genetic analysis of pathways involved in the removal of aromatic nitro groups (Suen and Spain 1993). Therefore, the three *Pseudomonas* strains studied by Spain and coworkers (DNT, R34, and PR7) are the most fully-characterized and documented bacterial strains that are known to degrade DNT oxidatively.

2.4 Biodegradation Kinetics

Knowledge of the kinetics of degradation is necessary for the design of reactor systems and for the prediction of system behavior as well as for the design and analysis of nonbioreactor bioremediation systems. The length of time required for the remediation of waste stores or contaminated sites must usually be estimated and has bearing on the cost of and feasibility of cleanup. Therefore sound models of the biodegradative processes involved are essential.

2.4.1 Modeling the Metabolism of a Substrate

Microbial growth in any system is a very complex phenomenon. However, the overall growth can often be regarded as a single chemical reaction with a simple rate expression. Although many equations could describe this rate of reaction, the simplest and most accepted is that proposed by Monod (Bailey and Ollis 1986). Monod assumed that a single essential substrate is the growth limiting factor (Monod 1942). The reaction can be described by:



and the Monod equation is expressed as:

$$\frac{1}{X} \frac{dX}{dt} = \mu = \frac{\mu_{\max} S}{K_s + S} \quad (2.2)$$

And because this limiting substrate is assumed to be utilized only for biomass production, the rate of substrate uptake can be written:

$$-\frac{dS}{dt} = \mu \left(\frac{X}{Y_{x/s}} \right) \quad (2.3)$$

In these equations, μ is the specific growth rate (the rate of production of new cells per unit time divided by concentration of cells at any time), μ_{\max} is the maximum specific growth rate, K_s is the Monod half-saturation constant, $Y_{x/s}$ is the yield of cells per amount of substrate consumed, and S is the substrate concentration. To describe the degradation kinetics of a specific substrate, it is necessary to determine the values of μ_{\max} , K_s , and $Y_{x/s}$. Methods of estimating the values of these parameters include linearized methods such as those of Lineweaver-Burk and Eadie-Hofstee (Bailey and Ollis 1986). Another method, described by Robinson and Tiedje (1983), is to fit the sigmoidal substrate depletion versus time data to the integrated Monod equation.

The Monod model is inherently simplistic and therefore has been used successfully to describe the growth kinetics of many different microorganisms. It does not, however, account for substrate inhibition and consequently may be unreliable when describing biodegradation kinetics at high concentrations of substrate. The Haldane equation is a modification of the Monod equation that accounts for inhibition by the substrate:

$$\mu = \frac{\mu_{\max} S}{K_s + S + \left(\frac{S^2}{K_i} \right)} \quad (2.4)$$

where K_i represents the substrate inhibition term. Similar expressions have been developed for inhibition of cell growth and substrate consumption by toxic or otherwise inhibitory products of substrate metabolism.

Yoshinaga, Hendricks, and Klein compiled data sets for microbial growth kinetics for natural and synthetic organics from six journals over the period 1965-1994. They found that for aerobic degradation, the Monod coefficients were as follows: μ_{\max} fell in the range of 0 - 0.8 h⁻¹ with an average of 0.21 h⁻¹, K_s fell in the range of 0 - 42 mg substrate/L with an average of 5.8 mg/L, and $Y_{x/s}$ fell in the range of about 0.01 - 0.98 g cells/g substrate with an average of 0.31g cells/g substrate (Yoshinaga, Hendricks et al. 1995). They also found that for growth of activated sludge on 26 different xenobiotic compounds the range of μ_{\max} was 0.1 - 0.54 h⁻¹ with an average of 0.25 h⁻¹, the range of K_s was 0.75 - 29 mg substrate/L with an average of 7.6 mg/L and the range of $Y_{x/s}$ was 0.22 - 0.62 g cells/g substrate with an average of 0.38 g cells/g substrate.

2.4.2 Biodegradation Kinetics for 2,4-Dinitrotoluene

The intrinsic kinetics of DNT metabolism by *P. PR7* were studied previously (Reardon 1992; 1995) . The kinetic parameters μ_{\max} and K_s were estimated to be 0.11 h⁻¹ and 34 μM (6.2 mg/L) respectively, from data obtained from continuous experiments. These results were obtained from continuous cultures grown in Spain's Mineral Salts Base (SMSB) and varied DNT feed rates at 32 °C, 250 RPM, and unadjusted pH (SMSB is pH 6.7 - 6.8).

2.5 Bioreactor Types

There are many different types of bioreactors which can be used for bioremediation. With respect to flow in and out of the reactor, however, there are three basic modes of operation: continuous, fed-batch, or batch. There are also two ideal types of mixing in reactors. One type is perfectly well mixed and the other is perfectly unmixed, or plug flow. Real bioreactors fall somewhere in between these two ideals. Well mixed reactors can be operated in any of the three modes, whereas plug flow reactors are generally only operated under continuous flow (although they can be batch or fed batch). Each of the types of reactors and flow modes offer their own advantages and disadvantages, and each can be applied to a biological or biochemical process. Any given biological process is better suited to one or a few reactor schemes, and the fundamentals behind reactor design should be used in designing a reactor system to optimize the biodegradation of DNT.

2.5.1 Immobilized versus Suspended Cells

A survey of the literature has shown that immobilized-cell bioreactors often perform more efficiently than suspended-cell continuous reactors. This has been attributed to many factors, including:

- (1) Immobilized cells are not susceptible to wash-out at dilution rates above their maximum specific growth rate, whereas suspended cells are.
- (2) A greater concentration of cells can therefore be achieved in reactors using immobilized cells.
- (3) Immobilized cells are usually able to adapt to environmental changes in variables such as pH and substrate concentration more easily than suspended cells.

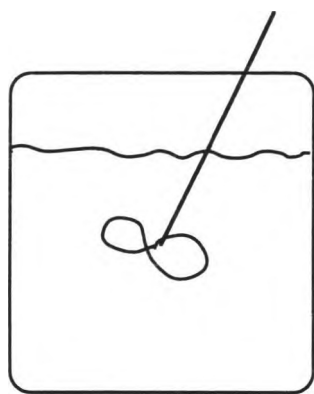
- (4) Immobilized cells are therefore more resistant to or better able to recover from shock loadings.
- (5) The immobilization medium may encourage adsorption of substrate, making it more available to the cells for consumption or degradation.

2.5.2 Chemostats (CSTRs) and Batch Bioreactors

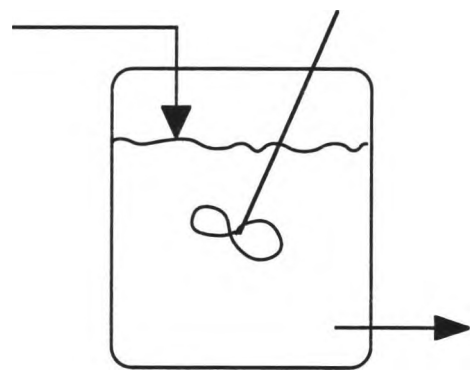
Many industrial biochemical processes are performed in batch processes due to the stringent quality control requirements of the pharmaceutical and food industries. Batch processes allow product tracking through batch or lot numbers. It also provides for shutdown and reactor cleaning and sterilizing at regular intervals. Although perfect mixing is difficult to obtain on a large scale, good mixing offers the advantages of distribution of substrate, increased oxygen availability, and dilution of toxic products.

2.5.3 Packed Bed Bioreactors

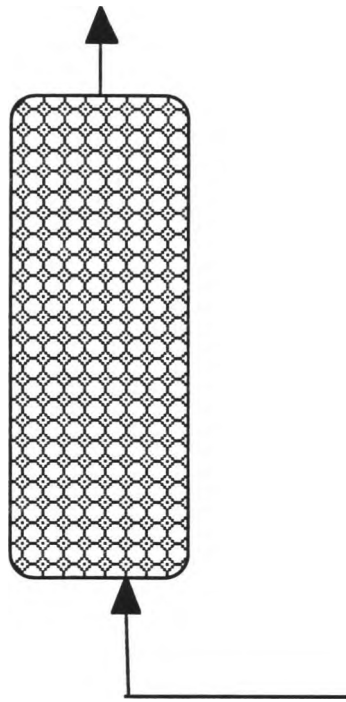
The use of columns packed with immobilized biocatalyst particles is applicable to many biochemical processes, examples of which are: glucose isomerization, selective penicillin hydrolysis, selective separation of proteins, and biodegradation of wastes. Many applications currently exist and new ones are developing rapidly. Packed-bed or fixed-bed reactor configurations are used with both immobilized enzymes and immobilized cells. Such reactors are advantageous because the biocatalyst is retained within the reactor rather than washed out with the reaction solution. Therefore immobilization offers the option of a continuous process rather than a conventional batch reactor. A continuous process simplifies separation techniques and often improves the utilization of feed stocks and biocatalysts.



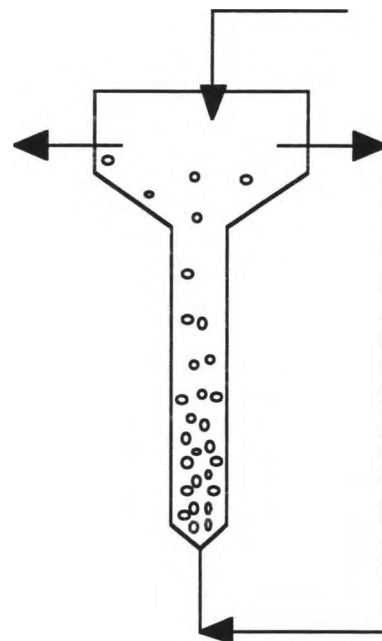
Batch Stirred Tank



Continuous Stirred Tank



Packed-Bed Bioreactor



Fluidized-Bed Bioreactor

Figure 2.2 Schematic diagrams of bioreactor types discussed in Section 2.5.

2.5.4 Fluidized-Bed Reactors

Liquid-air-solid, or three-phase, fluidized-bed reactors may fall under many categories depending upon the nature of the flows of each of the phases. The immobilized cells or enzymes make up the solid phase in fluidized-bed bioreactors. The use of air for fluidization provides an oxygen source to cells. The use of a nonoxygenated gas such as nitrogen provides a constant purge of oxygen for anaerobic processes. The bioreactor used in this study is a cocurrent upflow reactor in which the flows of liquid and of air are in the same upward direction. The bed of solid particles is expanded by the buoyant forces of the liquid and the air.

2.5.5 Fluidized- versus Packed-Bed Reactors

Packed-bed column reactors using immobilized cells have been found to be useful in many instances. The volume required for a packed-bed reactor can be smaller than for a mixed-type reactor, depending upon kinetics and desired effluent concentration. However, the depletion of oxygen, substrate, and nutrients as flow continues along the column can limit activity. In addition, high substrate concentrations at the inlet can be detrimental when there is substrate inhibition. Changes in pH or accumulation of toxic products are additional factors that can cause a decline in productivity and even death of cells downstream from the column inlet.

Fluidized-bed reactors offer the advantages of both immobilized cells and good mixing. In the case of DNT degradation, improved mixing is desired to increase oxygen availability and to decrease effects due to nitrite concentration and pH changes. Also, because cells grow slowly on DNT, immobilization is desired to allow for higher flow rates through the reactor.

2.6 Immobilized Cells

Microorganisms as well as plant and mammalian cells may be immobilized for the purpose of stabilization, for retention in a bioreactor or for other reasons. Immobilization of cells by confinement to particles or surfaces eases the separation of cells from products in solution, and may allow the use of continuous reactors while avoiding washout. It may also allow reactors to contain more cells and therefore to have higher volumetric reaction rates. Two principle considerations in the choice of a biological catalyst are the difficulty and cost of producing the catalyst, and the ability to maintain the desired activity and specificity of the catalyst under reaction conditions (Karel, Libicki et al. 1985). With respect to the use of immobilized cells, we will therefore be concerned with specificity, activity, and longevity. An immobilized-cell composite should have an operating lifetime ranging from weeks to months if it is to be useful. The potential for long operating lifetimes are exceptionally good considering viable cells will reproduce under growth-promoting conditions. Therefore the biocatalysts can be regenerated, either continuously or periodically.

2.6.1 Types of Immobilized Cell Aggregates

There are various means of immobilization (Figures 2.3 & 2.4). Some examples are: encapsulation in alginate beads, polyacrylimide beads or other polymers; entrapment in the matrix of a porous material such as activated carbon, diatomaceous earth, or glass; adhesion to the surface of glass, sand, granular activated carbon, diatomaceous earth, or polymeric particles; and self aggregation such as yeast flocs or mycelial pellets formed under special conditions.

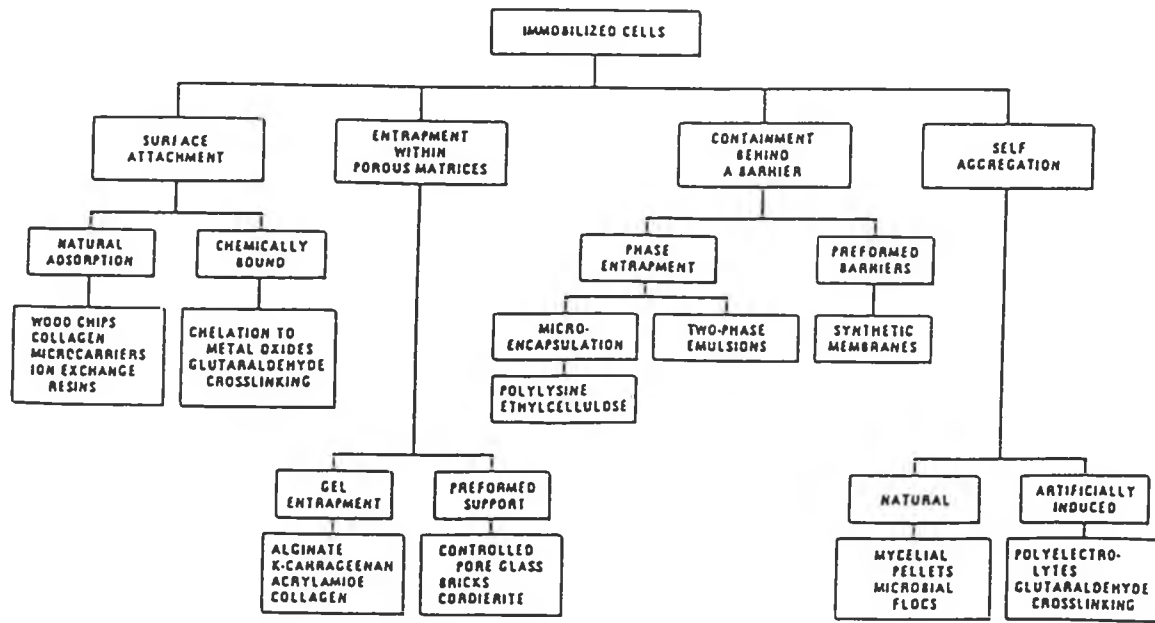
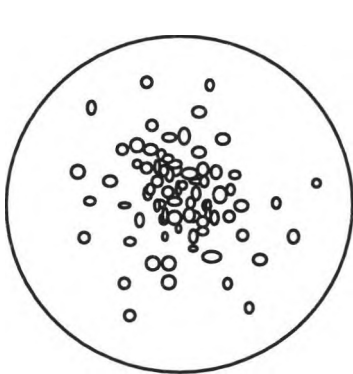


Figure 2.3: Various means by which cells might be immobilized (Karel, Libicki et al. 1985)

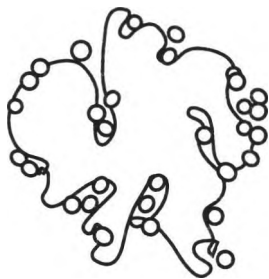
Particle sizes generally range from 1 to 5 mm in diameter for laboratory-scale systems utilizing bacterial cells. Mammalian cells are often immobilized on microcarriers in the micrometer size range which are usually surface treated with collagen or similar compounds that encourage attachment. The microcarriers are often stirred in a suspension or slurry. Fungal cells can be attached to wood chips or other particles or grown in an agitated vessel to form mycelial pellets. Some microorganisms, such as certain yeasts, will form flocs under special conditions, thus immobilizing themselves. Schematics of these methods of immobilization of cells are shown in Figure 2.4.



Entrapment within a gel
or behind a membrane



Attachment to the surface
of a particle



Attachment to and entrapment
within a porous matrix



Self aggregation or
self flocculation

Figure 2.4: Schematics of four general methods of cell immobilization.

2.6.2 *Immobilized Cells and Substrate Utilization*

In this work, bacterial cells were immobilized onto plastic particles or diatomaceous earth particles. Therefore the method of immobilization can best be described as attachment to a surface or within a porous matrix. In both instances, there is the likelihood that the formation of a biofilm occurs. When using immobilized cells for biodegradation, the diffusion of substrate to the biofilm where microbes can attack it must be considered. Also, it has

been asserted by several researchers that the intrinsic kinetics of the cells may change due to immobilization. According to Shreve and Vogel (1993), the phenomenon of changes in cellular activity upon immobilization has been well documented. They add that it remains unclear, however, whether the causes of these changes in cellular activity are due mainly to differences between an immobilized and suspended cell's physical and chemical environment, or to changes in the cellular physiology that are induced upon immobilization. Such changes raise speculation that immobilization may have a generalized effect on cellular metabolism (Shreve and Vogel 1993). It is also likely that a biofilm presents greater resistance to diffusion of substrate thus causing an apparent change in degradation kinetics. Conversely, weak adsorption of substrate to the particle matrix may make substrate more available to cells by bringing substrate in close vicinity to cells, causing an apparent increase in degradation kinetics. If the sorbed substrate is tightly bound to the particle, however, its availability to cells could be decreased. Increases in polysaccharides associated with the attachment process may also add error to estimates of biomass, again changing the apparent behavior of the biomass.

Shieh and Keenan (1986) describe substrate conversion in an immobilized-cell bioreactor such as a fluidized-bed bioreactor (FBB) in three steps (Figure 2.5):

1. transport of substrate from the bulk liquid to the liquid-biofilm interface (external mass transfer);
2. transport of substrate within the biofilm (internal mass transfer);
3. substrate conversion reactions within the biofilm.

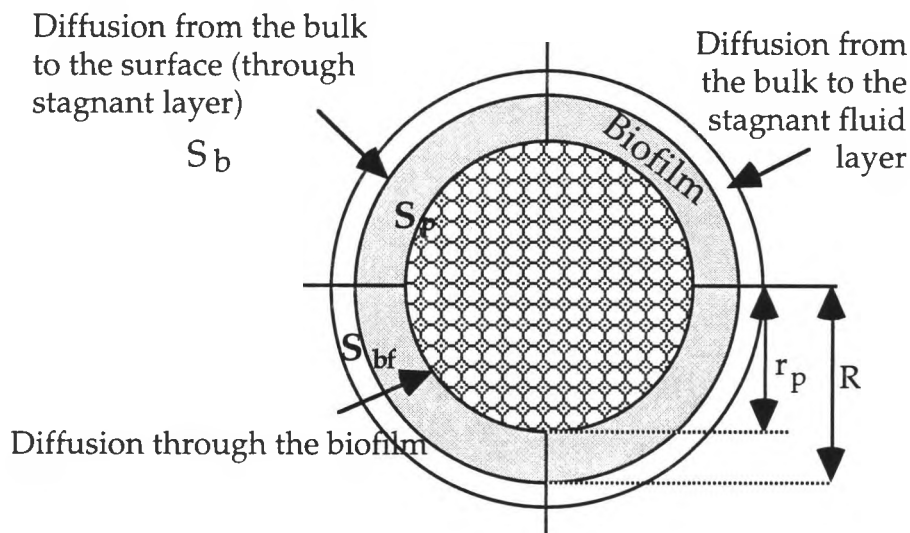


Figure 2.5: Representation of an immobilized-cell particle.

Using the assumption that steps 2 and 3 take place simultaneously whereas step 1 occurs in series with steps 2 and 3, Shieh and Keenan conclude that neither step 2 nor 3 can be said to be solely responsible for rate control. For intrinsic cell kinetics with a positive dependence on substrate concentration such as first-order, Monod, etc., the gradients established by external and internal mass transfer decrease the observed reaction rate by decreasing the local or intrabiofilm substrate concentration. For intrinsic zero-order kinetics, usually occurring with an excess substrate concentration, steps 1 and 2 can decrease the observed reaction rate by limiting substrate penetration into the biofilm (Shieh and Keenan 1986).

2.6.3 External Mass Transfer

Diffusion of the substrate through the stagnant fluid layer surrounding the immobilized-cell particle is referred to as external mass transfer. The flux

of substrate from bulk liquid to the stagnant layer and subsequently through the stagnant layer to the liquid-biofilm interface are usually accounted for using one mathematical expression. This is because the main resistance to diffusion of substrate is through the stagnant fluid layer, and it therefore dominates the overall rate. The expression describing the external diffusive flux to the interface is:

$$N_s = k_s(S_b - S_{bf}), \quad (2.5)$$

where N_s is the molar flux of substrate to the biofilm surface with respect to stationary coordinates, S_b is the bulk substrate concentration, S_{bf} is the substrate concentration at the liquid-biofilm interface, and k_s is the mass-transfer coefficient which is dependent upon hydrodynamic, physical, and substrate diffusional properties existing in the system. Because it describes both the convective and the diffusive transport of substrate, the mass-transfer coefficient k_s tends to increase with increasing flow and mixing in the system. The mass transfer coefficient can be evaluated through the use of correlations, such as the following correlation developed for use with fluidized beds (Shieh and Keenan 1986):

$$k_s = \frac{0.81}{\epsilon} \left[\frac{D^{4/3} U \rho_l^{1/3}}{\mu^{1/3} d_p} \right]^{1/2} \quad (2.6)$$

where ϵ is the bed porosity, D is the diffusivity of substrate in the bulk liquid, U is the superficial upflow velocity, ρ_l is the liquid density, μ is the dynamic viscosity of the liquid, and d_p is the bioparticle diameter. This equation was used by Shieh and Keenan (1986) to calculate the effect of external mass

transfer on observed denitrification rates in an FBB system because it was derived from experimentation at Reynolds numbers within the range common to fluidized bed bioreactor operation. A typical FBB external mass transfer coefficient calculated by Equation (2.6) is 0.01 cm/s. In their system, Shieh and Keenan determined that errors in the observed rate that resulted if external mass transfer effects were neglected ranged from 2.6 to 7.1% for bulk-liquid NO_3^- -N concentrations over the range 43 to 6 mg/L. They argued that errors of this magnitude are acceptable in light of the greatly simplified mathematics that result. Thus, external mass transfer was neglected in the development of their FBB kinetic model.

However, external mass transfer effects may be significant in other systems. Under steady-state conditions, substrate cannot accumulate at the particle interface, so the rate of mass transport to the biofilm surface must be balanced by the rate of degradation. Assuming Monod kinetics for substrate depletion, the rate of disappearance of substrate is described by Equation (2.3), which is related to the mass flux by Equation (2.7),

$$k_s(S_b - S_{bf}) = \mu \frac{X}{Y_{x/s} A_p} V_p = \mu_{\max} \frac{S_{bf}}{K_s + S_{bf}} \frac{X}{Y_{x/s} A_p} V_p. \quad (2.7)$$

V_p and A_p are the volume and the surface area of the particle.

With sufficient mixing, external diffusion occurs rapidly enough to not be the degradation-rate-limiting step (i.e. $S_{bf} \rightarrow S_b$, absence of stagnant layer), and the rate of degradation is controlled by either the rate of reaction within the biofilm or the rate of mass transfer in the biofilm. Assuming no rate limitations due to internal mass transfer, the effect of external mass transfer on the intrinsic reaction rate is commonly quantified by an effectiveness factor, defined here as:

$$\bar{\eta} = \left(\frac{\text{observed rate of reaction}}{\text{intrinsic reaction rate at bulk - liquid concentration}} \right) \quad (2.8)$$

The Damköhler II number (Da) can be used as a measure of the significance of external mass-transfer limitations. Assuming steady-state conditions once again and introducing the dimensionless variables $\xi = S_{bf}/S_b$ and $\kappa = K_s/S_b$ to equation (2.7) and rearranging yields:

$$\left(\frac{1-\xi}{\xi} \right) (\kappa + \xi) = \frac{\mu_{max} \left(\frac{X}{Y_{x/s}} \right) \left(\frac{V_p}{A_p} \right)}{k_s \cdot S_b} \quad (2.9)$$

The definition of the Damköhler II number is the right hand side of (2.9), and it can be defined physically as:

$$Da = \left(\frac{\text{maximum rate of reaction}}{\text{maximum rate of mass transfer}} \right) = \frac{\mu_{max} \left(\frac{X}{Y_{x/s}} \right) \left(\frac{V_p}{A_p} \right)}{k_s \cdot S_b} \quad (2.10)$$

If Da is very small, the maximum rate of mass transfer is much larger than the maximum rate of degradation. Thus reaction-rate limitation exists and is very significant. If Da is very large, then the slower mass-transfer rate dominates the process and mass transfer limitations are fairly significant, more so the further that Da is from 1. In order to evaluate Da , the intrinsic parameters μ_{max} and $Y_{x/s}$ must be known along with the external mass transfer coefficient k_s . To avoid the necessity of experimentally determining

values for μ_{max} and $Y_{x/s}$, an observable Damköhler number, Ω , can be used to assess the effects of external mass transfer on the degradation rate. The observable Damköhler number is a function of the effectiveness factor:

$$\Omega = \bar{\eta} Da = \frac{R_{obs}L}{k_s S_b} = \frac{\mu_{obs}}{k_s S_b} \quad (2.11)$$

where R_{obs} is the observed overall reaction rate, L is the particle characteristic length, V_p and A_p are the particle volume and surface area, and S_b is the bulk substrate concentration. When $\Omega \rightarrow 1$, the system is under external diffusion limitation. It is under reaction kinetics control when $\Omega \ll 1$.

It is easy to make the mistake of assuming that the observed rate of disappearance of substrate is the actual intrinsic rate of reaction. However, the observed rate is often a conglomerate of reaction kinetics and mass transfer effects. An "observed" specific growth rate μ_{obs}

$$\mu_{obs} = \mu_{max}S/(K_s + S) \quad (2.12)$$

is sometimes used to fit parameters. However, μ_{obs} is empirical and although it may represent data well, there are probably other hydrodynamic phenomena and fluid properties that are hidden in the parameters. To avoid this problem it is best to structure experiments for determining reaction rate data so that $\Omega \ll 1$ whenever feasible.

2.6.4 Internal Mass Transfer Considerations

Internal diffusion of substrate through the biofilm is assumed equal to degradation rate at steady-state. A steady-state mass balance on the shell of

biofilm on a spherical particle between r and $r+dr$ and subsequent simplification gives:

$$D_{es} \left[\frac{d^2 S}{dr^2} + \frac{2}{r} \frac{dS}{dr} \right] = \frac{\mu_{\max} S X}{(K_s + S) Y_{x/s}} \quad (2.13)$$

where D_{es} is the effective diffusivity of the substrate in the biofilm. D_{es} can be estimated through use of correlations and the diffusivity of the substrate in water. In the case of a dense biofilm, internal diffusion could be degradation rate limiting. To determine the extent to which internal mass transfer affects the overall rate (assuming no external mass transfer limitation), Equation 2.13 can be solved with the boundary conditions:

| | | |
|-----|--------------|-------------|
| | at $r = R$ | $S = S_b$ |
| | at $r = r_p$ | $dS/dt = 0$ |
| and | at $r = 0$ | $dS/dr = 0$ |

where r is the radius at any point within the biofilm-particle matrix, R is the radius of the entire biofilm-particle matrix, r_p is the radius of the particle without biofilm, and S is the substrate concentration at any r . The boundary conditions above imply that substrate concentration in the particle is symmetrical about the center, that at the particle-biofilm interface there is no change in substrate concentration with time and that at the center of the particle, there is no longer a concentration gradient.

In the case of internal mass transfer, the observed overall rate of substrate disappearance $R_{s,obs}$ is equal to the rate of mass transfer to the particle at steady state:

$$R_{s,obs} = (A_p/V_p)[D_{es}(dS/dr)_{r=R}], \quad (2.14)$$

where A_p is the particle external surface area and V_p is the particle volume.

Once again, an effectiveness factor η is introduced to evaluate the effect of diffusion on the overall rate:

$$\eta = \left(\frac{\text{observed rate}}{\text{rate which would be obtained with no concentration gradients within particle}} \right) \quad (2.15)$$

Unfortunately, η is difficult to evaluate analytically when the reaction rate takes the nonlinear form of Monod kinetics. It is necessary to solve the boundary-value problem posed by Equation (2.13) and its accompanying boundary conditions numerically and then to evaluate R_{obs} . It is necessary to transform the equations into equivalent dimensionless form in order to present as compact a solution as possible. Using v to represent $\mu(X/Y_{x/s})$, v_{max} to represent $\mu_{max}(X/Y_{x/s})$, ξ to represent S/S_b , and r to represent r/R , Equation (2.13) can be written as

$$\frac{d^2\xi}{dr^2} + \frac{2d\xi}{\bar{r}d\bar{r}} = \frac{vR^2}{DesSb} = 9\phi^2 \frac{\xi}{1 + \beta\xi} \quad (2.16)$$

Dimensionless parameters ϕ and β are defined by:

$$\phi = \frac{R}{3} \sqrt{\frac{v_{max}/K_s}{Des}} \quad \text{and} \quad \beta = \frac{Sb}{K_s} \quad (2.17)$$

and the dimensionless boundary conditions for (2.16) are:

$$\xi|_{\bar{r}=1} = 1, \quad \text{and} \quad \left. \frac{d\xi}{d\bar{r}} \right|_{\bar{r}=0} = 0 \quad (2.18)$$

The physical definition of the square of the Thiele modulus ϕ^2 is a first-order reaction rate divided by a diffusion rate. This implies that it may serve as a measure of the degree of rate limitation by internal mass transfer or by kinetics, as the Damköhler number does for external mass transfer. The saturation parameter β shows the extent to which the rate departs from first-order kinetics. A large value of β indicates an approach to zero-order kinetics. Examination of the Monod equation and the definition of β shows that if $K_s \ll S_b$, causing $\beta = S_b/K_s \gg 0$, then K_s is negligible and $\mu \rightarrow \mu_{max}$, implying zero-order kinetics due to excess substrate. Conversely, if $K_s \gg S_b$ such that $\beta \rightarrow 0$, then the rate equation becomes independent of S_b and dependent upon K_s and μ_{max} . However, the evaluation of the Thiele modulus is made difficult by the fact that intrinsic parameters v_{max} and K_s may not be known. Further manipulation yields new dimensionless observable modulus, Φ .

$$\Phi = \frac{v_o}{D_{es}S_b} \left(\frac{V_p}{A_p} \right)^2 \quad (2.19)$$

Plots of the η - Φ relationship for $\beta \rightarrow 0$ and $\beta \rightarrow \infty$ are given in Figure 2.6 (Bailey and Ollis 1986).

Since η for intermediate $1/\beta$ values lie between curves for the limiting cases of $\beta \rightarrow 0$ and $\beta \rightarrow \infty$, we see that η is relatively insensitive to the remaining intrinsic parameter, K_s/S_b (i.e., K_s). In conclusion, when using an immobilized-cell system, the effect of mass-transfer limitations on the overall

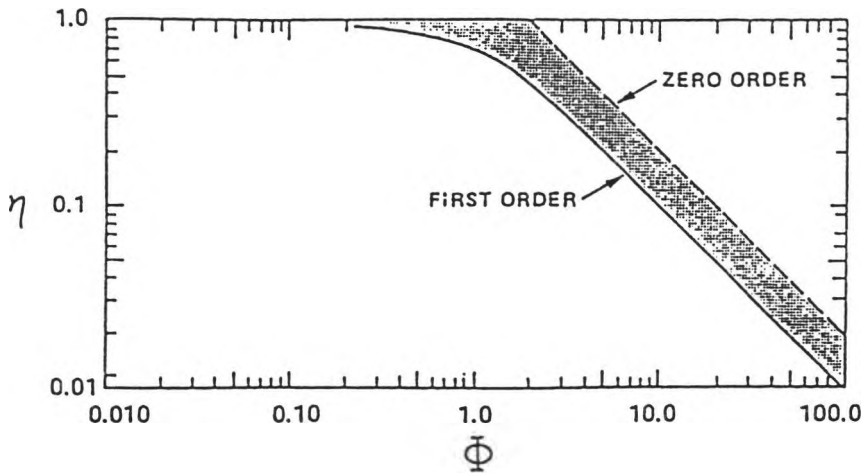


Figure 2.6: Calculated effectiveness factor as a function of the observable modulus (Bailey and Ollis 1986)

rate of degradation can be evaluated through the use of observable Damköhler number Ω and observable modulus Φ given relatively easily measured experimental data. As long as reasonable values are available for the observed rate of reaction and for the parameters k_s , A_p , V_p , and S_b , effectiveness factors can be estimated.

2.7 Fluidized Bed Reactor

There are several modes of operation for fluidized beds. Most of the possible modes of operation are illustrated in the diagram in Figure 2.7 (Fan 1989). The reactor scheme used in this work is a cocurrent upflow configuration in which the gas and liquid flows are in the upward direction.

Figure 2.7: Basic classification of gas-liquid-solid fluidization systems (Fan 1989).

| Expanded Bed Regime in Gas-Liquid-Solid Fluidization | Mode Designation | E-I-a-1 | E-I-a-2 | E-I-b | E-II-a-1 | E-II-a-2 | E-II-b | E-III-a | E-III-b |
|--|-----------------------|------------------------|-----------------|--------|-----------|----------|---------------------|----------|-----------------------------|
| | Schematic Diagram | | | | | | | | |
| | Continuous Phase | Liquid | | Gas | Liquid | | Gas | Liquid | Gas |
| | Flow Direction | Cocurrent Up-Flow | | | | | Countercurrent Flow | | Gas Up-Flow Liquid-Batch |
| | References (Chapters) | 1,2,3,6,7 8,10,11,A | 1,4,6,7,10,11,A | 1,2,11 | 1,5,6,7,8 | 5,9,11 | 1,5,7,9,11 | 1,4,7,11 | 1,5 |
| Transport Regime in Gas-Liquid-Solid Fluidization | Mode Designation | T-I-a-1 | T-I-a-2 | T-I-b | T-II-a | T-II-b | T-III-a | T-III-b | |
| | Schematic Diagram | | | | | | | | |
| | Continuous Phase | Liquid | | Gas | Liquid | Gas | Liquid | Gas | |
| | Flow Direction | Cocurrent Up-Flow | | | | | Countercurrent Flow | | Cocurrent Down-Flow |
| | References (Chapters) | 1,6,7,8,11 | 1,4,10,11,A | 1,6 | 1,9,11 | 1,9 | 1,6,11 | 1,6,9 | |

(S--) Independent Charge of Solids from Fluid (--)S) Independent Discharge of Solids from Fluid (+S) Charge or Discharge of Solids with Fluid

2.7.1 Fluidization of Particles

The minimum fluidization velocity for the fluidizing phase (gas or liquid) U_{mf} , can be predicted through correlations derived from equations for the pressure drop across a packed bed. One correlation, based on estimations involving the particle shape factor Φ_p and the particle void fraction or porosity at minimum fluidization, ε_{mf} , that hold for many fluidized systems, is presented in Equation 2.20 (Fan ; Geankolis 1983):

$$N_{Re,mf} = [(33.7)^2 + 0.0408 D_p^3 \rho_l (\rho_p - \rho_l) g / \mu^2]^{0.5} - 33.7 \quad (2.20)$$

where $N_{Re,mf} = D_p U_{mf} \rho / \mu$ (2.21)
 rearranging, $U_{mf} = N_{Re,mf} \mu / D_p \rho$.

$N_{Re,mf}$ is the particle Reynolds number at minimum fluidization, D_p is the diameter or effective diameter of particles, U_{mf} is the minimum fluidization velocity of the liquid, ρ_l is the density of the liquid, ρ_p is the density of the solids, μ is the viscosity of the liquid. For liquid-solid-air fluidized beds, the following correcting equation was developed by Song and coworkers (Song, Bavarian et al. 1987):

$$U_{lmf}/U_{lmfo} = 1 - 376 U_g^{0.327} \mu_l^{0.227} D_p^{0.213} (\rho_s - \rho_l)^{-0.423} \quad (2.22)$$

which is valid for the following conditions:

$$\begin{aligned} 0 &\leq U_g \leq 17 \text{ cm/s} \\ 0.9 &\leq \mu_l \leq 11.4 \text{ cP} \\ 0.046 &\leq D_p \leq 0.63 \text{ cm} \\ 1.8 &\leq \rho_s \leq 2.5 \text{ g/cm}^3 \end{aligned}$$

U_{lmf0} is calculated using the two-phase (liquid-solid) equation above, and U_g is the superficial gas velocity. Calculations to predict U_{mf} for various support particles have been performed. U_g versus U_{mf} for two particle diameters are shown in Figure 2.8, and the minimum fluidization liquid velocity without gas fluidization for a range of particle densities is shown in Figure 2.9.

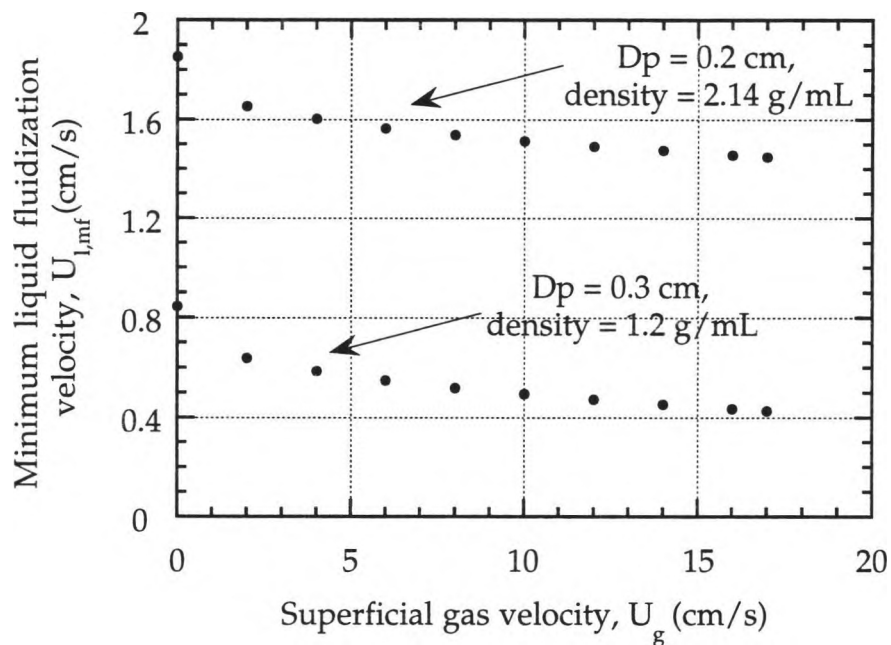


Figure 2.8: Minimum liquid fluidization velocities at varying superficial gas velocities for two particle diameters and densities.

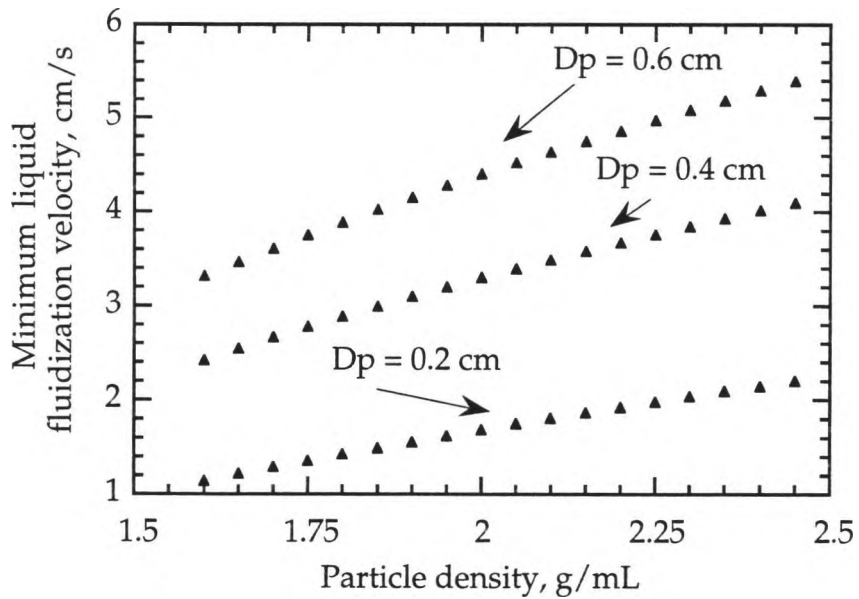


Figure 2.9: Minimum fluidization velocity for a range of particle densities.

The pressure drop at the minimum fluidization velocity is equal to the weight of particles in the bed (Kwauk 1992)

$$\Delta P = (\rho_s - \rho_f) (1 - \varepsilon_{mf}) L_o \quad (2.23)$$

where ρ_s is the density of the solid particles, ρ_f is the density of the fluid, ε_{mf} is the voidage, or void fraction in the solids bed at minimum fluidization, L_o is the height of fixed solids bed before fluidization starts. Once fluidization occurs, the pressure drop remains constant as flow increases (Figure 2.10) (Kwauk 1992). If the pressure drop at fluidization is measured, the void fraction of solids at minimum fluidization can be calculated.

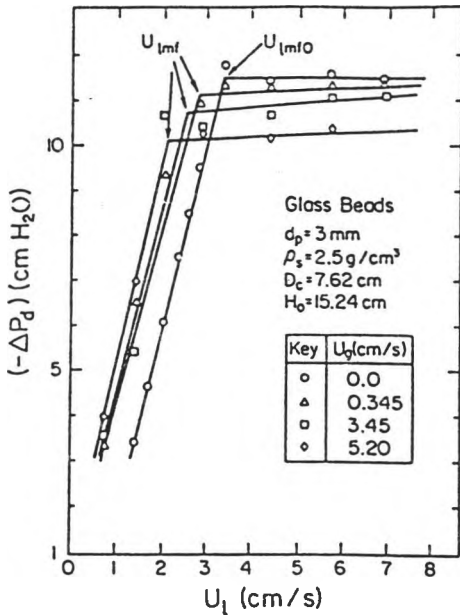


Figure 2.10: Pressure drop versus superficial fluid velocity. Note that the pressure drop ceases to increase at the minimum fluidization velocity.

It is known that the presence of small or light particles will promote bubble coalescence and that coalesced bubbles tend to result in the gas bypassing the emulsion phase rather than contributing to fluidization (Wu and Wisecarver 1990). Therefore increased bubble coalescence at high solids holdup requires a higher gas velocity to fluidize particles. Wu and Wisecarver (Wu and Wisecarver 1990) have found that there is an apparent tendency for bubble breakage and dispersion with increasing solids holdup for solids holdup below about 0.18, and for bubble coalescence with increasing solids holdup for solids holdup above 0.18. In the fluidized-bed bioreactor used in this work, the solids holdup was in the range of 0.1 to 0.2. Therefore it is expected that there was more of a tendency towards bubble breakage and dispersion rather than coalescence.

Chapter III METHODS AND MATERIALS

The first goal of this research was to determine the substrate degradation and microbial growth kinetics for *Pseudomonas* PR7 degrading 2,4-dinitrotoluene. Batch cultures were used for this part of the investigation. Batch experiments were chosen because they are easier to run than continuous experiments, they require far less medium, and the time required is less (Lee, Chang et al. 1991). However, batch experiments may have variable inocula, which can make it difficult to obtain useful data. In addition to the inoculum size, other elements influence the kinetics of microbial growth including substrate concentration, temperature, pH, availability of dissolved oxygen, ionic strength, salinity, and nutrients (Bauer and Capone 1988; Klecka and Maier 1988). All of these factors should be considered when designing experiments for gathering kinetic data. Oxygen mass transfer to the growth medium can be a major limiting factor due to the low solubility of oxygen in an aqueous solution (approximately 8.5 mg/L at room temperature and 1 atm pressure) (Yang and Wang 1992). Growth of *Pseudomonas* PR7 on DNT is not limited by oxygen under normal conditions. This is because the bacterium does not degrade large quantities of DNT quickly and therefore does not grow and consume oxygen as quickly as it would in the presence of another substrate such as glucose. For this reason, dissolved oxygen was monitored but not controlled or considered in model developments.

The second goal was to characterize the performance of a fluidized-bed bioreactor in degrading DNT with *Pseudomonas* PR7. This required the

design and construction of a fluidized bed reactor and the use of immobilized cells.

Batch and continuous experiments were performed and suspended as well as immobilized cells were used. A series of experimental protocols were developed, one protocol for each type of experiment. Several factors had to be taken into account when developing experimental procedures, among which were: ease of operation and equipment availability, economic feasibility for an environmental application, optimal growth conditions for bacterium in question, and desired experimental data. Protocols were developed for the experiments themselves and for the analysis of samples from the experiments.

3.1 Microorganism

Pseudomonas PR7, isolated by previous researchers (Spanggord, 1991; Suen, 1993), was used in this study and is thought to follow a pathway identical or similar to that of *Pseudomonas* DNT when using DNT as its sole carbon source. It oxidatively degrades DNT, releasing stoichiometric quantities of nitrite into solution.

Frozen stock cultures of the bacteria were maintained at -80 °C in a freezer. To make this stock, a flask of *Pseudomonas* PR7 was grown in 1/4-strength tryptic soy broth (BBL®) for one day. Cryogenic freezer vials were filled with 0.2 mL of glycerol (Aldrich) and then sterilized in an autoclave (steam, 121 °C, maintained for 20 minutes). Culture broth (1.2 mL) was aseptically pipetted into each vial and then frozen.

Culture solutions from each experiment were streaked onto 1/4-strength tryptic soy agar and onto DNT agar to check for contamination. Isolated colonies were then placed into test tubes with DNT and Spain's

Mineral Salts Base (SMSB) to check for the formation of the yellow intermediate MNC. If a yellow color formed, the bacteria was considered to be degrading DNT by the desired pathway, and the culture was assumed to be the *Pseudomonas* PR7 strain.

3.2 Inocula

In order to begin a batch experiment, an inoculum in the form of a suspension of bacteria is added to the media containing the substrate. The history of this inoculum can be important, since several researchers have suggested that the acclimation history of an inoculum significantly affects the degradation rates of the substrates (Templeton and Jr. 1988). Also, the size of the inoculum has been reported to affect degradation kinetics and the length of exponential growth (Chudoba 1989; Lee, Chang et al. 1991). Inocula were therefore prepared in a consistent manner for all batch fermentor experiments.

Batch fermentations were inoculated with a suspension of *P. PR7* that was taken from the frozen stock, inoculated into 500 μM DNT, streaked onto 1/4 TSA, reinoculated into 500 μM DNT from an isolated colony, and finally used as an inoculum when yellow color appeared, indicating production of MNC and exponential growth. A 0.5 % by volume inoculation was used in each experiment.

During flask experiments, culture conditions were still being explored, and the use of consistent inocula had not yet been established. Inocula history was recorded for flask experiments, but not deliberately manipulated. Results obtained from use of different inocula in these experiments are presented later.

3.3 DNT Recrystallization

Microorganisms were grown in solutions of DNT that were enriched with SMSB, outlined in the next subsection.

2,4-dinitrotoluene (DNT) was purchased from Aldrich Chemical at 97% purity. Recrystallization to further purify the compound was performed as follows:

(CAUTION: DNT AND METHANOL ARE HAZARDOUS MATERIALS, WEAR APPROPRIATE GLOVES, GOGGLES AND A LAB COAT AND WORK IN A FUME HOOD)

1. Dissolve DNT in methanol in a large Erlenmeyer flask while heating at low heat until solution is saturated (WORK IN FUME HOOD). Record mass of DNT used.
2. Place solution of DNT and methanol in an ice bath or freezer. Crystals should form within a few minutes. If crystals do not form within 5 to 10 minutes, scratch flask bottom with spatula or glass rod.
3. Allow flask to cool completely.
4. Once flask has cooled, vacuum filter solution over a Buchner funnel covered with filter paper to recover crystals. Wash crystals once briefly with cold methanol.
5. Allow crystals to dry. Remove from filter paper by scraping with spatula into a suitable dark glass container for storage for later use.
6. Evaporate methanol from filtrate in a fume hood. Gather crystallized impurities into suitable container and dispose of according to applicable hazardous waste regulations.

3.4 Media

The SMSB solution provided necessary mineral salts for the microorganisms and contains the following:

| | | |
|---|------------|--------------|
| MgSO ₄ ·7H ₂ O | 112.5 mg/L | (0.457 mM) |
| ZnSO ₄ ·7H ₂ O | 5.0 mg/L | (0.174 mM) |
| Na ₂ MoO ₄ ·2H ₂ O | 2.5 mg/L | (0.010 mM) |
| KH ₂ PO ₄ | 340 mg/L | (2.5 mM) |
| Na ₂ HPO ₄ ·7H ₂ O | 670 mg/L | (2.5 mM) |
| CaCl ₂ | 13.8 mg/L | (0.125 mM) |
| FeCl ₃ | 0.125 mg/L | (0.00077 mM) |
| NH ₄ Cl | 500 mg/L | (9.34 mM) |

Preparation of SMSB is detailed in Appendix II.

Microorganisms were also periodically grown on TSA or in TSB for the purpose of checking for contamination or for enriching prior to freezing for storage. Tryptic soy broth (BBL®) was prepared at 1/4-strength according to package instructions (7.5 g/L) and tryptic soy agar was prepared by combining 1/4 the suggested amount of tryptic soy broth with a full amount of Bacto plain agar (16 g/L) (Difco). Finally, *Pseudomonas* PR7 colonies were also maintained on plates containing SMSB, 500 µM DNT, and 16 g/L Bacto agar with and without 10 mM succinate (as sodium succinate·2H₂O).

3.5 Batch Shake Flask Experiments

Batch experiments were performed in shake flasks using 200 mL of 500, 750, or 1000 µM initial DNT concentration plus Spain's Mineral Salts Base (SMSB) solution in shake flasks incubated at 30 °C at 200 RPM. The shake

flasks were inoculated with 20 mL of a *P. PR7* culture in exponential growth. The inocula for these experiments were grown in a shake flask with 1000 µM DNT initial concentration, incubated at 30 °C at 200 RPM for 100 hours, or until the yellow color disappeared. Because the bacteria seemed to degrade all DNT before exponential growth began, the inocula were thought to be very low in DNT concentration with respect to the uninoculated shake flask solutions.

Samples were taken with sterile 10-mL pipets in a laminar flow hood. An unfiltered portion of each sample was used for optical density measurements. The remainder was immediately filtered through a 0.2 µm syringe filter to separate cells and stop degradative activity. Filtered samples were analyzed for NO₂⁻ concentration, DNT concentration, and pH.

3.6 Batch Stirred-Tank Bioreactor Experiments

Suspended-cell batch experiments were carried out under controlled conditions in 2- and 3-liter stirred-tank bioreactors. The bioreactors were filled to a specific volume (1.5 and 2 L respectively) with DNT at varying concentrations in SMSB. The bioreactors were equipped with impeller shafts and motors, temperature control, pH and D.O. probes and meters, air inlet and air outlet ports, inoculation septa, acid and base addition ports, and sample ports. Air filters (Gelman Bacterial Air Vent) were placed on air inlet and outlet lines to guard against contamination, and the bioreactors were then autoclaved (20 - 30 min.) after being double checked.

After autoclaving, a bioreactor was allowed to cool and then stabilize at 30 °C before inoculation. If pH control was a part of the experimental procedure, the desired pH was attained before inoculation.

The following sets of batch experiments were performed using suspended cells to determine intrinsic kinetics:

$S_0 = 250, 500, 750, 1000 \mu\text{M}$ DNT, no pH control

$S_0 = 500, 1000 \mu\text{M}$ DNT with pH controlled at 6.8, 5.0, and 4.0

For pH-control experiments, a BioController 1030 manufactured by Applikon was employed. A base-pump-only system was sufficient because the bacteria produced nitrous acid (HNO_2) continuously during the exponential growth and substrate degradation phase. Sodium hydroxide (1 M) was used successfully to control the pH. Since the SMSB solution buffers around pH 6.75, hydrochloric acid was added to lower-pH experiments before inoculation.

Samples were taken every three to eight hours, depending on the stage of the fermentation and the desired density of data points. Repeated experiments were generally sampled every six to eight hours. Samples of 4 mL were taken using sterile syringes. One mL of unfiltered sample was transferred to a polystyrene cuvette for optical density measurement. After this measurement, the sample was transferred to a microcentrifuge tube for later use in protein analysis. The remaining 3 mL was promptly filtered through a $0.2 \mu\text{m}$ Gelman Nylon Acrodisc syringe filter to remove cell activity and to filter for HPLC analysis and nitrite assay. Filtered and unfiltered samples were immediately frozen.

3.7 Fluidized-Bed Bioreactor

A fluidized-bed bioreactor was designed and built for this work. The bioreactor was fabricated from high-temperature glassware by the Colorado

State University Department of Chemistry scientific glass blower. A schematic of the bioreactor and associated plumbing is shown in Figure 3.1.

Air enters the fluidized-bed bioreactor through the bottom. Liquid feed enters the bioreactor through a port at the top, and a liquid recycle is drawn from the settling zone at the top of the reactor and pumped to the bottom of the reactor. The level of liquid is kept constant in the system by pumping overflow out of the effluent port, which is located one centimeter above the recycle outlet port.

Screw-cap connections fit with open-top screw-caps and septa are located along the length of the reactor for liquid sampling with needle and syringe. Larger diameter ports are located along the length, on the other side of the reactor, for particle sampling.

3.7.1 Diatomaceous-Earth Particle Experiments

The fluidized-bed bioreactor was loaded with 200 mL of calcinated diatomaceous earth particles (Manville Celite R-630) and about 300 mL of 1000- μ M DNT plus SMSB and autoclaved. Air was bubbled into the bottom of the vessel to provide oxygen. An inoculum of 10 mL of a culture of *P. PR7* (grown in a solution of 1000 μ M DNT initial concentration) in exponential growth was introduced through a septum near the bottom of the reactor. After inoculation, the bacteria were given 70 hours to begin exponential growth, 400 mL of 1000 μ M feed was added, and bacteria were again given time to grow. Once MNC (indicated by yellow color) appeared and disappeared, feed was added at a slow rate and continued until the reactor was full. Liquid in the reactor was then recycled until the appearance of a yellow color (MNC) occurred after about 72 hours. This was used as an indicator of

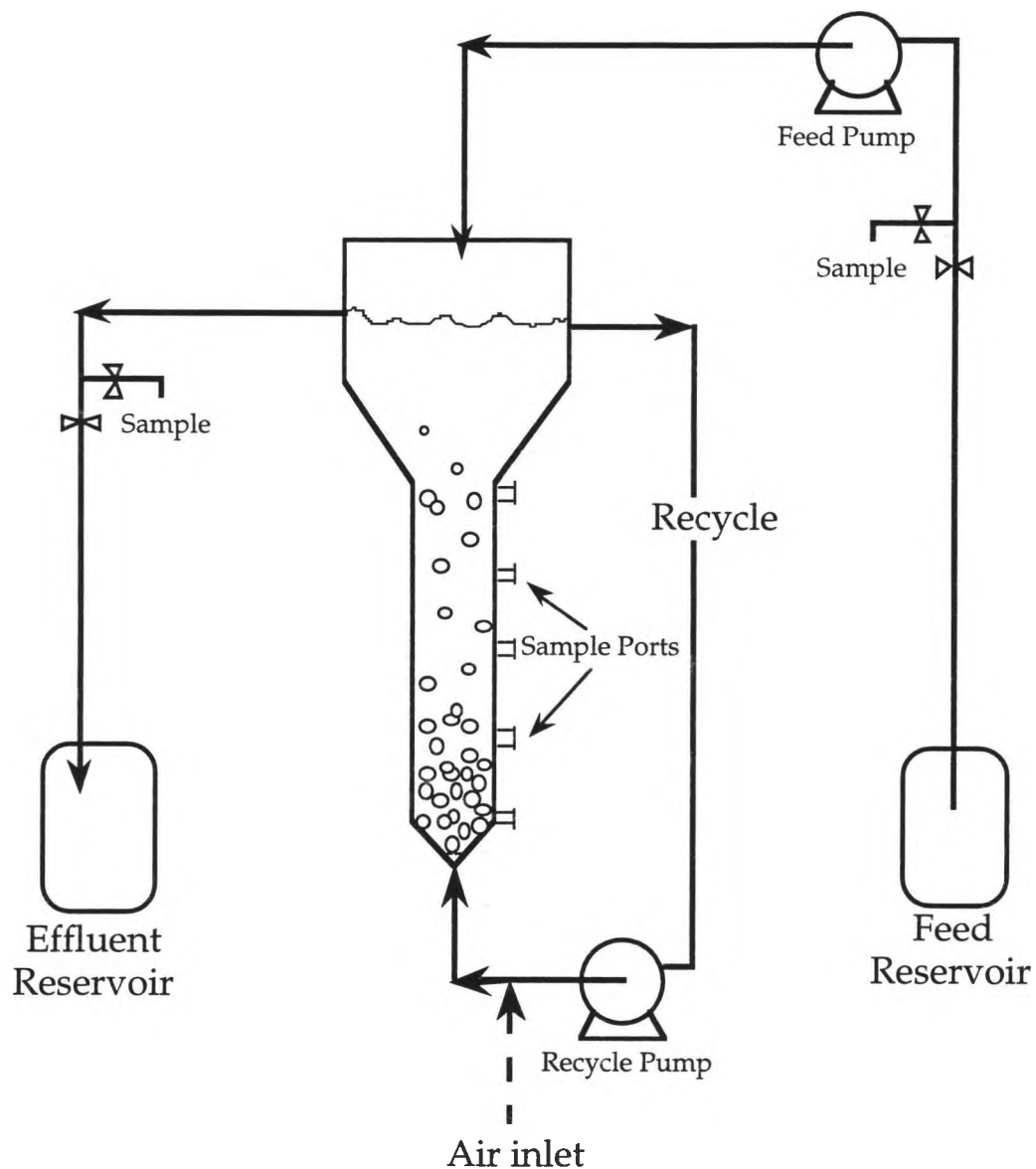


Figure 3.1: Schematic of the fluidized-bed bioreactor.

the initiation of growth soon to follow. Continuous feed was then started at a dilution rate of 0.03 h^{-1} , and the air rate was increased to between 1000 and $1100 \text{ cm}^3/\text{min}$. The liquid capacity of the reactor was 1.7 L when loaded with solids, but this did not remain constant due to the sloughing of particle mass during fluidization and reached as much as 1.9 L. The reactor volume was estimated at 1.7 for the calculation of dilution rates, however. Inlet DNT

concentration to the reactor was 1000 μM and dilution rates varied from 0.031 to 0.14 h^{-1} . Samples were taken from the top and bottom of the column through septa to avoid contamination of the reactor. Filtered samples were analyzed for DNT, NO_2^- , and pH.

3.7.2 Plastic Particle Experiments

After three experiments were performed using diatomaceous-earth particles, plastic particles were used in further experiments for several reasons. Diatomaceous-earth particles had a tendency to break apart after short operating periods, clogging associated tubing with fine particulate matter. In addition, they were more dense than desired, requiring high liquid flow rates for fluidization. Plastic particles were considered because of the large variety of polymeric compounds that have densities close to that of water. The plastic particle had to fit the following criteria: (1) be slightly more dense than water to fluidize readily yet settle as well, (2) have glass transition and melting temperatures high enough to withstand autoclave temperatures of 121 °C, (3) not be toxic to bacteria, (4) support bacterial attachment, (5) be economically feasible, and (6) available in the size range of 1 to 4 mm diameter. Cylindrically shaped polycarbonate particles (Sigma Chemical) with average length and diameter of 3 mm and density of 1.2 g/mL were chosen.

The fluidized-bed bioreactor was loaded with 200 mL (volume measured via water displacement) polycarbonate particles. The system was started-up by adding 500 mL of 500 μM DNT plus SMSB to the reactor and autoclaving. A large inoculum from frozen stock was added through septa. A feed of 1000 μM DNT plus SMSB was started several hours later to fill the reactor. Once full, the feed was turned off and the bacteria were allowed to grow. Once yellow MNC appeared and disappeared, feed was started and the

gathering of data began. The reactor was sampled as described previously and samples were analyzed by the same methods as other in experiments.

3.8 DNT and MNC Analyses

Concentrations of DNT and MNC in aqueous solution were measured using high-pressure liquid chromatography (HPLC). Analysis was performed using a 4.6 x 150 mm Rainin Microsorb type C8 column with 5- μ particle size and 100- \AA pore size as the stationary phase and acetonitrile and water acidified to 0.004 N with H₂SO₄ as the mobile phase. The column was protected by a 5- μm Microsorb C8 precolumn.

The solvent gradient was 35% acetonitrile for 2 minutes, increased to 60% over 5 minutes and sustained for 5 minutes, decreased back to 35% over 2 minutes and held there for the remaining 8 minutes.

Solvent flow was 1.0 mL/min, sample injection volume was 20 μL , and absorbance was read at 230 nm by a Millipore Waters 486 Tunable Absorbance Detector. Sample queue, injection volume, and solvent gradient were controlled by a Maxima 820 Chromatography Workstation. Calibration curves and integration of chromatograms were also performed using the Maxima Workstation. Aqueous solutions of DNT and MNC were periodically made up for use as standards for calibration. MNC was positively identified in cultures by comparing diode array scans of the MNC peak in culture-sample chromatograms to diode array scans of the pure compound. Pure MNC was obtained from Shirley Nishino. HPLC chromatograms were compared for pure MNC and MNC in culture solutions. The time that the peak for the pure MNC was detected was the same as that for MNC in culture solutions. Examples of calibration curves for DNT and MNC are shown in Figures 3.2 and 3.3. Concentration is plotted versus peak response for both.

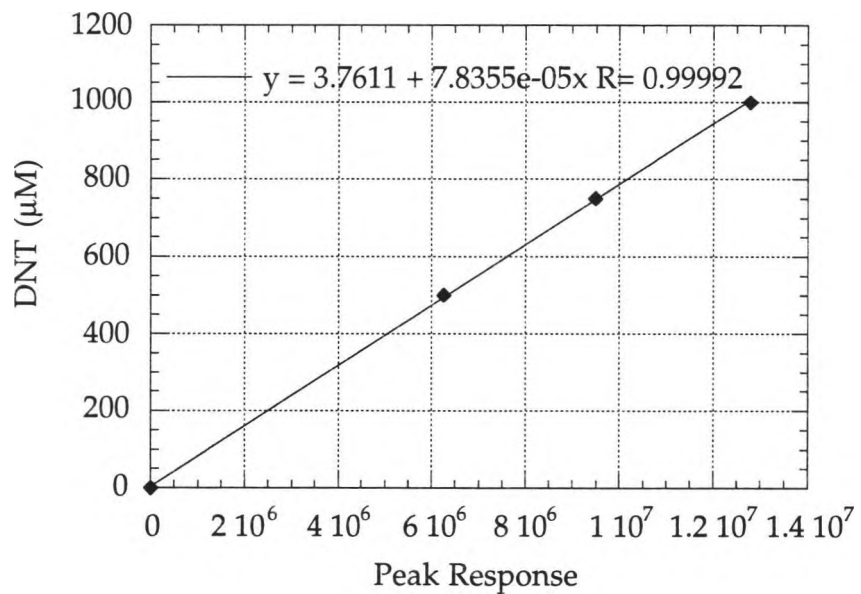


Figure 3.2: Calibration of DNT concentrations versus absorption peak response at $\lambda = 230$ nm from HPLC analysis.

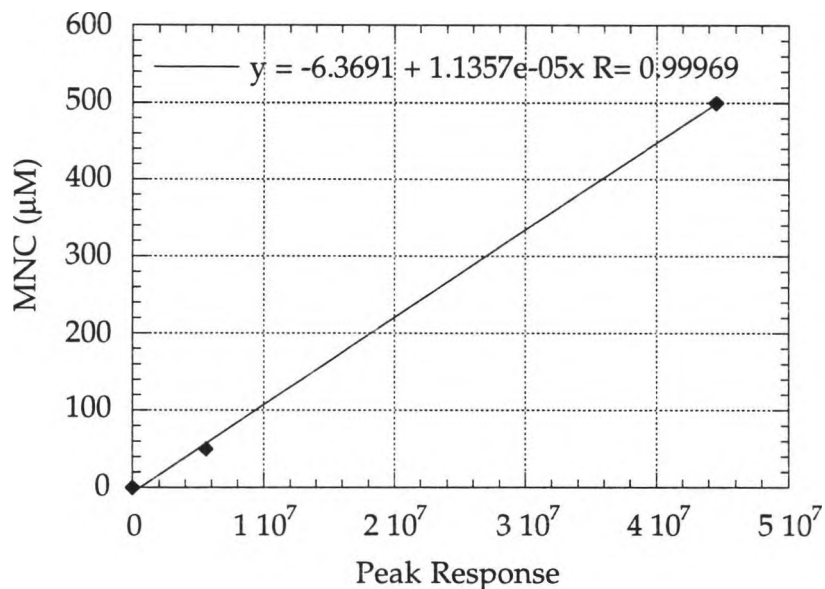


Figure 3.3: Calibration of MNC concentration versus absorption peak response at $\lambda = 230$ nm from HPLC analysis.

3.9 Nitrite Analysis

The sulfanilamide method described in Methods for General and Molecular Biology (1994) was used to measure nitrite ion concentrations. The analysis of nitrite nitrogen is based on the reaction of NO_2^- with sulfanilamide in an acid solution to form a diazo compound. This compound reacts with *N*-(1-naphthyl)ethylenediamene to form a colored dye whose absorbance at a wavelength of 543 nm is measured in a spectrophotometer. The reaction can detect as little as 1 $\mu\text{g}/\text{L}$ of NO_2^- using a 10-cm light path. In this work, however, a 1-cm light path was used. The absorbance of the compound follows Beer's law up to 180 $\mu\text{g}/\text{L}$ NO_2^- . Ions which interfere by causing precipitation are Cl^- and Fe^{3+} . Although these ions are present in very low concentrations, the sulfanilamide method was chosen because the reduction to NH_4^+ and subsequent analysis would involve interference by any ammonium or nitrate in solution. Also, samples required 1:100 dilution due to high NO_2^- concentrations, so any interfering Cl^- or Fe^{3+} ions were diluted further. Interference by colored substances (such as the yellow MNC) could occur, but the absorbance of MNC at 543 nm is insignificant and there are no other known interferences. Absorbance spectra of random samples from fermentations showed no absorbances at 543 nm in the absence of reagents A and B. Samples were filtered to remove any bacterial activity and any particulate matter and then frozen until analysis.

Reagents A and B were prepared according to the protocol below. Standard calibration curves were periodically prepared by plotting $[\text{NO}_2^-]$ versus A_{543} for a set of NO_2^- standards made with NaNO_2 and deionized water.

Table 3.1: Reagents A and B for the sulfanilamide method for nitrite ion concentration determination.

| | | |
|------------|---|--|
| Reagent A: | 5 g Sulfanilamide 300 mL conc. HCl deionized H ₂ O | (1) Dissolve sulfanilamide in 300 mL conc. HCl, (2) dilute to 500 mL with deionized water |
| Reagent B: | 0.5g <i>N</i> -(1-naphthyl) ethylenediamene deionized H ₂ O | Dissolve <i>N</i> -(1-naphthyl) ethylenediamene in deionized water to make 500 mL solution |

1. Add 0.02 mL of reagent A to 1 mL of filtered sample. Allow it to react for a minimum of 2 minutes but no longer than 8 minutes.
2. Add 0.02 mL of reagent B, and mix immediately.
3. Allow the magenta color to develop for at least 10 minutes before absorbance is measured at $\lambda = 543$ nm (1994).

A typical calibration for the nitrite assay is shown in Figure 3.4.

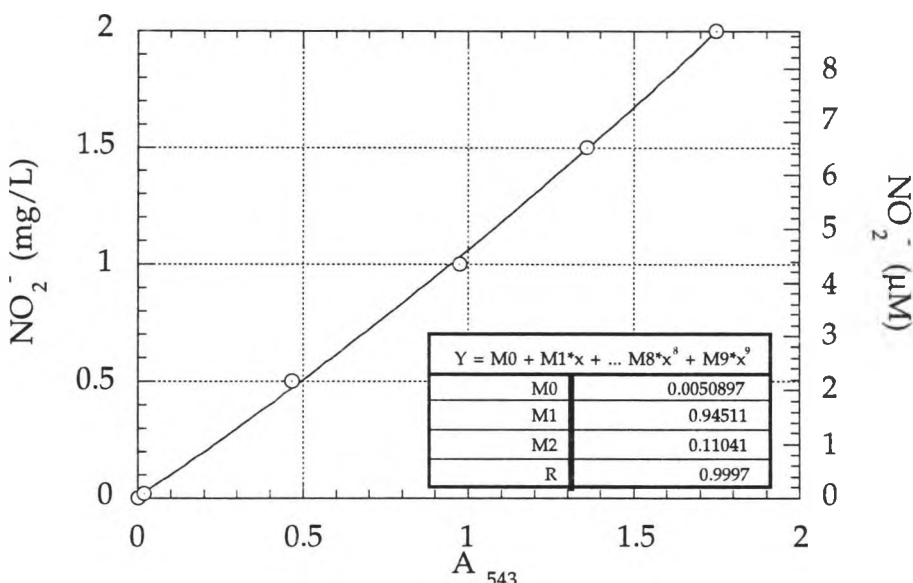


Figure 3.4: Standard calibration of sulfanilamide method for nitrite analysis.

3.10 Cell Concentrations/Absorbance

Optical density (OD) was measured at $\lambda = 600$ nm. Optical density measurements were used to measure cell concentrations in the suspended-cell shake flasks only. Optical density measurements were not used in the FBB because this method cannot determine the concentration of cells attached to particles.

Dry cell weights were measured by centrifuging 1.0 L (split into four equal volumes) of liquid cell suspensions from flasks at various stages of growth and drying in a 105 °C oven to constant weight. Optical density measurements were taken before centrifugation in order to relate dry cell weight to optical density. A calibration of dry cell weight versus optical density at $\lambda = 600$ nm is shown in Figure 3.5.

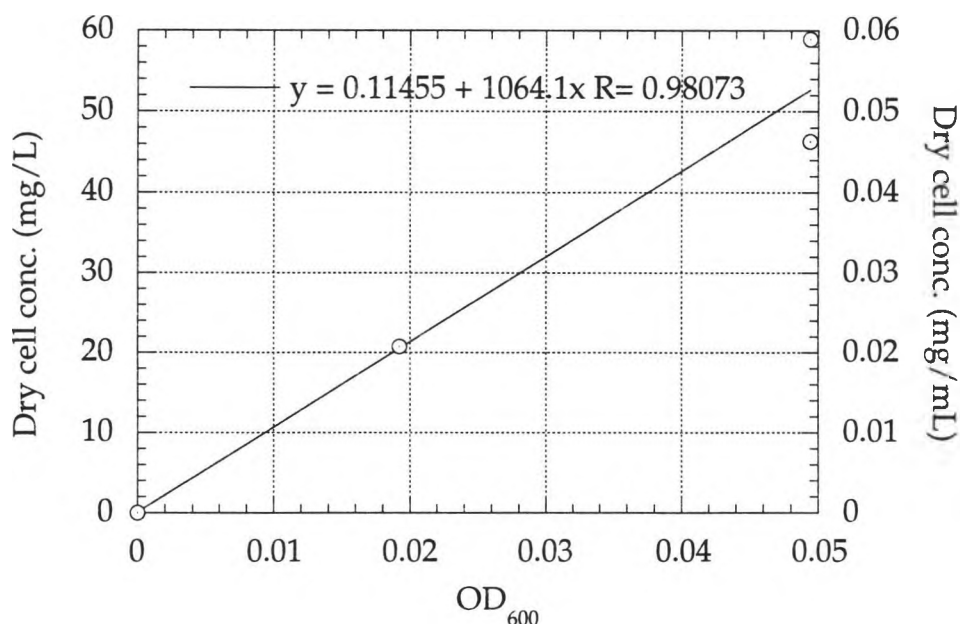


Figure 3.5: Dry cell concentration versus optical density measured at 600 nm.

Two assays were performed in an attempt to quantify the cell mass attached to immobilized-cell particles. The BCA protein assay (Pierce) (Conuel 1994) and a spectrofluorometric method employing fluorescein diacetate were performed on samples from suspended-cell cultures and on cells attached to known volumes of particles.

BCA Assay:

To sample the particles with bacteria growing on them, washed and autoclaved polycarbonate particles were aseptically transferred into test tubes containing DNT plus SMSB. Test tubes were then inoculated with *P. PR7*. Test tubes were incubated both with and without gentle stirring until yellow MNC had appeared and disappeared. The solutions containing the particles were then gently poured over a piece of screen attached to a spatula to drain particles. Then sterile SMSB was poured over the particles to rinse any free cell matter from the particles.

Samples of five or ten polycarbonate particles were bathed in 2 mL of pH 13 NaOH at 70 °C for 1 hour in a test tube to lyse the cells. The alkaline solution was prepared by diluting 5 N NaOH 1:10 with SMSB solution. SMSB has a slight buffering capacity, so the final pH of the solution was about 13, which is expected for a 0.1 N NaOH solution.

After incubation, 0.1 mL of the solution from each test tube was added to 2 mL of the BCA working reagent in a small glass test tube. The contents of each vial were immediately mixed and placed in a water bath at 60 °C for 30 minutes. Protein standard solutions of bovine serum albumin were prepared with the same diluent (NaOH-SMSB solution) and incubated with the unknown samples. After cooling briefly, test tube contents were transferred to spectrophotometer cuvettes and their absorbance at 562 nm was measured.

The absorbance of a blank prepared with diluent and incubated with BCA working reagent was subtracted from all samples. The calibration curve for albumin standards is shown in Figure 3.6.

Samples of suspended-cell solutions were also analyzed for protein concentration using the BCA method. Culture solutions in different phases of growth were diluted with the diluent 1:2 and then incubated to lyse cells. After this step, 0.1 mL of each solution was added to 2 mL of working reagent and incubated at 60 °C for 30 minutes and then measured in the spectrophotometer.

Although no problems occurred with standard curves, problems repeatedly arose with unknown samples. Absorbance readings were erratic and often very low. Because a set of standards was prepared each time that unknown samples were prepared and there were no problems with standard curves, the preparation technique was not suspected to be causing problems with the unknowns.

Several factors could have caused the problems with the assay. Catecholamines are known to interfere with the BCA assay due to their reducing properties, so 4-methyl-5-nitrocatechol could cause interference as well. Clean, sterile polycarbonate particles gave relatively high absorbance readings with the BCA assay, so the polycarbonate probably interfered with protein determination on the particles. Cell concentrations did not usually exceed 80 mg/L dry-cell weight in the suspended-cell cultures. The BCA assay is most likely not sensitive enough to detect the protein concentrations in such dilute cultures typical in this work. If all dry cell matter were protein, then 80 µg/mL protein would be expected to be the maximum protein concentration. The range of the most sensitive BCA assay protocol is 5 - 250 µg/mL protein. Because only a percentage of cell matter is protein, the most

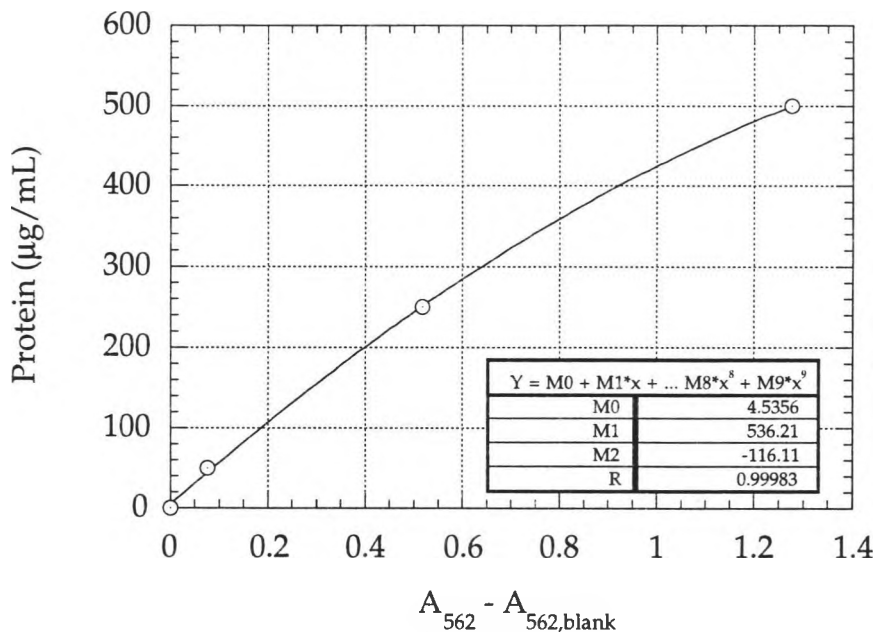


Figure 3.6: Typical BCA protein assay calibration.

concentrated cell suspension would be at the low end of the BCA assay range. Centrifugation for concentration was considered, but the aim of the assay was to measure protein concentration attached to the polycarbonate particles. In order to cleave the cells from the particles, cells had to be lysed first. Centrifugation would be impractical in this case, especially considering the interference with the BCA reagent from the polycarbonate particles.

Fluorescein diacetate:

The two ester bonds on fluorescein diacetate will be cleaved by esterases in viable cells. Once cleaved of the ester linkages, the fluorescein is fluorescent, especially when excited with light at a wavelength of 490 nm. The emission wavelength is in the range of 515 - 535 nm. A calibration of this

method was performed by preparing dilutions of suspended-cell cultures in exponential growth, and measuring fluorescence versus colony forming units obtained from spread plates of each dilution. A linear calibration was obtained, but the lower cell concentrations were not above background fluorescence levels. Particles harvested from the fluidized-bed bioreactor were loaded with the same concentration of fluorescein diacetate under the same conditions as the suspended cell dilutions. No fluorescence above the level obtained from the control solutions (no cell concentration) was detected.

Scanning electron micrographs (See Chapter V, Figures 5.10 - 5.12) were taken of the biomass-free polycarbonate particles and of polycarbonate particles containing cells to obtain an idea of the characteristics of the biofilm and to obtain an idea of the magnitude of cell concentrations on the particles.

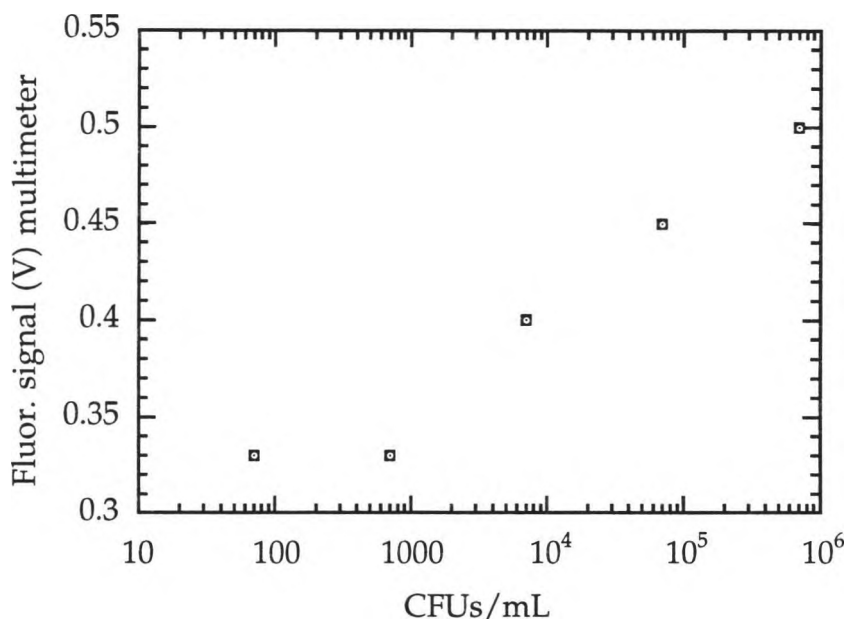


Figure 3.7: Voltage signal from the spectrofluorometer as a function of CFUs/mL of *P. PR7* grown in DNT plus SMSB. Particles with bacteria attached loaded with the fluorescein diacetate dye did not give signals above the background value of 0.33 volts, corresponding to < 10000 CFUs/mL above.

3.11 Residence Time Distribution (RTD) Analysis

Residence time distribution analysis was performed using sodium chloride as a tracer. Chloride ion concentrations were measured using Orion chloride ion and reference probes, a conductivity meter calibrated in millivolts and a stripchart. Instruments were calibrated with sodium chloride solutions from 0 to 200 mg/L in deionized water. The fluidized-bed reactor was filled with deionized water and Manville Celite R-630 particles and fluidized with air and recycled water. Deionized water was pumped through the reactor at a dilution rate of 0.30 h^{-1} for a short time to establish steady state. Feed was then switched to a 150 ppm NaCl solution and conductivities were recorded until reactor concentration reached a maximum of 150 ppm NaCl (about 5.5 residence times). The concentration versus time data obtained is given with the results sections.

Chapter IV SUSPENDED-CELL EXPERIMENTAL RESULTS & DISCUSSION: Intrinsic Kinetics of Biodegradation of 2,4-DNT by *Pseudomonas PR7*

Experiments for the determination of the intrinsic kinetics of DNT degradation by *Pseudomonas PR7* were restricted to suspended-cell batch experiments. Results from preliminary shake-flask experiments revealed the necessity of proper inoculum size and consistent inocula history in batch experiments. Subsequent bench-scale reactor experiments were performed to gather the kinetic data. Inocula size and history were kept consistent for these experiments.

4.1 Batch Shake-Flask Experiments

4.1.1 Results

Table 4.1 lists the conditions used for experiments SF1 - SF7. Flasks were shaken in an incubated shaker at 200 RPM and 30 °C. Results from shake flask experiments are presented in Figures 4.1 through 4.6.

The medium for Experiment SF1 contained twice the concentration of the phosphate buffer solution (SMSB Solution B). This was done as an attempt to decrease the fall in pH due to the production of nitrous acid.

Table 4.1: Suspended-cell shake-flask experiments and conditions.

| <u>Exp.#</u> | <u>DNT₀</u> (μ M) | <u>DNT_f</u> (μ M) | <u>X₀</u> (mg/mL) | <u>X_f</u> (mg/mL) | <u>pH₀</u> | <u>pH_f</u> | <u>inoc.</u> | <u>hrs until</u> <u>DNT=0</u> |
|--------------------------|--------------------------------------|--------------------------------------|---------------------------------|---------------------------------|-----------------------|-----------------------|--|----------------------------------|
| SF1; double buffer | 498 | 0 | 20 | 30 | 6.71 | 6.5 | 8%v/v; 500- μ M DNT | 27 |
| SF2 | 496 | 0 | 15 | 24 | 6.67 | 6.34 | " | 17.5 |
| SF3 | 492 | 0 | 15 | 31 | 6.67 | 6.43 | " | 27 |
| SF4 | 651 | 0 | 14 | 30 | 6.65 | 6.25 | " | 34 |
| SF5 | 990 | 0 | 13 | 34 | 6.67 | 6.23 | " | 43.5 |
| SF6 | 220 | 0 | 4 | 14 | - | - | 1%v/v; 10 ³ - μ M DNT | 52 |
| SF7 | 440 | 0 | 4 | 23 | - | - | " | 57 |

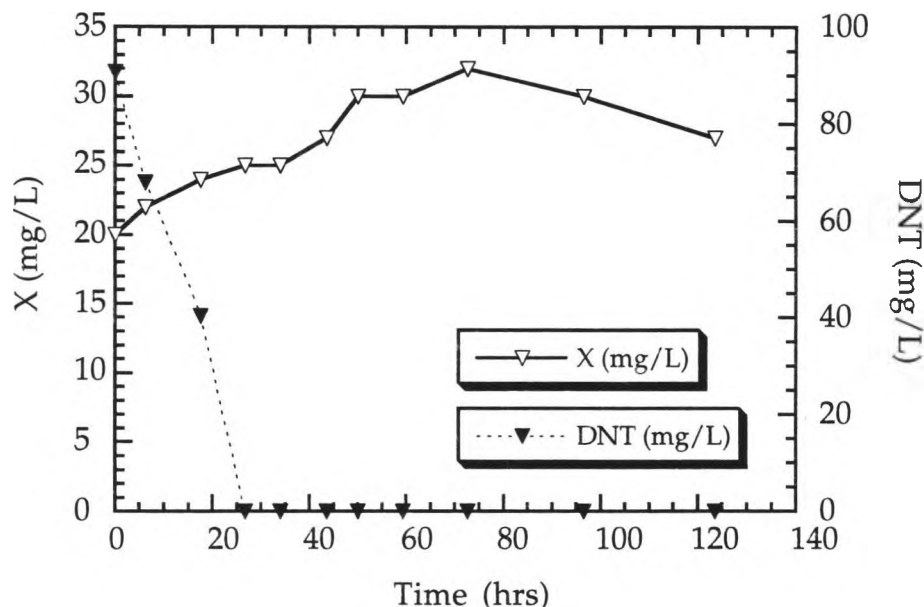


Figure 4.1: Cell growth and DNT degradation in Shake-Flask Experiment SF1. Initial phosphate buffer strength was increased two-fold.

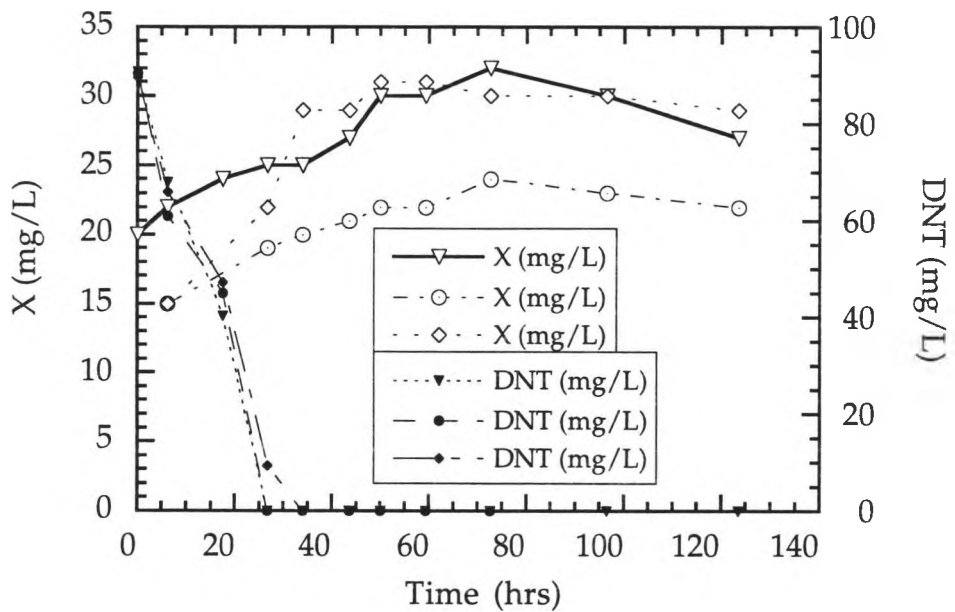


Figure 4.2: Shake-flask cultures SF1 (triangles), SF2 (circles), and SF3 (diamonds) with initial DNT concentration of 500 μM .

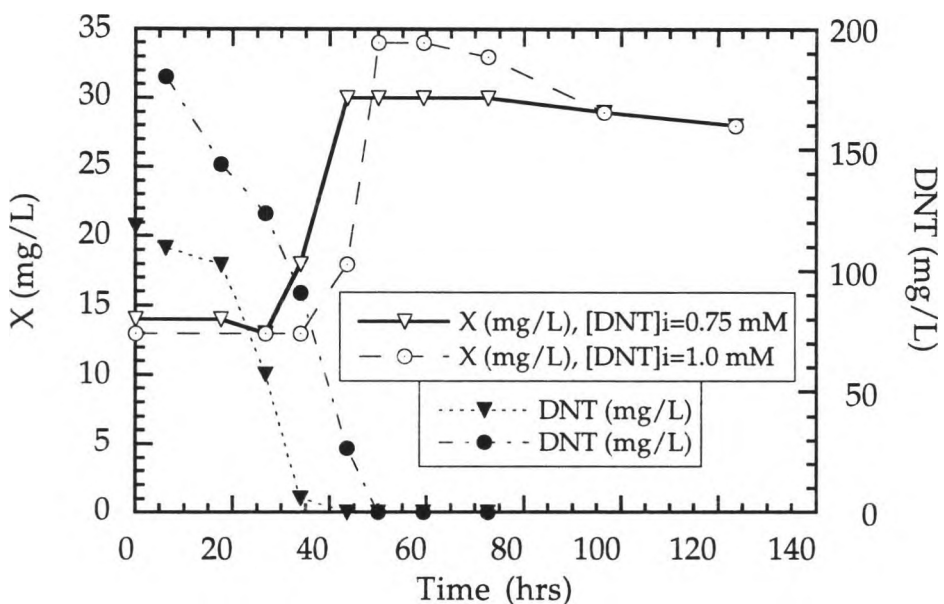


Figure 4.3: Experiments SF4 (triangles) and SF5 (circles) with different initial DNT concentrations.

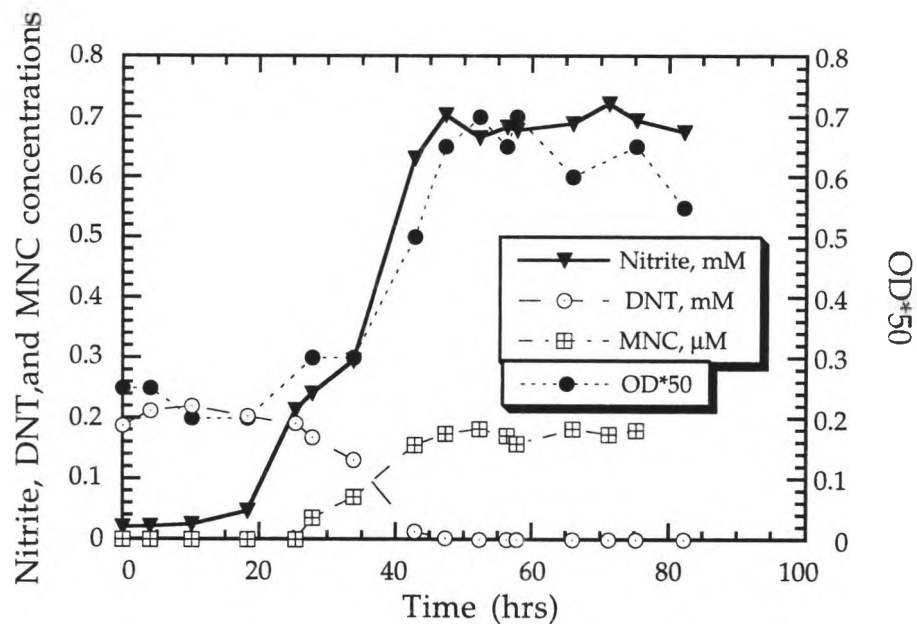


Figure 4.4: Experiment SF6; initial DNT concentration was 220 μM .

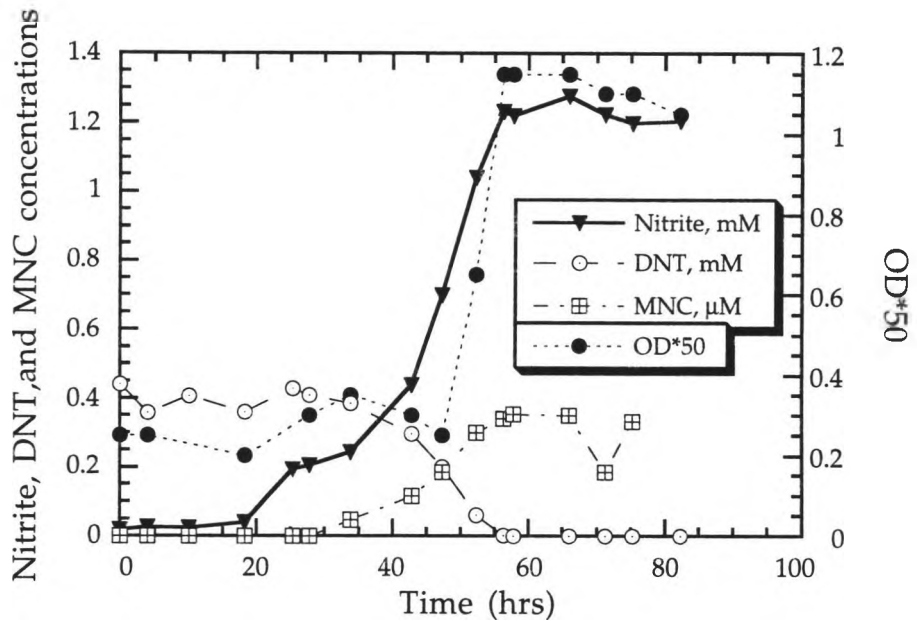


Figure 4.5: Experiment SF7; initial DNT concentration was 440 μM .

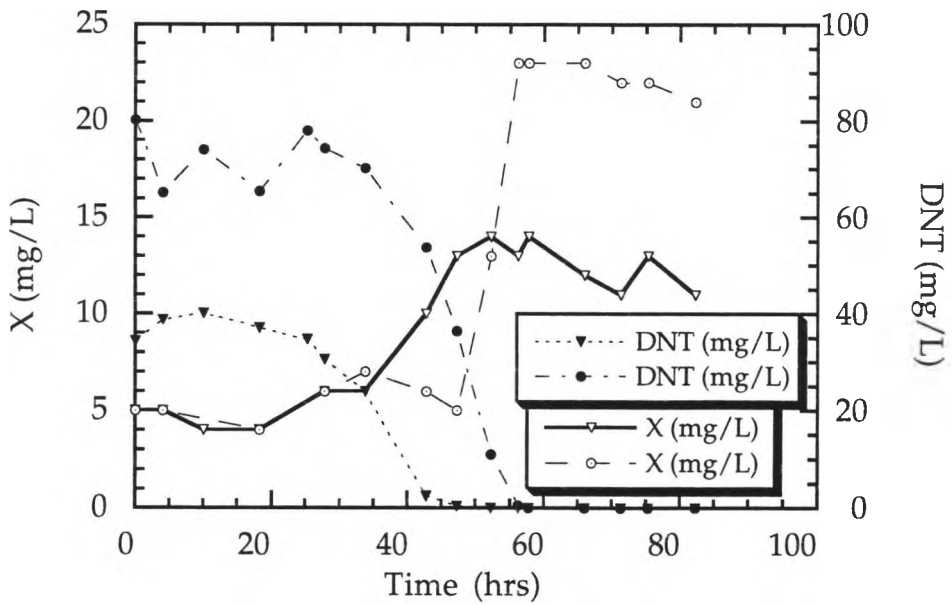


Figure 4.6: Experiments SF6 (triangles) and SF7 (circles); initial DNT concentrations were 220 and 440 μM (40 and 80 mg/L) respectively.

4.1.2 Analysis and Discussion

The results shown in Figures 4.1 through 4.6 show that, as expected from earlier reports (Reardon 1992), *P. PR7* can utilize DNT as its sole carbon and energy source for growth. Also, MNC was positively identified in small quantities, supporting the hypothesis that *P. PR7* uses the oxidative pathway shown previously in Figure 2.1.

Figures 4.4 and 4.5 show cell growth, DNT depletion and formation of MNC and NO_2^- . In order for the increases in MNC to show on the plots, the MNC concentrations are plotted in μM while the DNT concentrations are plotted in mM. The appearance of MNC was detected in small quantities as expected. The yellow color of the intermediate disappeared at the end of each experiment, but the concentration detected did not decrease. It is possible that

the concentrations appearing on the plots are residual amounts of MNC since not more than 0.2 and 0.4 μM appeared in SF6 and SF7 respectively. The peak of the transient accumulation of MNC may have occurred too quickly to detect without continuous sampling. MNC concentrations of the same order of magnitude were detected in all experiments once DNT depletion was nearly complete. These results also show that the bacteria are capable of completely converting DNT into products that do not have nitrite bound to their structure. Although an analysis of the end products of metabolism was not performed, products are most likely not nitrated since analysis of Experiments SF6 and SF7 (Figures 4.4 and 4.5) shows a greater than stoichiometric increase in nitrite levels. An explanation for this is unknown. Standards of known nitrite concentration and spiked samples were analyzed. Values obtained were not in excess of expected values. One hypothesis is that MNC interferes with the analytical method, but this seems unlikely because the nitrite is still bound to the aromatic ring and it would not explain such a large excess of nitrite. Another hypothesis is that some ammonium in the culture medium is converted to nitrite by *P. PR7*. This type of phenomenon would probably have been observed in previous experiments conducted by Reardon, however. One last possible explanation is that mistakes were made in preparation of DNT for both the media and the standards such that in SF6 the DNT concentration was actually twice that thought and in SF7 it was one and one-half times that thought. This is probably not the case because standards were prepared separately from media. The same DNT standards were used for Experiments SF6 and SF7 because samples were analyzed in the same HPLC run.

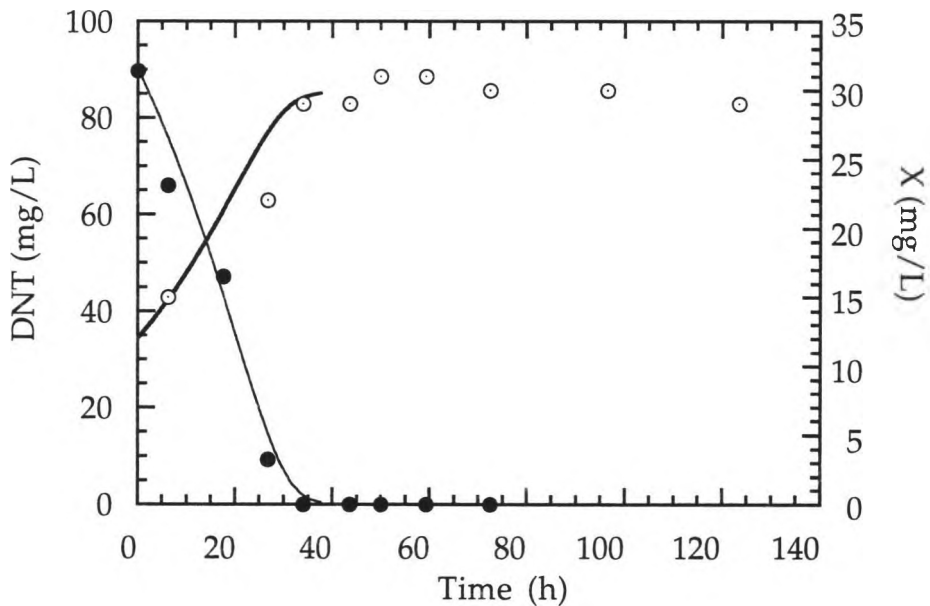


Figure 4.7: Monod model fit to experiment SF3. Model parameter values were: $\mu_{\max} = 0.04 \text{ h}^{-1}$, $K_s = 14.97 \text{ mg/L}$, and $Y_{x/s} = 0.198$.

In experiments SF6 and SF7, cell concentrations more than doubled over the course of an experiment. In experiments SF3, SF4, and SF5 cell concentrations just doubled. Because a rapid growth and substrate depletion phase was observed in experiments SF3, SF4, and SF5, it might be thought that the intrinsic kinetics could be accurately estimated from these experiments. It was determined that the Monod model could approximately fit the data (e.g., Figure 4.7), but the parameters μ_{\max} , K_s , and $Y_{x/s}$ estimated were different for each experiment. Similar μ_{\max} values near 0.04 h^{-1} were found, but K_s values varied from 10 to 40 mg/L, and the yield factor varied from as little as 0.16 to as much as 0.95 mg cells/mg substrate. The μ_{\max} parameter values did not agree with the value of 0.11 h^{-1} previously reported (Reardon 1992). The previously reported K_s value of 6.2 mg/L was outside

the range found from these experiments, but because the range was relatively broad, this is not conclusive. The combination of inoculum size and history was suspected to be the root cause of the variation in parameter values (Chudoba 1989; Templeton and Grady 1988). Therefore, future experiments were limited to an inocula size of 0.5% (v/v) and inoculum history was monitored and kept as consistent as possible between experiments.

4.1.3 Qualitative Results Observed

Effects of MNC on growth

Because MNC concentrations were not determined until later experiments, a quantitative analysis of the effect of MNC concentration on culture behavior was not performed at this stage. However, it was observed that exponential cell growth did not begin until the intensity of yellow color, indicating the presence of MNC, began to wane. It was concluded that the growth of *P. PR7* in the presence of DNT as a sole carbon and energy source does not occur until the metabolism of MNC has begun. The MNC is most likely ultimately metabolized to pyruvate, which is responsible for the production of energy in the form of ATP. It follows that an energy gain and subsequent growth does not result from the conversion of DNT to MNC but does result from the metabolism of the MNC or subsequent metabolites.

Effects of increased temperature

Several times throughout this work, an incubator thermostat malfunctioned and culture temperatures increased to 37 °C in one instance and to about 40 °C in others. Following such temperature increases, the culture solutions would turn a bright or even "dark" yellow color, presumably indicating the accumulation of MNC. When temperatures came

down to near 30 °C, the cultures remained yellow, indicating that the MNC was not being degraded. Transfer of culture solution into fresh SMSB/DNT medium resulted in growth without any appreciable increase in lag time. In some cases, MNC accumulation occurred without subsequent degradation and in others MNC accumulation occurred followed by disappearance. Different hypotheses on the results of temperature shock are presented. It could be that two similar strains coexist and that the strain responsible for MNC metabolism is more heat sensitive than the other. Another hypothesis is that a plasmid is responsible for the coding for MNC monooxygenase synthesis, induction, or both. Because plasmids are known to be sensitive to heat shock, and because previous research indicated that the genes for DNT and MNC degradation are on plasmids (Suen and Spain 1993), this is likely.

Effect of inoculum history on lag time

A final observation concerns the lag time before DNT degradation observed in cultures that were inoculated from cultures with varying histories. More than once, it was observed that in cultures transferred between test tubes for culture maintenance, lag times before the appearance of yellow intermediate were significantly shorter in tubes inoculated from TSB into DNT than in tubes inoculated from DNT into DNT. This partially contradicts the hypothesis that a microbial culture acclimated to a certain xenobiotic should degrade that xenobiotic more readily than a culture not acclimated to the xenobiotic. The basis of this hypothesis is that a culture accustomed to growing on a specific compound has induced the enzymes necessary for metabolism of the compound in larger concentrations than a culture not growing on that compound. An explanation of the observed phenomena could be that the culture grown in TSB carried the plasmids

necessary to code for the DNT degradation enzymes and also had sufficient stores of amino acids, carbohydrates, or other stored compounds to survive in large numbers in a new environment, and to begin producing enzymes rapidly, whereas the culture grown on DNT alone may have lacked sufficient stores of such building blocks and thus exhibited an extended lag time before the onset of DNT consumption and growth.

4.2 Batch Stirred-Tank Bioreactor Experiments

4.2.1 Results

The results from batch experiments performed in stirred-tank bioreactors are presented in Table 4.2 and in Figures 4.8 through 4.12. Experiments BR1, BR2, BR4, BR5, and BR6 were not pH-controlled, whereas experiments BR3, BR7, BR8, and BR9 were pH-controlled experiments.

Table 4.2: Suspended-cell stirred bioreactor experiments and conditions; all batches inoculated with a 0.5%v/v inocula grown in 1000 μM DNT until MNC had just disappeared.

| Exp.# | DNT ₀ (μM) | DNT _f (μM) | X ₀ (mg/mL) | X _f (mg/mL) | pH ₀ | pH _f | hrs until DNT=0 |
|-------|---------------------------------------|---------------------------------------|---------------------------|---------------------------|-------------------|-------------------|--------------------|
| BR1 | 694 | 10.4 | 1 | 38 | -- | -- | >145.5 |
| BR2 | 806 | 16 | 1 | 39 | 6.6 | 5.3 | >108 |
| BR3* | 320 | 0 | 4 | 60 | 6.9 | 6.8 | 75.33 |
| BR4 | 885 | 0 | 2 | 59 | 5.55 [†] | 3.0 [†] | 149 |
| BR5 | 440 | 0 | 2 | 40 | 6.02 [†] | 5.53 [†] | 69.5 |
| BR6 | 160 | 0 | 4 | 31 | 6.7 | 6.03 | 45 |
| BR7* | 800 | 0 | 1 | 60 | 6.81 | 6.9 | 130 |
| BR8* | 760 | 129 | 1 | 38 | 5.56 | 5.53 | ? |
| BR9* | 700 | 161 | 1 | 36 | 4.08 | 4.7 | ? |

*pH-controlled experiments; [†]pH probes thought to have gone out of calibration during autoclave cycle.

The data from all experiments is presented in one table. This was done to facilitate the discussion of intrinsic kinetics that were determined to be

common to pH-controlled and noncontrolled experiments. It was also done to ease comparisons between experiments that have one experimental condition varied, e.g., experiments BR2 and BR7 both had an initial DNT concentration of about 800 μM but BR7 was pH controlled and BR2 was not.

4.2.2 Analysis and Discussion

The Monod equation for growth and the corresponding equation for substrate depletion (Eqns. 2.2 and 2.3) were used as an initial attempt to mathematically describe the intrinsic kinetic behavior of DNT biodegradation by *P. PR7* in suspended-cell batch conditions. Parameters were estimated using SimuSolvTM Modeling and Simulation Software, a program for solving nonlinear differential equations. The parameters from the best fit of the

Table 4.3: Parameter values for best fit of Monod Model to experimental data

| Parameters from best fit of model | | | | | | Parameters used for model prediction | |
|-----------------------------------|-----------------------|-----------------------|-------------------|--------------------------------|-----------------------|--------------------------------------|-----------------------|
| Exp. # | X ₀ , mg/L | S ₀ , mg/L | Y _X /s | μ_{\max} , h ⁻¹ | K _S , mg/L | μ_{\max} , h ⁻¹ | K _S , mg/L |
| BR1 | 0.2 | 126.37 | 0.33 | 0.102 | 35.2 | 0.1 | 14 |
| BR2 | 0.2 | 147 | 0.26 | 0.099 | 14.0 | 0.1 | 14 |
| BR3,pH6.5* | 1.0 | 57.9 | 0.97 | 0.1128 | 14.34 | 0.1 | 14 |
| BR4 | 0.2 | 160 | 0.37 | 0.095 | 14.2 | 0.1 | 14 |
| BR5 | 0.1 | 81 | 0.40 | 0.10 | 13.0 | 0.1 | 14 |
| BR6 | 0.8 | 29.2 | 0.96 | 0.11 | 11.0 | 0.1 | 14 |
| BR7,pH6.5* | 0.005 | 145 | 0.4 | 0.08 | 11.0 | 0.1 | 14 |
| BR8,pH5.5* | 0.1 | 138 | 0.3 | 0.1 | 11.0 | 0.1 | 14 |
| BR9,pH4.5* | 0.1 | 128 | 0.27 | 0.1 | 11.0 | 0.1 | 14 |

* pH controlled experiments; model did not fit data as well as experiments without pH control.

model for each experiment are presented in Table 4.3. The right section of Table 4.3 shows the parameters used for model prediction of experimental data using the initial cell concentration and initial DNT concentration determined from initial samples. Figure 4.8 shows a Monod-model fit of experimental data and Figures 4.9 through 4.12 show subsequent predictions of experimental data by the model using parameter values shown in Table 4.3 ($\mu_{\max} = 0.1 \text{ h}^{-1}$ and $K_s = 14 \text{ mg/L}$). Model predictions are plotted with actual experimental data.

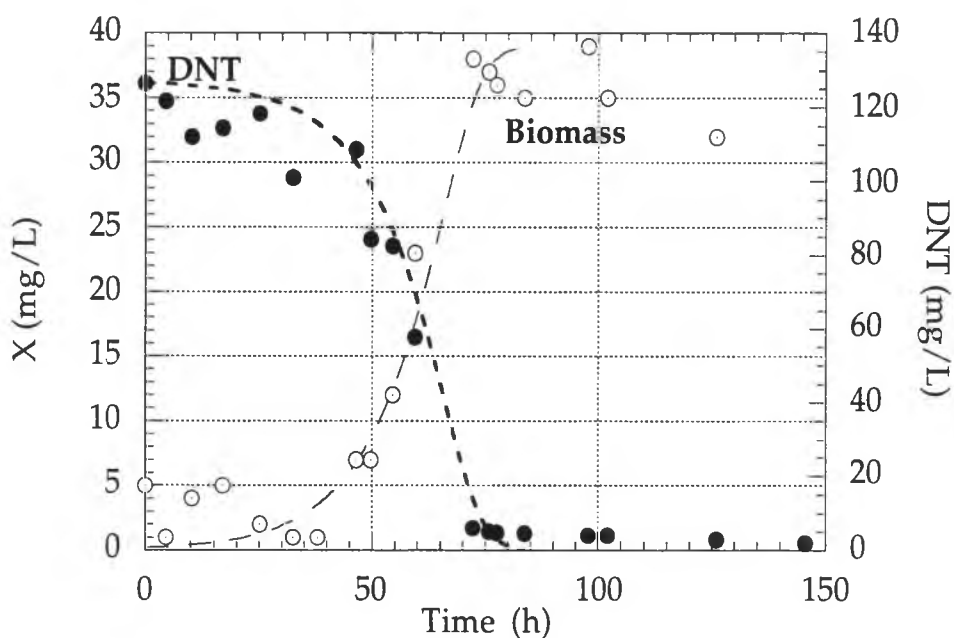


Figure 4.8: Monod-model fit of BR1 experimental data is represented by the dashed lines. Initial DNT concentration = 126 mg/L (694 μM); $Y_{X/s} = 0.33$; $\mu_{\max} = 0.102 \text{ h}^{-1}$; $K_s = 35.2 \text{ mg/L}$.

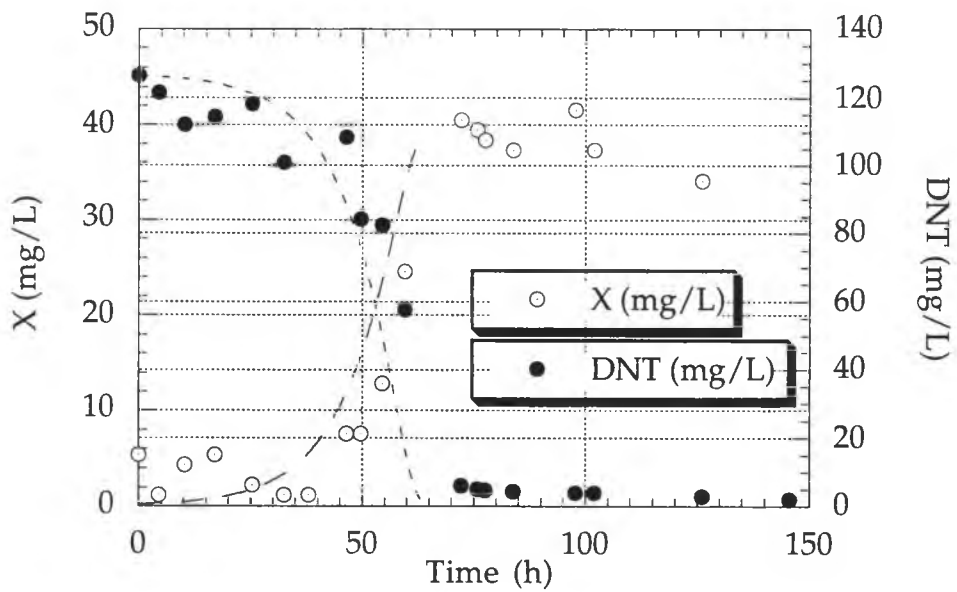


Figure 4.9: Model prediction of BR1 experimental data. Initial DNT concentration = 126 mg/L (694 μ M); $Y_{x/s} = 0.3$; $\mu_{max} = 0.1 \text{ h}^{-1}$; $K_s = 14.0 \text{ mg/L}$.

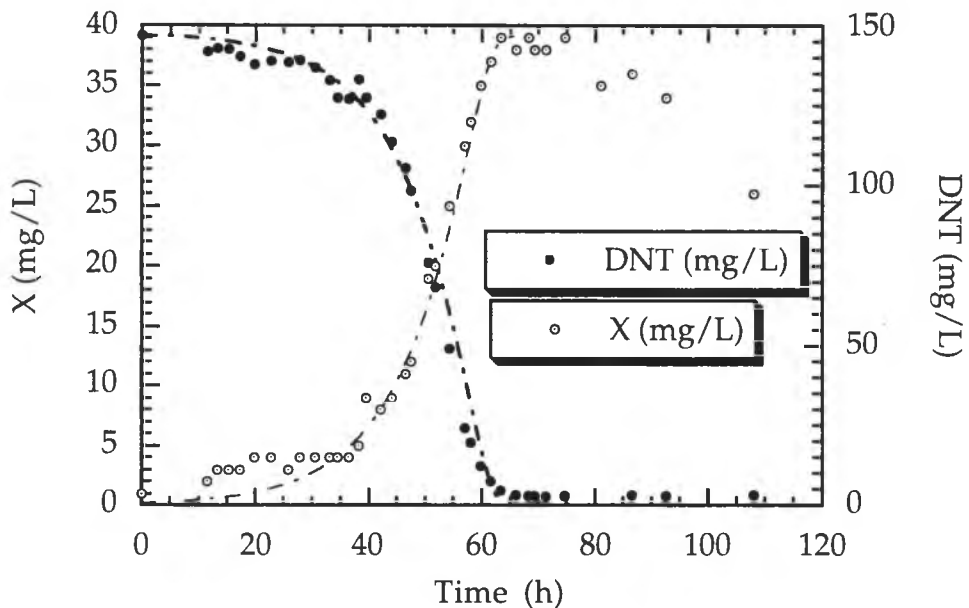


Figure 4.10: Monod-model prediction of BR2 experimental data. Initial DNT = 147 mg/L (806 μ M); $Y_{x/s} = 0.3$; $\mu_{max} = 0.1$; $K_s = 14.0 \text{ mg/L}$.

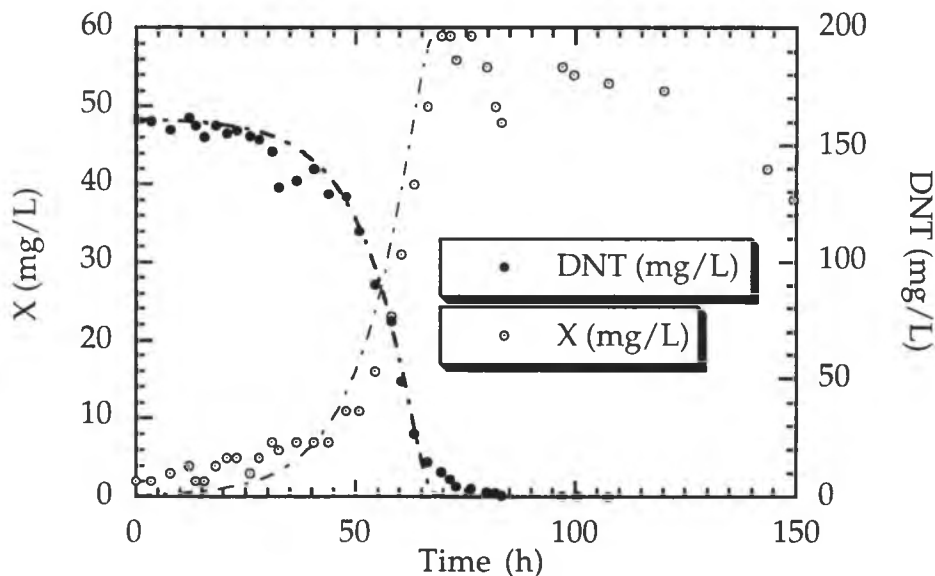


Figure 4.11: Monod-model prediction of BR4 experimental data. Initial DNT concentration = 160 mg/L (885 μ M); $Y_{x/s} = 0.3$; $\mu_{max} = 0.1$; $K_s = 14.0$ mg/L.

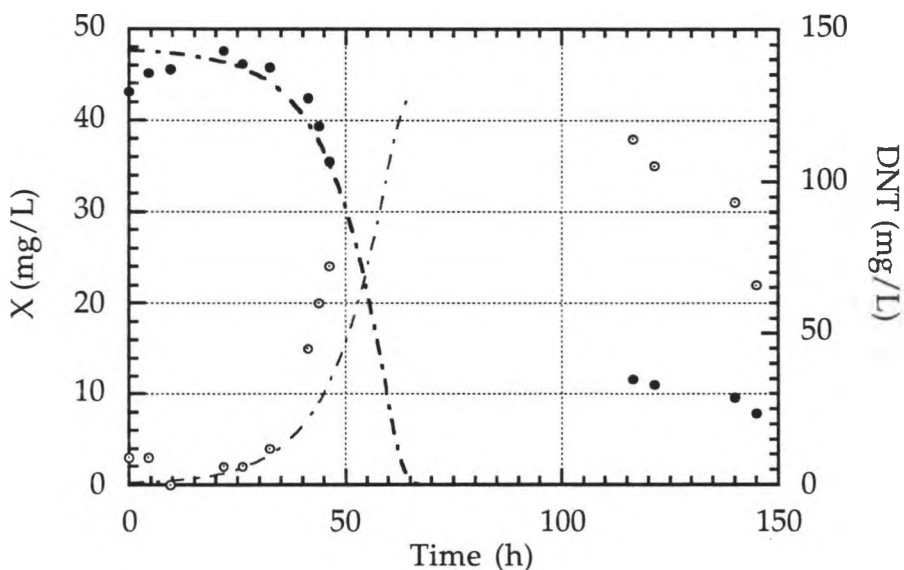


Figure 4.12: Monod-model prediction of BR8 experimental data, pH controlled at 5.5.

Figure 4.8 shows a fit of experimental data using the Monod model and SimuSolv™ to find values of the parameters μ_{\max} and K_s that best fit the data. The yield $Y_{X/s}$ was determined by calculation of the overall yield of cell mass produced per substrate mass utilized. The Monod model fit the data well, and the first attempt at fitting data gave μ_{\max} and K_s values of 0.1 h^{-1} and 14.0 mg/L respectively. Later, K_s was varied above and below 14.0 mg/L and for experiment BR1, a value of 35.2 mg/L was found to fit the data better. In other experiments, values of K_s were close to 14.0 mg/L . Model fits of experimental data for varying initial substrate concentrations gave similar parameters, with the exception of $Y_{X/s}$ which was usually calculated to be 0.3 but jumped to near 0.95 in a few experiments. The value of μ_{\max} was essentially the same as that found previously by Reardon, but the K_s value was not. The variation in K_s could be due to the fact that the previous value was determined by continuous experiments and the K_s value found here was determined by batch experiments. Due to the repeated prediction of experimental batch data with a K_s of 14.0 mg/L (Figures 4.9 to 4.11), this value can be used with confidence. These parameters also fall within the range found in the literature by Yoshinaga and coworkers. The $Y_{X/s}$ value of 0.30 is the same as the average found by their study (Yoshinaga, Hendricks et al. 1995).

Data from pH controlled experiments did not, however, fit the model as well. The initial rates of growth and substrate depletion matched model prediction fairly well (Figure 4.12), but substrate depletion tapered off and stopped altogether before DNT concentrations reached zero, with the exception of BR3.

4.3 Conclusions

Shake flask experiments gave some insight into the behavior of *P. PR7* under various conditions. Inocula size and history appears to have an effect on the lag time in an experiment. A small inoculum (0.5-1.0%) was found to give a more distinct exponential growth phase and to facilitate the determination of intrinsic kinetics through the estimation of Monod model parameters. Temperature also had an effect on the degradation of DNT. Temperatures over 35 °C disabled the degradation of DNT beyond the MNC intermediate in several cases. The optimum pH for the degradation of DNT by *P. PR7* in the experiments performed in this study is between 6.5 and 7.0.

As stated previously, with the exception of Experiment BR3, data from pH controlled experiments did not fit the model as well as data from noncontrolled experiments did. This phenomenon could be due to interaction of NaOH with DNT or with MNC. It is known that nitroaromatics react with alkaline chemicals to form colored, often red or orange compounds. An orange color appeared in all pH controlled experiments after addition of 1-N NaOH began. In some cases the color was more intense than in others. Experiments BR3 and BR9 showed more intense orange than BR7 and BR8. In BR7 and BR8 the orange color was barely more than a very deep yellow, and it disappeared as the experiment progressed. Further repetition of pH-controlled experiments would give more conclusive evidence. The repeat of the pH 6.5 experiment (BR3 and BR7) did not give similar enough data to be considered conclusive.

It is possible that *P. PR7* is capable of using MNC or DNT that has reacted with NaOH as long as it is in small concentrations. Another possibility is that DNT is transported into the cells easily when NaOH is not

present, but that a change in ionic strength, salt concentration, or a similar property interferes with the transport.

Finally, the degradation of DNT by *P. PR7* in batch experiments with an initial DNT concentration between 160 - 885 μM (29 - 161 mg/L) is described by the Monod model with $\mu_{\max} = 0.1 \text{ h}^{-1}$, $K_s = 14.0 \text{ mg/L}$, and $Y_{x/s} = 0.30$. Because the growth of *P. PR7* on DNT is slow, high suspended-cell concentrations were not reached. For this reason, it is concluded that continuous cultures of *P. PR7* degrading DNT would have to be operated at a very low dilution rates ($<0.1 \text{ h}^{-1}$). One method of increasing dilution rates possible and thereby increasing degradation rates is the use of immobilized cells. Immobilized-cell experiments were therefore carried out and are presented and discussed in the next chapter.

Chapter V FLUIDIZED-BED BIOREACTOR RESULTS & DISCUSSION

The fluidized-bed bioreactor (FBB) designed for this work was used for two main types of experiments: abiotic tracer studies to determine the mixing characteristics and continuous flow biotic experiments to determine the performance of the FBB using *Pseudomonas* PR7 immobilized on various particles and under various 2,4-DNT loading rates.

5.1 Mixing Analysis

Mixing experiments were performed to characterize the liquid mixing within the FBB during continuous flow conditions. The degree of liquid mixing can affect reaction conditions and productivity. Poor mixing can cause significant temperature, substrate, product, and pH gradients within the reactor. Gradients can cause such problems as accumulation of toxic products. The problems caused by gradients can often be alleviated by an increase in the degree of mixing. The mixing characteristics of a reactor must be known before it can be determined whether the desired mixing is achieved and whether or not a change in mixing could solve a problem.

5.1.1 Results

A step input tracer experiment was chosen for mixing analysis of the fluidized bed bioreactor system. Results of the experiment using a step input of 150 ppm NaCl are shown in Figure 5.1.

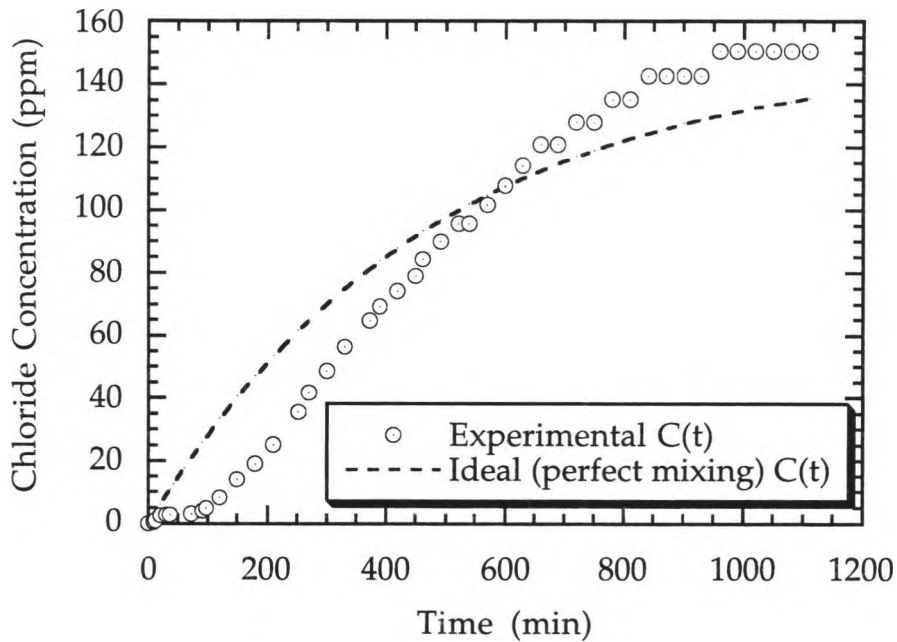


Figure 5.1: Result of mixing study in the fluidized-bed bioreactor.

5.1.2 Analysis and Discussion

A comparison of these data with the prediction for perfect mixing shows that there was not ideal mixing in the FBB. A tank-in-series model was plotted with the data to determine if the system behaved as two or more well-mixed tanks in series, but this did not appear to be the case. There are zones within the reactor that, due to the accumulation of particles, do not appear to have been well mixed. The bottom section of the reactor (approximately 200 mL) contained particles that recirculated slowly and in some places not at all. There was also periodic accumulation of particles visible in sampling ports along the sides of the bottom half of the reactor and constant accumulation of particles in the two bottom-most side ports. The

flow of particles was used as a visual indication of the flow of liquid within the FBB and the accumulation of particles in certain zones indicated poorer circulation of fluid through these zones.

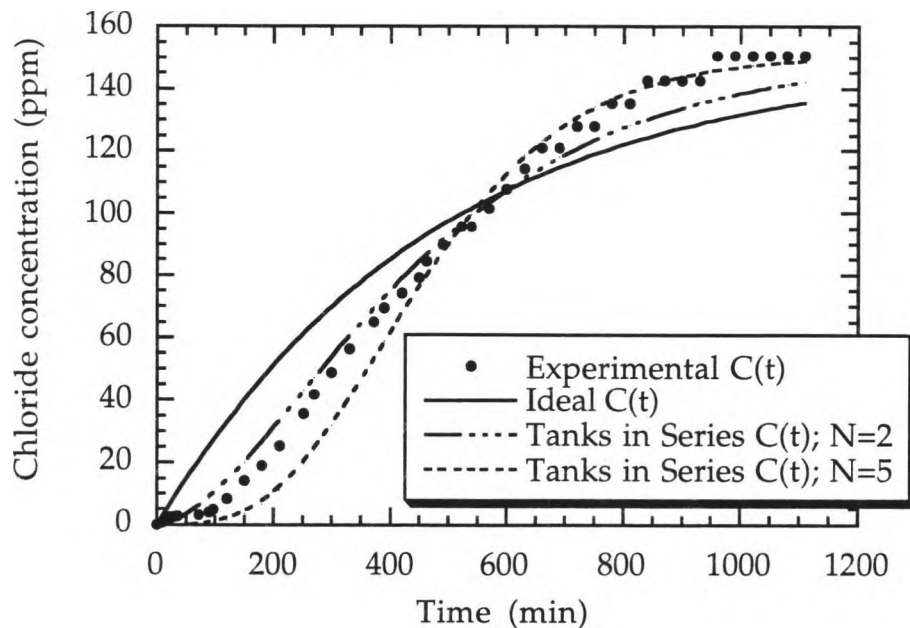


Figure 5.2: Experimental results of mixing study with tank-in-series models for $N=1$, $N=2$, and $N=5$ tanks.

The results from the mixing experiment therefore indicate the probable presence of dead zones and bypasses within the fluidized-bed bioreactor. It was estimated from the mixing experiment that approximately 200 mL of the system was not active. This was accomplished through an estimation of the total volume of the reactor based upon the mixing study results (Levenspiel 1989). The estimated active volume of the FBB based on the mixing experiment was approximately 200 mL less than the actual liquid volume.

5.2 DNT Degradation Experiments

5.2.1 Results

Results from the first FBB experiment (FBB1) are shown in Figure 5.3. *P. PR7* was immobilized on diatomaceous earth particles and feed substrate concentration was constant at 1000 μM (182 mg/L). The DNT loading rate was changed by shifting the dilution rate from 0.03 h^{-1} to 0.14 h^{-1} after 200 hours of continuous operation. At the lower dilution rate of 0.03 h^{-1} , the effluent DNT concentration stayed around 50 μM after a 55- to 65-hour acclimation or startup period. At the higher dilution rate of 0.14 h^{-1} , the effluent DNT concentration stabilized around 140 μM after approximately 24 hours for the remaining 20 hours of the experiment.

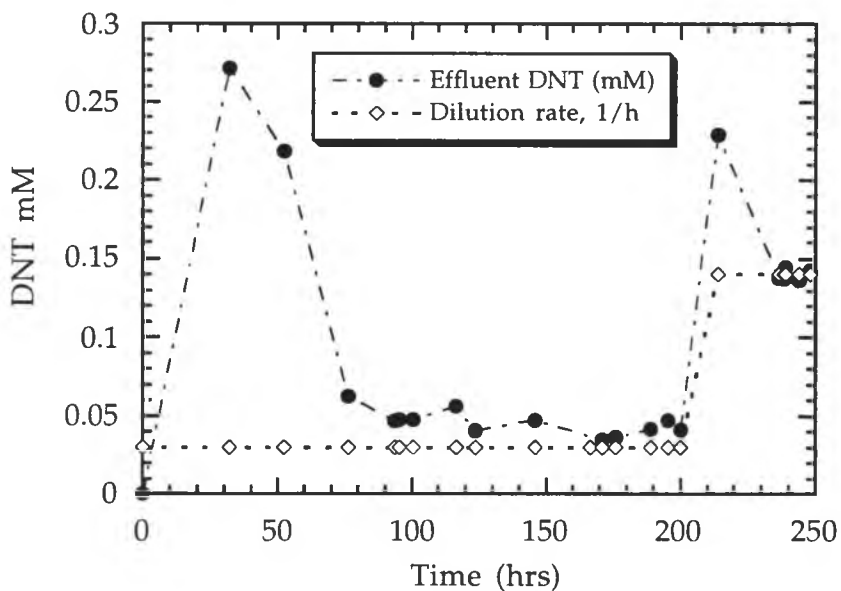


Figure 5.3: Fluidized-Bed Bioreactor Experiment FBB1 using diatomaceous-earth particles and feed DNT concentrations of 1000 μM .

A plot of the degradation rate as a function of the dilution rate for Experiment FBB1 is shown in Figure 5.4. For the two dilution rates used, the DNT degradation rate increased with an increase in the dilution rate.

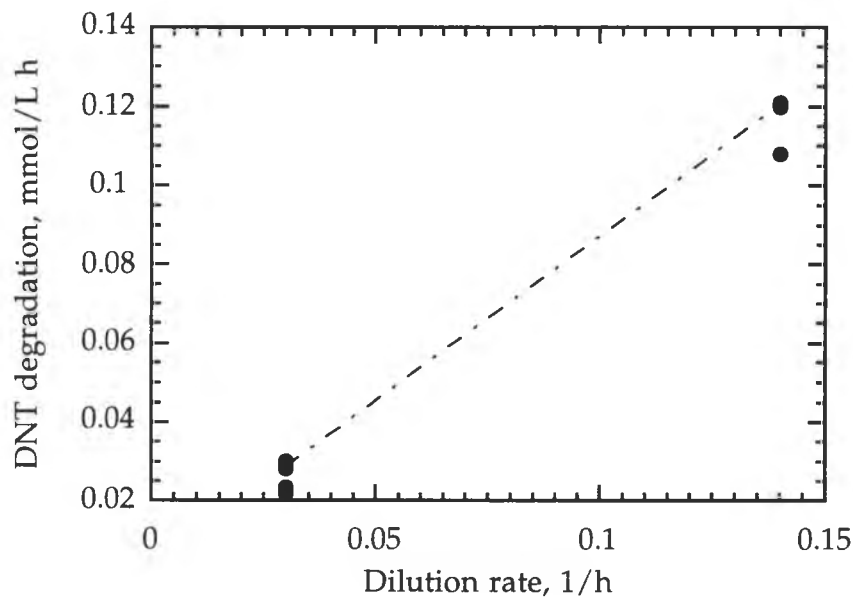


Figure 5.4: DNT degradation rate in the fluidized-bed bioreactor as a function of dilution rate for Experiment FBB1.

Results from the second and third FBB experiments (FBB2 and FBB3) are plotted in Figures 5.5 and 5.6. Cells were immobilized on polycarbonate particles in these experiments. In Experiment FBB2, the dilution rate was increased stepwise from 0.03 h^{-1} to 0.28 h^{-1} . Several times during the experiment, the tubing from the feed bottle to the feed pump developed a leak and suction from the feed bottle was lost. This resulted in no feed flow to the FBB for short periods of time. These instances are shown as dilution rates of zero in Figure 5.5.

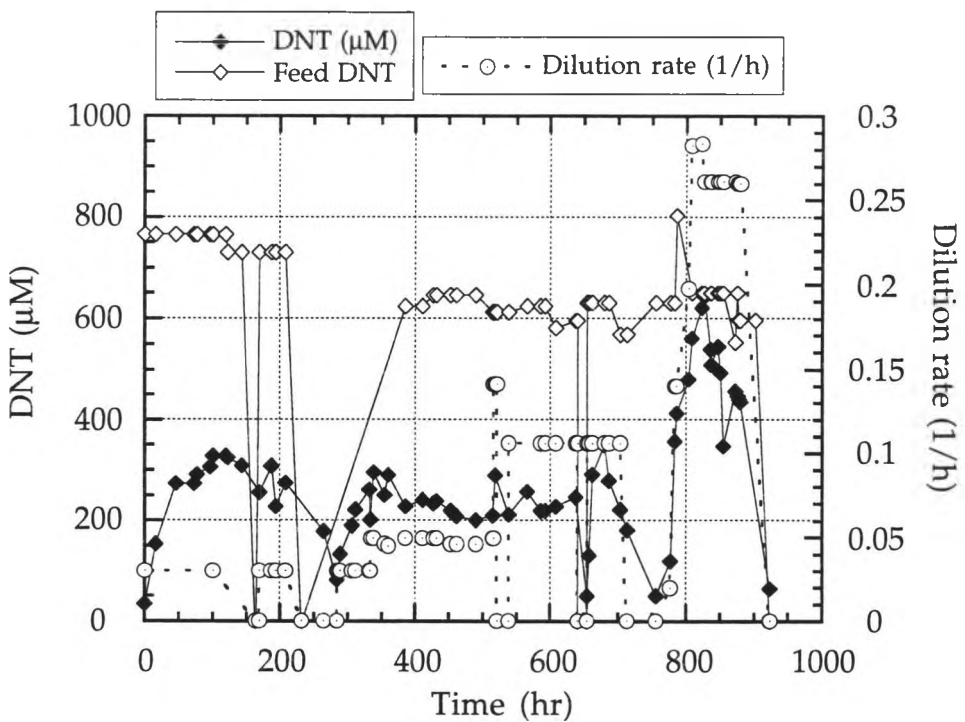


Figure 5.5: Experiment FBB2 using polycarbonate particles.

Experiment FBB3 was a repeat of Experiment FBB2. The feed line was secured to the fitting and new tubing was used to avoid further problems with erratic feed and dilution rates. The dilution rate was increased from 0.03 h^{-1} to 0.28 h^{-1} . Towards the end of the experiment, the DNT concentration in the effluent was lower than in the FBB, as shown in Figure 5.6. This was thought to be caused by accumulation of bacteria in the effluent lines and on a screen placed over the effluent port to keep particles in the FBB. Accumulation and growth of bacteria was also observed during the experiment in crevices in a clear plastic fitting on the effluent tubing and in tubing when the experiment was dismantled.

In both Experiment FBB2 and FBB3, the DNT concentration fell below 100 μM quickly when the feed was stopped. Overall, however, the DNT concentrations were higher than in Experiment FBB1 (diatomaceous earth particles) at comparable loading rates.

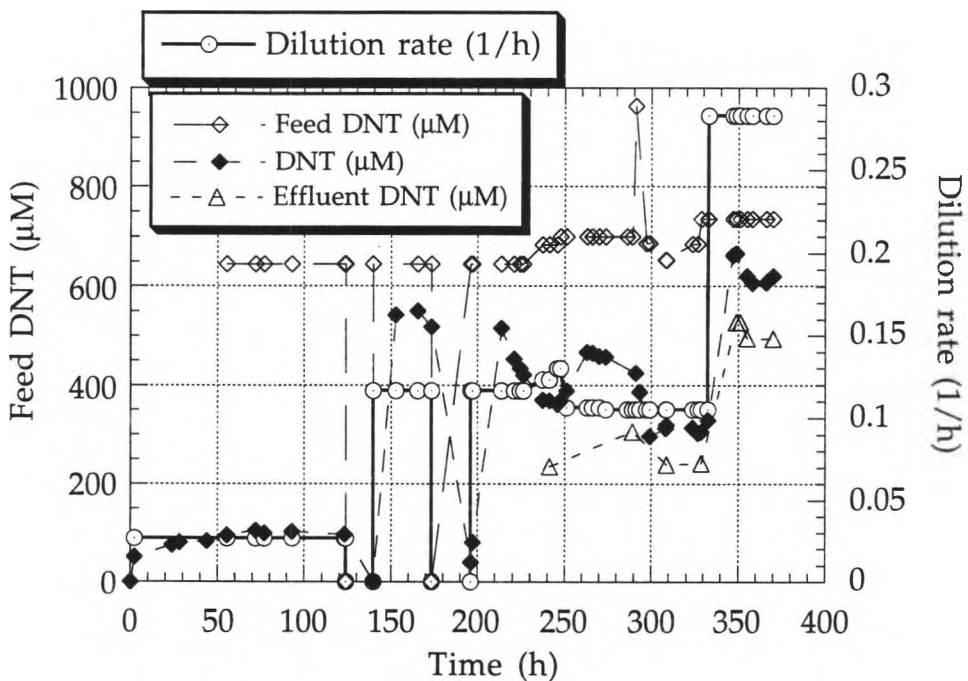


Figure 5.6: Repeated fluidized-bed bioreactor experiment (FBB3) using polycarbonate particles.

Experiment FBB4 incorporated pH control. Two different dilution rates and two different feed DNT concentrations were used in this experiment. The dilution rate was increased from 0.047 h^{-1} to 0.4 h^{-1} . At this point, the feed DNT concentration was increased from $675 \mu\text{M}$ to $880 \mu\text{M}$. The feed rate was then decreased after nine hours to return to the original dilution rate of 0.047 h^{-1} . The feed DNT concentration was kept at $880 \mu\text{M}$, however, so the final loading rate was higher than the first loading rate. The DNT concentrations in the FBB averaged around $35 \mu\text{M}$ during the first dilution rate, and returned to $45 \mu\text{M}$ after the dilution rate was increased and

then decreased. This could indicate that the cells recovered well from the disturbance. Further investigation is necessary for conclusive information.

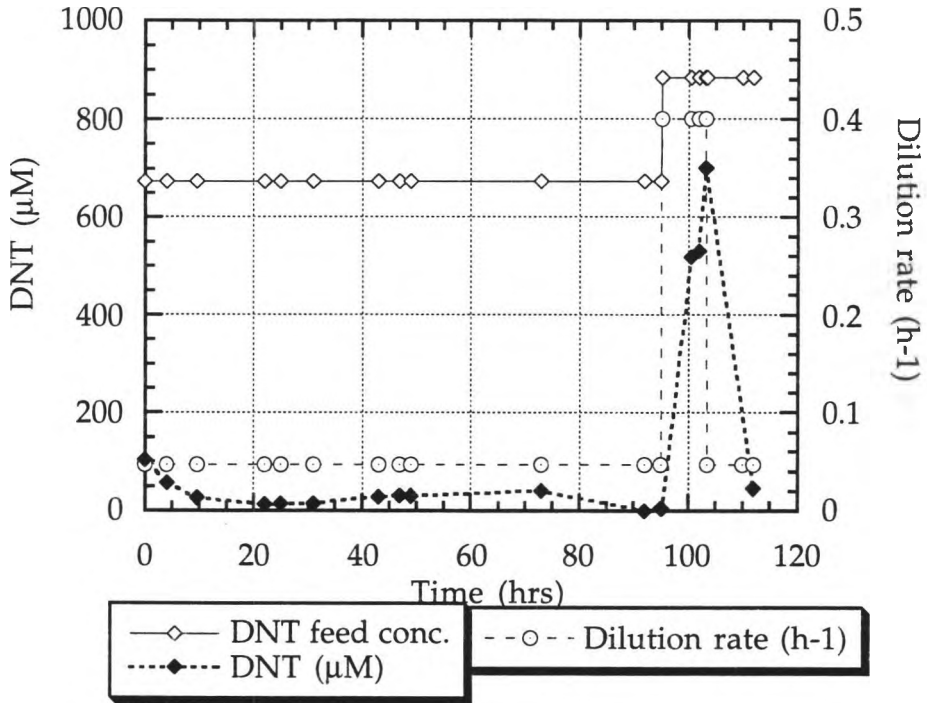


Figure 5.7: Experiment FBB4 using polycarbonate particles with pH controlled between 6.7 and 7.0 and DNT feed concentrations of 675 μM and 880 μM . Solid diamonds represent the effluent DNT concentration in μM .

5.2.2 Analysis and Discussion

In Experiment FBB1, DNT degradation rates increased with small increases in the loading rates. In experiments FBB2 and FBB3, DNT degradation rates increased with loading rates when loading rates were below 100 $\mu\text{M/L/h}$. At loading rates from 150 to 210 $\mu\text{M/L/h}$, degradation rates did not increase and at times decreased (Figures 5.8 and 5.9).

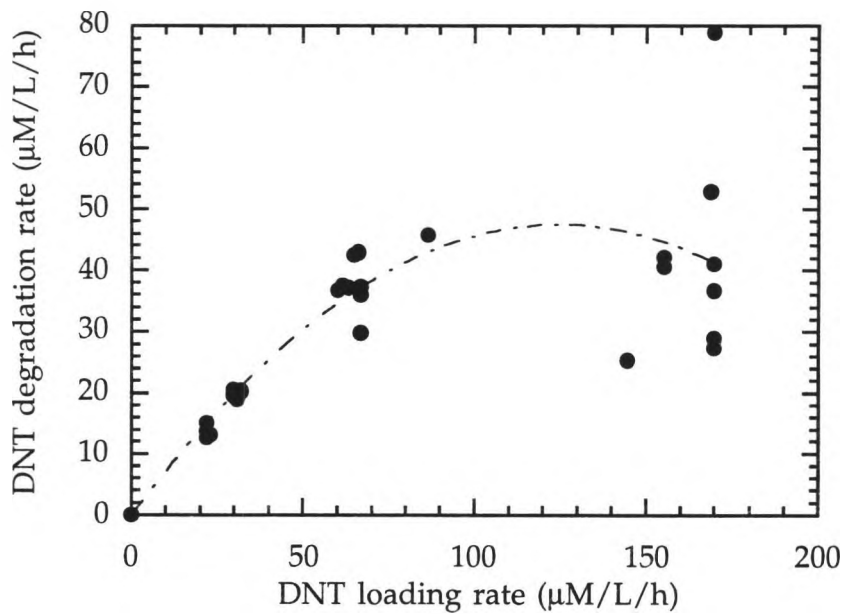


Figure 5.8: DNT degradation versus loading rates in the FBB for Experiment FBB2 using polycarbonate particles.

The highest degradation rates reached in these experiments were scattered between 35 and 52 $\mu\text{mol/L/h}$ at loading rates from 70 $\mu\text{mol/L/h}$ to 210 $\mu\text{mol/L/h}$. The maximum degradation rate using diatomaceous earth particles in the FBB was 120 $\mu\text{mol/L/h}$ at a loading rate of 140 $\mu\text{mol/L/h}$. The maximum degradation rate achieved with polycarbonate particles without pH control was 52 $\mu\text{mol/L/h}$ at a loading rate of 170 $\mu\text{mol/L/h}$. The maximum degradation rate achieved in the FBB using pH control and polycarbonate particles was 150 $\mu\text{mol/L/h}$ at a loading rate of 350 $\mu\text{mol/L/h}$. Previous experiments in a packed-bed recycle bioreactor system resulted in a maximum degradation rate of 325 $\mu\text{mol/L/h}$ at a loading rate of 450 $\mu\text{mol/L/h}$ (Reardon 1992).

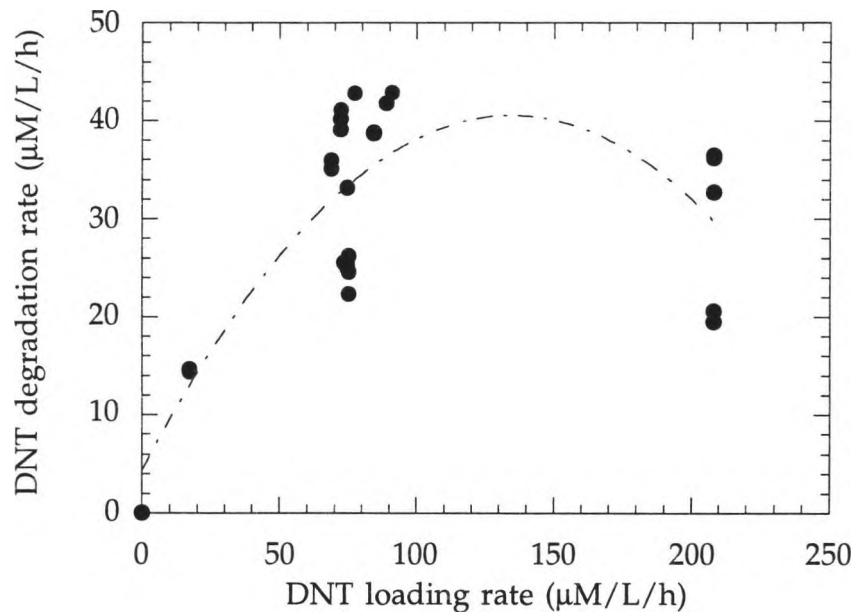


Figure 5.9: DNT degradation rates versus loading rates for Experiment FBB3 with polycarbonate particles.

The FBB using *P. PR7* bacteria performed better with respect to DNT degradation at various loading rates than did a suspended-cell continuous reactor studied previously (Reardon 1992). It did not, however, perform better than the recycle packed-bed system also characterized by Reardon. See Figure 5.10 for a comparison of degradation versus loading rates in the FBB to those in the packed-bed with recycle system. Higher cell loadings possible in the packed-bed column due to significantly lower shear rates are thought to be responsible for the difference in performance between these two systems.

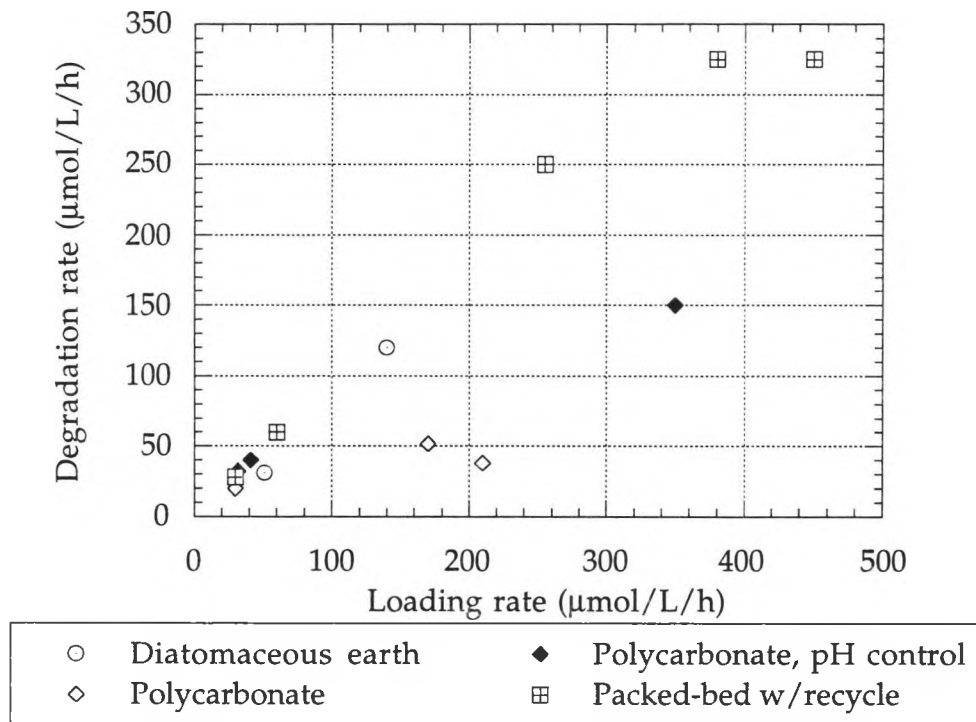


Figure 5.10: Comparison of the fluidized-bed bioreactor experiments to previous experiments in a packed-bed with recycle system.

5.3 Mass Transfer Considerations

The diffusivity D of DNT in water was estimated to be $0.92 \times 10^{-5} \text{ cm}^2/\text{s}$ by the Wilke-Chang correlation. An estimate of the mass-transfer coefficient k_s was calculated from this using the correlation given in Chapter 2 (Equation 2.6). For this FBB system, the estimated k_s is 0.003 cm/s . Particle volume/area V_p/A_p was calculated as 0.015 cm . Using these values and a cell concentration, X , of 10 mg/L and a bulk substrate concentration, S_b , of 45 mg/L , the Damköhler number Da was calculated as 0.0001 . This indicates an absence of external mass-transfer limitations under these conditions. Using a higher X , lower S_b , and a characteristic length of 0.1 cm (rather than V_p/A_p), Da was recalculated to be 0.003 . At steady-state conditions from the FBB

experiments, assuming $X = 30 \text{ mg/L}$, Da and the observable Damköhler number Ω were estimated to be less than 1.0 in all instances, indicating kinetic rather than external mass-transfer limiting conditions in the FBB. For FBB1, FBB2, FBB3, and FBB4, the square of the Thiele modulus ϕ^2 and the observable modulus Φ were also estimated. Values for the Damköhler number, observable Damköhler number, square of the Thiele modulus, and the observable modulus at various conditions are shown in Table 5.1. All values indicated the absence of either external or internal mass transfer limitations in the FBB.

Table 5.1: Estimated values of the Damköhler and observable Damköhler numbers and the Thiele and Observable moduli at various conditions where $D = 0.92 \times 10^{-5} \text{ cm}^2/\text{s}$ and $k_s = 0.003 \text{ cm/s}$.

| Expt. | S_{feed} mg/L | S_b mg/L | X mg/L | V_p/A_p or L, cm | $Y_{x/s}$ | μ_{\max} s ⁻¹ | R_{obs} mg/s | Da | Ω | ϕ^2 | Φ |
|-------|---------------------------|---------------|-----------|-----------------------|-----------|---------------------------------|--------------------------|--------|----------|----------|--------|
| Theo. | -- | 45.5 | 10.0 | 0.015 | 0.30 | 2.8E-5 | -- | 0.001 | -- | 0.013 | -- |
| Theo. | -- | 5.0 | 30.0 | 0.1 | 0.30 | 2.8E-5 | -- | 0.018 | -- | 0.024 | -- |
| FBB1 | 182 | 25.5 | 30.0 | 0.1 | 0.30 | 2.8E-5 | 0.0104 | 0.0036 | 0.014 | 0.024 | 0.26 |
| FBB1 | 109 | 36 | 30.0 | 0.1 | 0.30 | 2.8E-5 | 0.0017 | 0.0025 | 0.0016 | 0.024 | 0.03 |
| FBB2 | 123 | 56 | 30.0 | 0.1 | 0.30 | 2.8E-5 | 0.0033 | 0.0016 | 0.0019 | 0.024 | 0.037 |
| FBB3 | 137 | 91 | 30.0 | 0.1 | 0.30 | 2.8E-5 | 0.0060 | 0.0010 | 0.0022 | 0.024 | 0.042 |
| FBB4 | 123 | 8 | 30.0 | 0.1 | 0.30 | 2.8E-5 | 0.0027 | 0.012 | 0.0113 | 0.024 | 0.22 |
| FBB4 | 164 | 118 | 30.0 | 0.1 | 0.30 | 2.8E-5 | 0.0095 | 0.0007 | 0.0027 | 0.024 | 0.051 |

Due to the degree of mixing and high shear environment in the FBB, the estimated values of such numbers as the Damköhler number, the observable Damköhler number, the Thiele modulus, and the observable modulus, and the minimal amounts of growth on the polycarbonate particles, it was not necessary to take steps to improve mass-transfer in this system. Because Ω , Da , Φ , and ϕ^2 are always $\ll 1.0$, the process is always under

reaction rate control. It was noted, however, that in several instances these dimensionless numbers were significantly lower than 1.0, indicating severe reaction kinetics limitation. Practically, this indicates that mixing is higher than necessary to carry out an efficient reaction or that the biofilm density could be increased to some degree before mass transfer limitations occur. In experiments with higher degradation rates (FBB1 and FBB4), the dimensionless observable modulus Φ was close to 0.25 and the Damköhler and observable Damköhler were close to 0.01. The significance of this could be that external mass transfer was very fast compared to the kinetic rate but the internal mass transfer was only somewhat faster than the kinetic rate. A conclusion from this is that greater degradation efficiency might be gained more easily from decreasing the degree of mixing than from increasing the biofilm density. But because the two numbers are within an order of magnitude of one another and the values determined are estimations, the only significance might be that they are less than one, indicating no mass-transfer limitation and that is all.

Scanning electron microscope photographs of polycarbonate particles with and without biomass are shown in Figures 5.11, 5.12 and 5.13. The polycarbonate particles did not appear to support large amounts of *P. PR7* growth in the fluidized-bed bioreactor. The bacteria attached themselves to the polycarbonate particles when grown in low-shear (a culture tube shaken at low RPM) and no-shear (an unshaken and undisturbed culture tube) environments in significantly greater numbers than they did in the high-shear/high-abrasion environment of the fluidized bed. Nevertheless, a distinct biofilm was absent even from these particles. The plastic may not have been rough enough or porous enough to support a large biofilm.



Figure 5.11: SEM of the polycarbonate particles without bacteria attached.



Figure 5.12: SEM of *Pseudomonas* PR7 bacteria attached to the surface of a polycarbonate particle that was incubated in an unshaken test tube of DNT and SMSB.

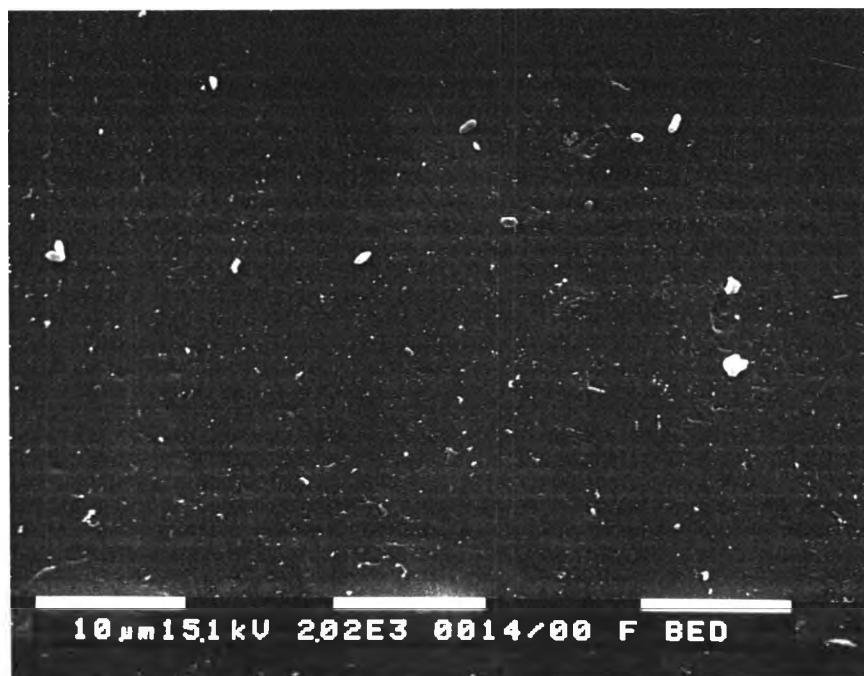


Figure 5.13: SEM of *Pseudomonas* PR7 bacteria attached to the surface of a polycarbonate particle that was from the fluidized-bed bioreactor while growing on DNT.

5.4 Conclusions

The mixing experiment performed in the FBB indicated that the mixing within the bioreactor was not ideal, or perfect, mixing. The mixing in the FBB also did not approximate a tank-in-series model. The estimated volume of the bioreactor based on the mixing experiment was 200 mL less than the actual measured liquid volume, indicating the presence of dead zones and/or bypasses. The presence of dead zones was also indicated by the apparent lack of liquid flow in some regions indicated by lack of particle flow.

With respect to DNT removal, the FBB performed better than a suspended-cell system but not better than a packed-bed system with recycle. The *P. PR7* immobilized on diatomaceous earth particles gave better

degradation versus loading rates in the FBB than cells immobilized on polycarbonate particles. But the diatomaceous earth particles sloughed and broke apart easily, clogging effluent and recycle lines. Experiment FBB4 using polycarbonate particles and pH control gave good degradation versus loading rates. A plastic particle may give better results than occurred here if it is more amenable to the attachment of bacteria. Bacteria did adhere to the inside surface of those polycarbonate particles that were hollow in the center. A more porous particle that has a density slightly greater than that of water and that can be autoclaved would probably fluidize well and give DNT degradation rates comparable to those in the packed-bed with recycle. Until further research is performed with the fluidized-bed bioreactor system, however, it is recommended that a packed-bed with recycle system be used.

Often during fluidization experiments, the air used for fluidization formed slugs of air that traveled up the length of the FBB carrying particles with them. The fluidization in the pH controlled experiment (FBB4) appeared to be significantly better. The bubbles were much finer and the particle motion formed a definite pattern. The particles traveled up through the center of the reactor, disengaged from the air flow, and settled down along the sides of the expansion at the top of the FBB. It is thought that the NaOH used for pH control may have acted as a surfactant, reducing bubble size therefore improving fluidization.

In the pH controlled experiment (FBB4), the DNT concentrations in the FBB averaged around 35 μM during the first dilution rate, and returned to 45 μM after the dilution rate was increased and then decreased. This could indicate that the cells recovered well from the disturbance of a sudden increase in the DNT loading rate. Further experiments should be performed

to confirm this because this experiment was not continued long enough at the higher dilution rate or after the return to the lower dilution rate.

Chapter VI SUMMARY

The oxidative degradation of 2,4-dinitrotoluene (DNT) by the bacterium *Pseudomonas* PR7 was studied in batch suspended-cell experiments and in continuous immobilized-cell fluidized-bed bioreactor experiments. *Pseudomonas* PR7 degrades DNT via the oxidative pathway studied by Suen and Spain (1993) for *Pseudomonas* DNT (Figure 2.1).

The intrinsic kinetics of the biodegradation of DNT were studied using suspended-cell batch experiments. It was determined that the biodegradation could be described by the Monod model for substrate consumption and cell growth (Equations 2.2 and 2.3). The parameter values determined by fitting experimental data to the Monod model are as follows: the maximum specific growth rate $\mu_{\max} = 0.1 \text{ h}^{-1}$, the Monod half-saturation constant $K_s = 14 \text{ mg/L}$, and the yield coefficient $Y_{x/s} = 0.30$. These values were successfully used in Monod-model predictions of experimental data (Figures 4.9 through 4.12).

The degradative capability of *P. PR7* was studied in an immobilized-cell three-phase fluidized-bed bioreactor using both diatomaceous earth and polycarbonate particles as immobilization media. Experiments with diatomaceous earth particles showed comparable degradative capacities to a previously studied packed-bed system at the low loading rates tested. However, the diatomaceous earth particles broke apart and sloughed fine particles during fluidization, causing clogging in effluent and recycle lines. Polycarbonate particles were chosen for study due to their durability, autoclavability, lack of toxicity, size and shape, cost, availability, and density

which was slightly greater than that of water. Although the polycarbonate particles did not break apart in the FBB, it was thought that they did not encourage cell adhesion to the extent that the diatomaceous earth particles did. The degradative rates in the FBB using polycarbonate particles were lower than those using diatomaceous earth particles. It was thought that the surface of the polycarbonate particles was too smooth to support cell adhesion under the abrasive conditions occurring in the FBB. It may be possible to roughen the surface of the polycarbonate particles to cause greater cell adhesion. This could be accomplished by treatment with a solvent such as acetone or with an acid which may alter and perhaps pit the surface of polycarbonate. It is also suggested that other, more porous polymeric materials with properties similar to polycarbonate be investigated for use as immobilization media.

Both suspended-cell batch and immobilized-cell continuous experiments were performed with and without pH control. The pH-controlled suspended-cell experimental data could be partially described by the Monod model using the parameters found from experimental data obtained without pH control. The Monod model predicts more complete degradation of DNT than occurred in pH-controlled batch experiments, however. The performance of the FBB using polycarbonate particles improved in an experiment where pH was controlled at approximately 7.0. Degradation rates in this experiment were higher than in FBB polycarbonate-particle experiments without pH control, but not as high as in the packed-bed with recycle system. The pH-controlled experiment should be repeated to obtain more conclusive evidence for the benefits of pH control in the FBB.

It is recommended that further experiments with the FBB be performed using higher dilution rates and higher DNT loading rates in order

to obtain more conclusive data to compare to the previously studied packed-bed system. Further experiments using pH control in the FBB should also be performed for comparison to the packed-bed system.

References

(1994). *Methods for General and Molecular Bacteriology*, American Society for Microbiology, Washington, D.C.

An, D., D. T. Gibson and J. C. Spain. (1994). "Oxidative release of nitrite from 2-nitrotoluene by a three-component enzyme system from *Pseudomonas* sp. strain JS42." *J. Bacteriol.*, **176**(24), 7462-7.

Bailey, J. E. and D. F. Ollis. (1986). *Biochemical Engineering Fundamentals*, McGraw-Hill.

Bauer, J. E. and D. G. Capone. (1988). "Effects of Co-Occurring Aromatic Hydrocarbons on Degradation of Individual Polycyclic Aromatic Hydrocarbons in Marine Sediment Slurries." *Applied and Environmental Microbiology*, **54**(7), 1649-1655.

Cain, R. B. (1958). "The microbial metabolism of nitroaromatic compounds." *J. Gen. Microbiol.*, **19**, 1-14.

Cain, R. B. (1966). "Utilization of anthranilic and nitrobenzoic acids by *Norcardia opaca* and a flavobacterium." *J. Gen. Microbiol.*, **42**, 219-235.

Chudoba, J. (1989). "Discussion of: Effect of culture history on the determination of biodegradation kinetics by batch and fed-batch techniques." *Journal of Water Pollution Control Federation*, **61**(3), 367-369.

Conuel, J. (1994). "Cometabolic Biodegradation of TCE & Toluene," Master's Thesis, Colorado State University, Fort Collins, CO.

Dey, S., P. Kanekar and S. H. Godbole. (1986). "Aerobic microbial degradation of *m*-dinitrobenzene." *Indian J. Environ. Health*, **29**, 118-128.

Ecker, S., H.-J. Knackmuss and C. Bruhn. "Catabolism of 2,6-dinitrophenol by *Alcaligenes eutrophus* JMP222, abstr. Q-198." *89th Annu. Meet. Am. Soc. Microbiol.*, Washington, D. C., 168.

Fan, L.-S. (1989). *Gas-Liquid-Solid Fluidization Engineering*, Butterworth Publishers, Stoneham, MA.

Feist, C. F. and G. D. Hegeman. (1969). "Phenol and Benzoate Metabolism by *Pseudomonas putida*: Regulation of Tangential Pathways." *Journal of Bacteriology*, **100**(2), 869-877.

Fernando, T., J. A. Bumpus and S. D. Aust. (1990). "Biodegradation of TNT (2,4,6-trinitrotoluene) by *Phanerochate chrysosporium*." *Appl. Environ. Microbiol.*, **56**, 1666-1671.

Geankoplis, C. (1983). *Transport Processes and Unit Operations*, Allyn and Bacon, Inc., Newton, Massachusetts.

Gorontzy, T., J. Kuver and K. H. Blotevogel. (1993). "Microbial transformation of nitroaromatic compounds under anaerobic conditions." *J. Gen. Microbiol.*, **139**(6), 1331-6.

Gundersen, K. and H. L. Jensen. (1956). "A soil bacterium decomposing organic nitro-compounds." *Acta Agric. Scand.*, **6**, 100-114.

Haigler, B. E. and J. C. Spain. (1991). "Biotransformation of Nitrobenzene by Bacteria Containing Toluene Degradative Pathways." *Applied and Environmental Microbiology*, **57**(11), 3156-3162.

Hallas, L. E. and M. Alexander. (1983). "Microbial transformation of nitroaromatic compounds in sewage effluent." *Appl. Environ. Microbiol.*, **45**, 1234-1241.

Hutchinson, D. H. and C. W. Robinson. (1988). "Kinetics of the simultaneous batch degradation of *p*-cresol and phenol by *Pseudomonas putida*." *Applied Microbiology and Biotechnology*, **29**, 599-604.

Karel, S. F., S. B. Libicki and C. R. Robertson. (1985). "The Immobilization of Whole Cells: Engineering Principles." *Chemical Engineering Science*, **40**(8), 1321-1354.

Klecka, G. M. and W. J. Maier. (1988). "Kinetics of Microbial Growth on Mixtures of Pentachlorophenol and Chlorinated Aromatic Compounds." *Biotechnology and Bioengineering*, **31**, 328-335.

Kulpa, C. and M. Wilson. "Degradation of trinitrotoluene by a mixed microbial culture isolated from soil, abstr. A-159." *91st Annu. Meet. Am. Soc. Microbiol.*, Washington, D. C., 303.

Kwauk, M. (1992). *Fluidization: idealized and bubbleless, with applications*, Science Press, Bejing, China.

Lee, J., H.-L. Chang, S. J. Parulekar and J. Hong. (1991). "An Alternate Method for Estimation of Cell Growth Kinetics from Batch Cultures." *Biotechnology and Bioengineering*, **37**, 26-34.

Levenspiel, O. (1989). *The Chemical Reactor Omnibook*, OSU Book Stores, Inc., Corvallis, OR.

Liu, D., K. Thomson and A. C. Anderson. (1984). "Identification of Nitroso Compounds from Biotransformation of 2,4-Dinitrotoluene." *Appl. Environ. Microbiol.*, **47**, 1295-1298.

McCormick, N. G., J. H. Cornell and A. M. Kaplan. (1978). "Identification of Biotransformation Products from 2,4-Dinitrotoluene." *Appl. Environ. Microbiol.*, **35**, 945-948.

McCormick, N. G., F. E. Feeherry and H. S. Levinson. (1976). "Microbial Transformation of 2,4,6-Trinitrotoluene and Other Nitroaromatic Compounds." *Appl. Environ. Microbiol.*, **31**, 949-958.

Monod, J. (1942). *Recherches sur la croissance des cultures bactériennes*, Herrmann et Cie, Paris.

Neumeier, W., R. Haas and E. V. Low. (1989). "Microbieller Abbau von Nitroaromaten aus einer ehemaligen Sprengstoffproduktion." *Forum Staedte-Hyg.*, 37, 32-37.

Nishino, S. F. (1994). Personal communication.

Prescott, L. M., J. P. Harley and D. A. Klein. (1993). *Microbiology*, Wm. C. Brown Publishers, Dubuque, IA.

Reardon, K. F. (1992). "Immobilized Cell Bioreactor for 2,4-Dinitrotoluene Degradation." , Colorado State University, Fort Collins, CO.

Reardon, K. F. and J. C. Spain. (1995). "2,4-Dinitrotoluene Biodegradation by Free and Immobilized *Pseudomonas PR7*." (in preparation).

Sax, N. I. and R. J. Lewis. (1987). *Hazardous Chemicals Desk Reference*, Van Nostrand Reinhold Company Inc., New York.

Shieh, W. K. and J. D. Keenan. (1986). "Fluidized Bed Biofilm Reactor for Wastewater Treatment." *Advances in Biochemical Engineering/Biotechnology*, A. Fiechter, ed., Springer-Verlag, Berlin, 132-167.

Shreve, G. S. and T. M. Vogel. (1993). "Comparison of Substrate Utilization and Growth Kinetics Between Immobilized and Suspended *Pseudomonas* Cells." *Biotechnology and Bioengineering*, **41**, 370-379.

Song, G. H., F. Bavarian, L.-S. Fan, R. D. Buttke and L. B. Peck. "paper presented at AIChE Annual Meeting." *AIChE Annual Meeting*, New York.

Spain, J. C., O. Wyss and D. T. Gibson. (1979). "Enzymatic oxidation of *p*-nitrophenol." *Biochem. Biophys. Res. Commun.*, **88**, 634-641.

Spain, J. C., G. J. Zylstra, C. K. Blake and D. T. Gibson. (1989). "Monohydroxylation of Phenol and 2,5-Dichlorophenol by Toluene Dioxygenase in *Pseudomonas putida* F1." *Applied and Environmental Microbiology*, **55**(10), 2648-2652.

Spanggord, R. J., J. C. Spain, S. F. Nishino and K. E. Mortelmans. (1991). "Biodegradation of 2,4-Dinitrotoluene by a *Pseudomonas* sp." *Applied and Environmental Microbiology*, **57**(11), 3200-3205.

Stayner, L. T., A. L. Dannenberg, T. Bloom and M. Thun. (1993). "Excess Hepatobiliary Cancer Mortality among Munitions Workers Exposed to Dinitrotoluene." *Journal of Occupational Medicine*, **35**(3), 291-296.

Stayner, L. T., A. L. Dannenberg, M. Thun, G. Reeve, T. F. Bloom, M. Boeniger and W. Halperin. (1992). "Cardiovascular mortality among munitions workers exposed to nitroglycerin and dinitrotoluene." *Scand J Work Environ Health*, **18**, 34-43.

Suen, W.-C. and J. C. Spain. (1993). "Cloning and Characterization of *Pseudomonas* sp. Strain DNT Genes for 2,4-Dinitrotoluene Degradation." *Journal of Bacteriology*, **175**(6), 1831-1837.

Templeton, L. L. and C. P. L. Grady Jr. (1988). "Effect of culture history on the determination of biodegradation kinetics by batch and fed-batch techniques." *Journal of Water Pollution Control Federation*, **60**(5), 651-658.

Tewfik, M. S. and W. C. Evans. (1966). "The metabolism of 3,5-dinitro-o-cresol (DNOC) by soil microorganisms." *Biochem. J.*, **99**, 31-32.

Unkefer, P. J., M. A. Alvarez, J. L. Hanners, C. J. Unkefer, M. Stenger and E. A. Margiotta. (1990). "Bioremediation of explosives." JANNAF Safety and Environmental Protection Subcommittee Workshop: alternatives to open burning/open detonation of propellants and explosives, Chemical Propulsion Information Agency, Laurel, Md., 307-326.

Valli, K., B. J. Brock, D. K. Joshi and H. M. Gold. (1992). "Degradation of 2,4-Dinitrotoluene by the Lignin-Degrading Fungus *Phanerochaete chrysosporium*." *Appl. Environ. Microbiol.*, **58**, 221-228.

Wu, K.-Y. A. and K. D. Wisecarver. "Biological Phenol Degradation in a Countercurrent Three-Phase Fluidized Bed Using a Novel Cell Immobilization Technique." *Advances in Fluidization Engineering*.

Yang, J.-D. and N. S. Wang. (1992). "Oxygen Mass Transfer Enhancement via Fermentor Headspace Pressurization." *Biotechnology Progress*, **8**, 244-251.

Yoshinaga, J. K., D. W. Hendricks and D. A. Klein. (1995). "Microbial Growth Kinetics for Natural/Synthetic Organic Compounds: Kinetic Coefficients and Influences of Operating Conditions." , Colorado State University, Fort Collins, CO.

Zeyer, J. and P. C. Kearney. (1984). "Degradation of *o*-nitrophenol and *m*-nitrophenol by a *Pseudomonas putida*." *J. Agric. Food Chem.*, **32**, 238-242.

Appendix I: Physical Properties of DNT and Other Nitroaromatics

The physical properties of 2,4-dinitrotoluene, 2,6-dinitrotoluene, 2,4,6-trinitrotoluene and 4-methyl-5-nitrocatechol are listed in Table A1.1 below.

Table A1.1: Physical properties of selected nitroaromatic compounds.

| Compound | Molecular Weight | Melting Point (°C) | Boiling Point (°C) | Solubility in water (mM) | Solubility in methanol |
|--------------------------|------------------|--------------------|---------------------------|--------------------------|------------------------|
| 2,4-dinitrotoluene | 182.14 | 70-1 | 300 (slightly decomposes) | 1400 mM | soluble |
| 2,6-dinitrotoluene | 182.14 | -- | | | slightly soluble |
| 2,4,6-trinitrotoluene | 227.13 | 82 | 240 exp | | slightly soluble |
| 4-methyl-5-nitrocatechol | 169.14 | | | very soluble | soluble |

Appendix II: Preparation of Spain's Mineral Salts Base

Stock solutions of the mineral salts base are diluted by addition to a specific volume of deionized water in which the desired concentration of 2,4-dinitrotoluene, succinate or other carbon source has been dissolved. The final concentrations of the salts are:

| | | |
|---|------------|--------------|
| MgSO ₄ ·7H ₂ O | 112.5 mg/L | (0.457 mM) |
| ZnSO ₄ ·7H ₂ O | 5.0 mg/L | (0.174 mM) |
| Na ₂ MoO ₄ ·2H ₂ O | 2.5 mg/L | (0.010 mM) |
| KH ₂ PO ₄ | 340 mg/L | (2.5 mM) |
| Na ₂ HPO ₄ ·7H ₂ O | 670 mg/L | (2.5 mM) |
| CaCl ₂ | 13.8 mg/L | (0.125 mM) |
| FeCl ₃ | 0.125 mg/L | (0.00077 mM) |
| NH ₄ Cl | 500 mg/L | (9.34 mM) |

First, prepare the DNT solution: dissolve 1.82 g DNT in 10 L deionized water or 1.467 g DNT in 8 L deionized water for a 1000 µM solution. Heat fairly vigorously but not to boiling (about 3 or 4 on most stirrer/hot plates). It will take 8 to 10 hours to dissolve. If a few small crystals remain undissolved, they will dissolve in the autoclave, but large crystals (about 8-10 mm +) will melt and not dissolve. Allow to cool until tepid or at room temperature before adding salts. If solution is warm, a precipitate will form. Usually somewhere below 30 °C is sufficient.

Add the SMSB solutions while stirring in the order given in Table A2.1, allowing a minute or two between additions to ensure

fairly uniform concentrations. This will decrease the likelihood of precipitation of insoluble salts.

Table A2.1: Preparation of Spain's Mineral Salts Base.

| Stock Solution | Constituents | Add to 1 Liter: | Add to 10 Liters: | Add to 8 Liters: |
|--------------------------|---|-----------------|-------------------|------------------|
| Solution A: | MgSO ₄ ·7H ₂ O, 22.5 g/L ZnSO ₄ ·7H ₂ O, 1.0 g/L Na ₂ MoO ₄ ·2H ₂ O, 0.5 g/L | 5 mL | 50 mL | 40 mL |
| Solution B: | KH ₂ PO ₄ , 68 g/L Na ₂ HPO ₄ ·7H ₂ O, 134 g/L or anhydrous, 70.98 g/L | 5 mL | 50 mL | 40 mL |
| Solution C: | CaCl ₂ , in 0.50 L use 13.75g OR CaCl ₂ ·2H ₂ O, 18.38g/0.5L | 0.5 mL | 5 mL | 4 mL |
| Solution D: | FeCl ₃ ·6H ₂ O, 0.208 g/0.5L OR FeCl ₃ , 0.125 g/0.5L | 0.5 mL | 5 mL | 4 mL |
| NH₄Cl: | NH ₄ Cl, 100 g/L | 5 mL | 50 mL | 40 mL |

Appendix III: Calibrations of Analytical Methods

Calibrations of analytical methods for DNT and MNC were performed on the Maxima Workstation that controlled the HPLC analytical system. Calibrations of analytical methods for nitrite and protein (BCA method) were performed on the spectrophotometer. Calibration curves are shown in Figures A3.1 through A3.4. Examples of calibration reports for each method are included in this appendix.

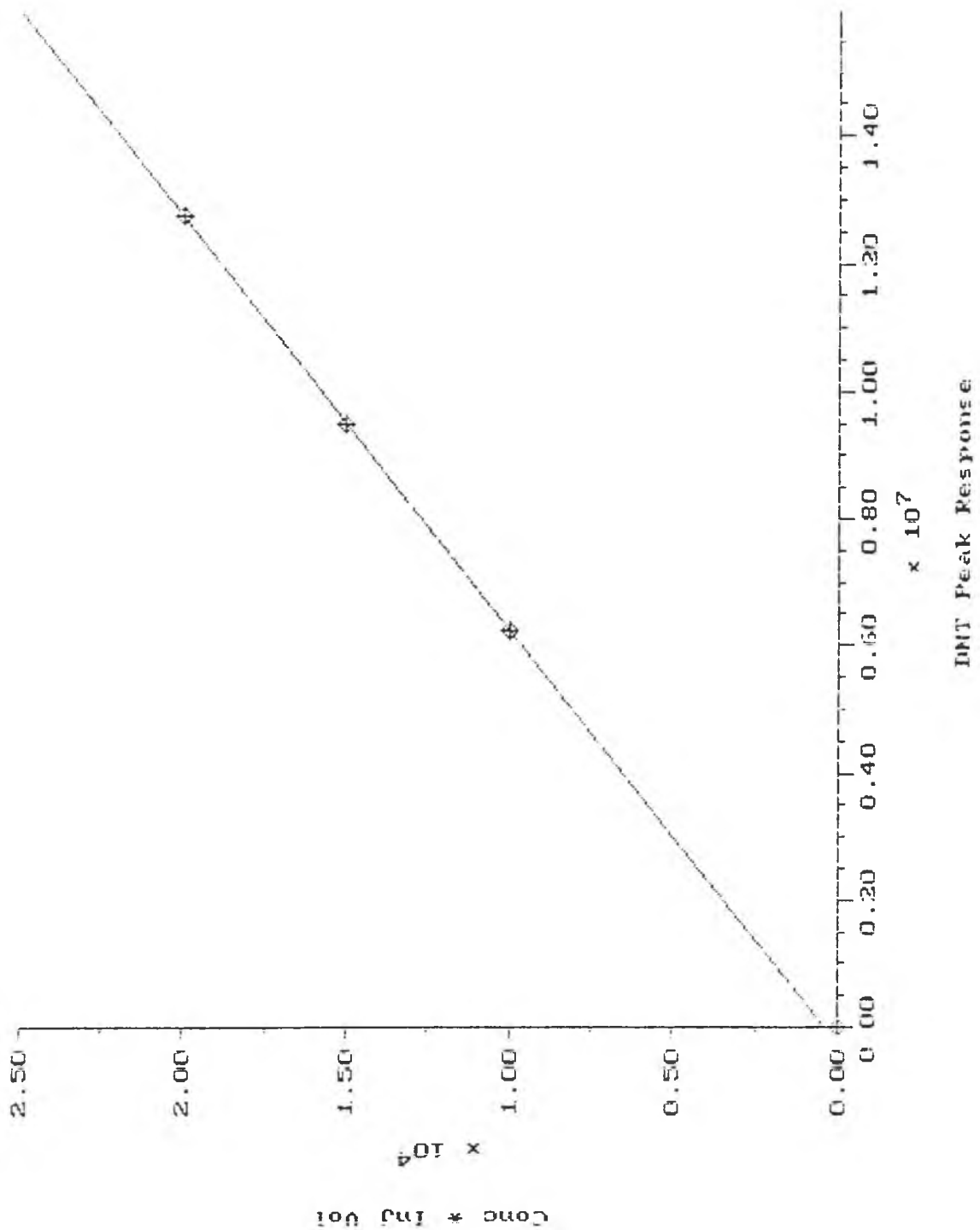


Figure A3.1: Calibration of DNT concentration versus absorption peak response at $\lambda = 230$ nm from HPLC analysis.

DNT Calibration Report

Printed: 1-JUN-1995 15:20:36

Quant Basis: Area Rejection Tolerance: None Internal Standard: None
Curve Type: Linear Weighting: None Forced Through Origin: No
Y-axis Label: Concentration
Corr. Coef. (r): 0.9999833 Coef. of Determination (r²): 0.9999665

Equation: Conc^t(Inj Vol) = 4.201132E+02 + 1.533465E-03 * R

| Sample | File Name | Valid | Concentration | Response | Calc'd Concentration | S Deviation | Response Factor |
|------------|-----------|-------|---------------|----------------|----------------------|-------------|-----------------|
| BLANK | BLANK | Y | 0.000000E+00 | 0.0000000E+00 | 2.100566E+01 | -1.00E+02 | Invalid |
| S95DNT500 | S95DNT5 | Y | 5.000000E+02 | 6.2582240E+06 | 5.008440E+02 | -1.69E-01 | 1.597897E-03 |
| S95DNT750 | S95DNT75 | Y | 7.500000E+02 | 9.4860090E+06 | 7.483287E+02 | 2.23E-01 | 1.581276E-03 |
| S95DNT1000 | S95DNT10 | Y | 1.000000E+03 | 1.27791858E+07 | 1.000827E+03 | -8.27E-02 | 1.563045E-03 |

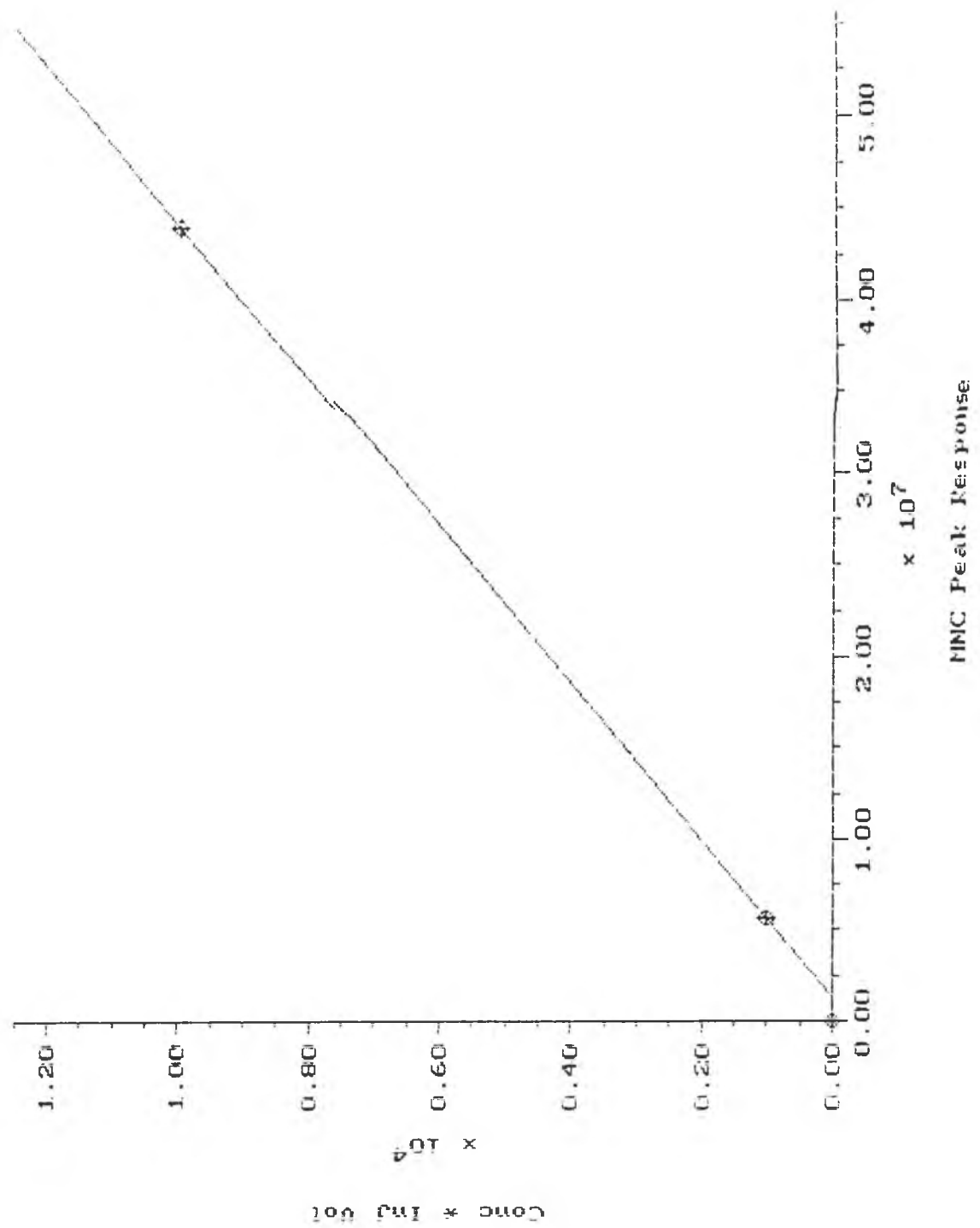


Figure A3.2: Calibration of MNC concentration versus absorption peak response at $\lambda = 230$ nm from HPLC analysis.

MNC Calibration Report

Printed: 7-AUG-1995 14:32:12

Quant Basis: Area Rejection Tolerance: None Internal Standard: None
Curve Type: Linear Weighting: None Forced Through Origin: No
Y-axis Label: Concentration
Corr. Coef. (r): 1.000000 Coef. of Determination (r²): 1.000000

$$\text{Equation: Conc} \times \{\text{Inj Vol}\} = -2.967585E+02 + 2.313482E-04 \times R$$

| Sample | File Name | Valid | Concentration | Response | Calc'd Concentration | % Deviation | Response Factor |
|-----------|-----------|-------|---------------|---------------|----------------------|-------------|-----------------|
| BLANK | BLANK | Y | 0.000000E+00 | 0.0000000E+00 | -1.483792E+01 | -1.00E+02 | Invalid |
| 795DNT100 | 795DNT1 | Y | 0.000000E+00 | 0.0000000E+00 | -1.483792E+01 | -1.00E+02 | Invalid |
| 795DNT500 | 795DNT5 | Y | 0.000000E+00 | 0.0000000E+00 | -1.483792E+01 | -1.00E+02 | Invalid |
| 795DNT750 | 795DNT75 | Y | 0.000000E+00 | 0.0000000E+00 | -1.483792E+01 | -1.00E+02 | Invalid |
| 295WNCS0 | 295WNCS | Y | 5.000000E+01 | 5.6052245E+06 | 5.000000E+01 | 0 | 1.784050E-04 |
| 295WNCS00 | 295WNCS0 | Y | 5.000000E+02 | 4.4507628E+07 | 5.000000E+02 | 0 | 2.246806E-04 |

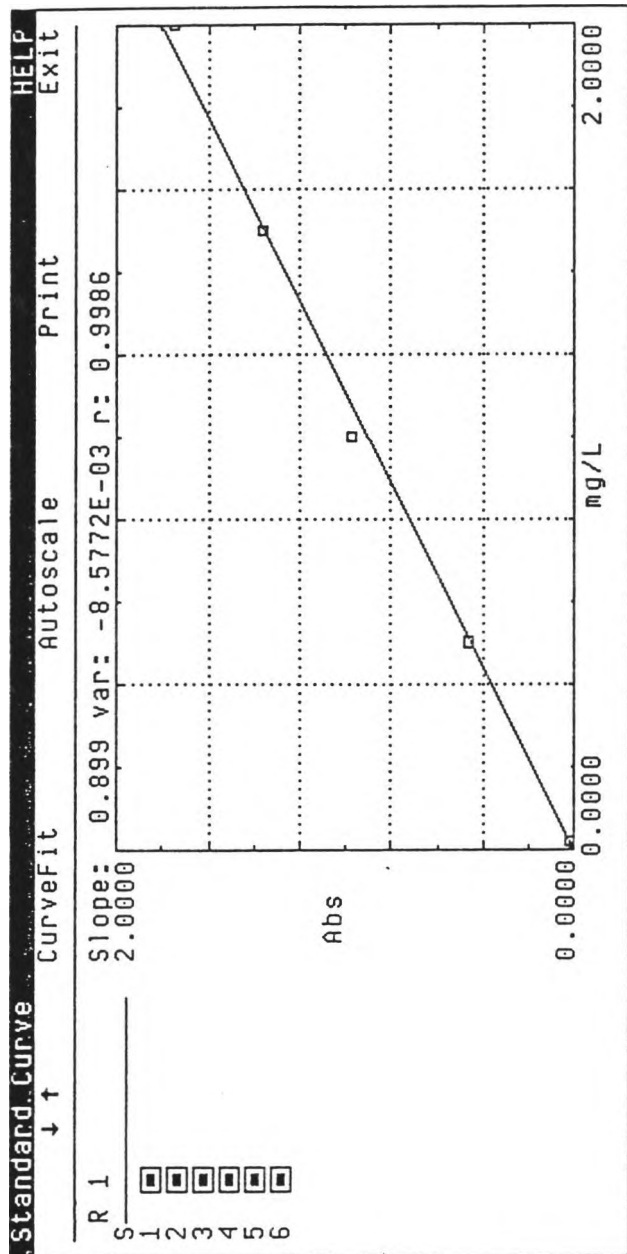


Figure A3.3: Calibration of nitrite ion concentration versus absorption at $\lambda = 543 \text{ nm}$.

COLORADO STATE UNIVERSITY
CHEMICAL ENGINEERING

Date: 08/13/95
Time: 18:11

Single Component Analysis: Standards
Samples DispStdCurve ViewStats Method SaveClear Print Quit

| | |
|---|--------------------------------|
| Standards file: A:\STD2 | Method name: A:\NO2 ↑ ↑ |
| Component name: Nitrite ion concentration | Analytical wl: 543.00 nm |
| Units: mg/L | Bkg1: [No] 500.00 nm |
| Curve fit: Non-linear, non zero intercept | Bkg2: [No] 560.00 nm |
| Sampling device: Auto smplr | |
| Number of standards: 6 | Number of replicates: 1 |
| Read average time: 0.50 sec | Flag standards over: 1.000% CV |

| Std # | Rep # | Std Conc | Calc Conc | Diff | Analyt abs | Bkg1 abs | Bkg2 abs | Net abs | Use |
|--------|-------|----------|-----------|---------|------------|----------|----------|---------|-----|
| Read 1 | | 0.0000 | 0.0048 | 0.0048 | 0.0017 | | | 0.0017 | [Y] |
| Read 2 | | 0.0200 | 0.0234 | 0.0034 | 0.0207 | | | 0.0207 | [Y] |
| Read 3 | | 0.5000 | 0.4734 | -0.0266 | 0.4655 | | | 0.4655 | [Y] |
| Read 4 | | 1.0000 | 1.0293 | 0.0293 | 0.9733 | | | 0.9733 | [Y] |
| Read 5 | | 1.5000 | 1.4887 | -0.0113 | 1.3383 | | | 1.3583 | [Y] |
| Read 6 | | 2.0000 | 2.0004 | 0.0004 | 1.7503 | | | 1.7503 | [Y] |
| Read 7 | | | | | | | | | |

COLORADO STATE UNIVERSITY
CHEMICAL ENGINEERING

Date: 06/13/95
Time: 17:28

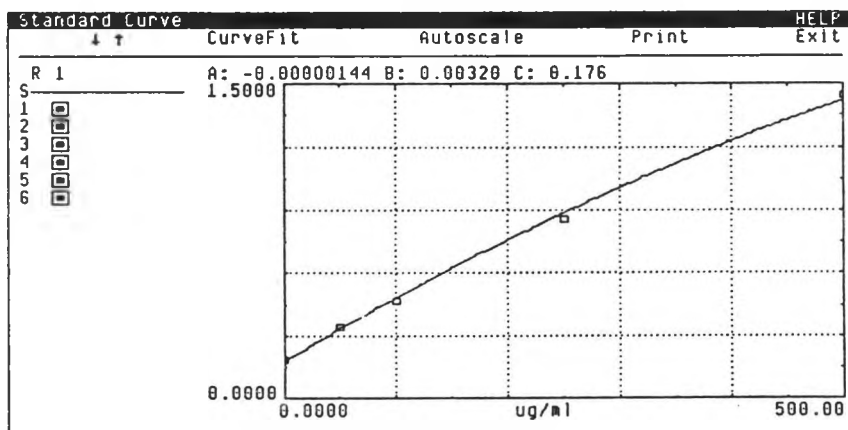
Protein Analysis: Standards
Samples DispStdCurve ViewStats Method SaveClear Print Quit

Assay type: Bicinchoninate (BCA)
Standards file: A:\KAT_STD2
Component name: PROTEIN
Curve fit: Non-linear, non-zero intercept
Sampling device: Auto smplr
Number of standards: 6
Read average time: 0.50 sec

Analytical wl: 562.0 nm
Method name: A:\KAT_STD1
Units: ug/ml

Number of replicates: 1
Flag standards over: 1.000% CV

| Std# | Rep# | Std Conc | Calc Conc | Diff | %CV | Analytical abs | Use | Flag |
|--------|------|----------|-----------|----------|-----|----------------|-----|------|
| Read 1 | | 0.0000 | 3.5720 | 3.5720 | | 0.1870 | [Y] | |
| Read 2 | | 50.000 | 53.4668 | 3.4668 | | 0.3428 | [Y] | |
| Read 3 | | 100.00 | 95.1152 | -4.8848 | | 0.4673 | [Y] | |
| Read 4 | | 250.00 | 239.1308 | -10.8692 | | 0.8597 | [Y] | |
| Read 5 | | 500.00 | 513.4489 | 13.4489 | | 1.4422 | [Y] | |
| Read 6 | | 1000.0 | 988.3447 | -11.6553 | | 1.9398 | [Y] | |
| Read 7 | | | | | | | | |



COLORADO STATE UNIVERSITY
CHEMICAL ENGINEERING

Figure A3.4: Calibration of BCA method with protein concentration versus absorption at $\lambda = 562$ nm.

Appendix IV: SimuSolv™ Modeling and Simulation Software: user program and example of input data file

```
PROGRAM dnt1
'WARNING--DO NOT USE TABS IN SETTING UP YOUR PROGRAM'
INITIAL
  VARIABLE TIME    = 0.   $ 'RENAME THE INDEPENDENT VARIABLE'
  ALGORITHM IALG   = 2   $ 'CHANGE INTEGRATION METHOD TO GEARS STIFF'
  constant umax = 0.10  $ 'max specific growth rate, 1/h'
  constant ks = 13.    $ 'mg/L'
  constant Yxs = 27.   $ 'yield cells per substrate, mg/mg'
  constant xic = 0.5   $ 'initial cell conc., mg/L'
  constant sic = 145.  $ 'initial substrate conc., mg/L'
  constant kat = 100.

  CONSTANT TSTOP   = 110. $ 'LENGTH OF EXPERIMENT, hours'
  CONSTANT POINTS = 550. $ 'NUMBER OF OUTPUT POINTS'

CINT = TSTOP/POINTS      $ 'SPECIFY COMMUNICATION INTERVAL'
END $'end of initial segment'

DYNAMIC
  TERMT(TIME .GE. TSTOP) $ 'DEFINE TERMINATION CONDITION'

DERIVATIVE
  mu = (umax*s)/(ks+s)
  dx = mu*x
  ds = -mu*x/Yxs
  x = integ(dx,xic)
  s = integ(ds,sic)

END $'end of derivative'

END $'end of dynamic'

TERMINAL
END $'end of terminal'

END $'end of program'
```

```

' This optional file is provided to enter frequently used Simusolv*' 
' commands (such as PREPARE), definition of PROCs, and experimental' 
' data (in a DATA block). Commands will be read from the terminal' 
' if this file is not used or after all commands entered here are' 
' processed. '
'* Trademark of the Dow Chemical Company'

prepare time x s
proc allone
data

time      x          s
0.0000    1.0        146.9
11.500   2.0        141.8
13.250   3.0        142.85
15.25    3.0        142.63
17.25    3.0        140.36
19.75    4.0        137.88
22.75    4.0        138.83
25.75    3.0        138.44
27.75    4.0        139.15
30.5     4.0        136.77
33.0     4.0        132.8
34.5     4.0        127.53
36.5     4.0        126.93
38.25   5.0        133.04
39.5     9.0        127.39
42.00   8.0        122.20
44.00   9.0        113.67
46.5     11.0       105.48
47.5     12.0       98.556
50.5     19.0       76.207
51.75   20.0       68.357
51.25   25.0       49.378
57.0     30.0       24.37
58.0     32.0       19.78
59.75   35.0       12.451
61.5     37.0       7.557
63.333  39.0       4.6191
66.0     38.0       3.2312
68.16666 39.0       2.9998
69.3333  38.0       2.978
71.3333  38.0       2.8942
74.6666  39.0       2.9325
81.00   35.0       2.9352
86.5     36.0       3.1474
92.5     34.0       3.1346
108.0    26.0       3.2038

end $'data'
end $'procedure'

```